



Universidade Federal de Uberlândia - UFU
Faculdade de Engenharia Mecânica - FEMEC

**AEROACOUSTIC EFFECT GENERATED BY THE INTERACTION ROTOR-
AIRFRAME IN AN UNMANNED AERIAL VEHICLE'S STRUCTURE**

Gino Rodrigo Lavagnino Sanchez

UBERLANDIA - MG

November, 2021

Gino Rodrigo Lavagnino Sanchez

**AEROACOUSTIC EFFECT GENERATED BY THE INTERACTION ROTOR-
AIRFRAME IN AN UNMANNED AERIAL VEHICLE'S STRUCTURE**

Bachelor thesis submitted to the Undergraduate's Course of Aeronautical Engineering of Universidade Federal de Uberlândia, as a partial requirement for the bachelor's degree in Aeronautical Engineering.

Advisor: Prof. Dr. Odenir de Almeida

UBERLANDIA - MG

November, 2021

AEROACOUSTIC EFFECT GENERATED BY THE INTERACTION ROTOR-AIRFRAME IN AN UNMANNED AERIAL VEHICLE'S STRUCTURE

Bachelor thesis submitted for the Undergraduate's Course of Aeronautical Engineering of Universidade Federal de Uberlândia, as a partial requirement for the bachelor's degree in Aeronautical Engineering. Approved by:

Prof. Dr. Odenir de Almeida
Faculdade de Engenharia Mecânica
Universidade Federal de Uberlândia

Prof. Dr. Marcus Antonio Viana Duarte
Faculdade de Engenharia Mecânica
Universidade Federal de Uberlândia

Prof. Dr. Tobias Souza Morais
Faculdade de Engenharia Mecânica
Universidade Federal de Uberlândia

UBERLANDIA - MG

November, 2021

ACKNOWLEDGMENTS

First, I would like to thank my mentor Odenir de Almeida for his unconditional support, teachings and availability throughout all the process, especially on the late night of the testing.

We would like to thank Prof. Fernando Martini Catalano from EESC/USP for helping in this research by providing the microphone for the acoustic measurements.

I would like to thank Paulo Almeida, for his unselfish help, availability and technical support during the set-up of the experimental equipment, especially on the last day of the testing.

I would also like to thank my family and my girlfriend Gabriela, for the support through the entire journey in Brazil and university, for always believing in me, motivating me to keep going and picking me up when I was down or feeling away from home.

Also, I would like to thank Marcio Dias and Rafael Cyrino, for all their love and support throughout these years, especially during the pandemic.

To my friend Cristyan Lucas, thank you for all the late nights of study and support to keep on going throughout the University.

I would also like to thank my boss, Nora Paredes, for her unconditional support, patience and motivation throughout this year.

To Anderson and Denise, thank you for your help and support in my search for internship.

Last but not least, I would like to thank Brazil for the life-changing opportunity and especially Federal University of Uberlandia for all the knowledge and support.

LAVAGNINO. G. R. **Aeroacoustic effect generated by the interaction rotor-airframe in an unmanned aerial vehicle's structure.** 2021. Bachelor's Thesis, Federal University of Uberlândia, Uberlândia Brazil.

ABSTRACT

As the years go by, UAVs become more accessible, their operation properties improve and companies like Embraer get closer and closer to apply this type of vehicles for their operations and become their future product. These vehicles are evolving fast and the possibility of skies being filled with buzzing multicopters has raised major concerns about security, health and control. For this reason, a vast number of researches, in the area of Aeroacoustics, need to be done to solve major problems as mentioned before, including problems such noise pollution in our modern society. Knowing this, the present work is dedicated to study a possible source of noise in UAVs, known as the interaction rotor-airframe, which causes a tonal noise given by pressure fluctuations between these components. As a possible solution and based on some studies, were projected and manufactured three different airframes; each one with a distinctive noise reduction concept. To test these concepts, an experimental process was conducted using a high-definition microphone, as a data acquisition system to measure the different pressure levels through a determinate period of time and through a code in Matlab® interpret and plot the signals as a A-weighting signal to identify a possible noise reduction in each case in the human acoustic domain.

Keywords UAVS, Aeroacoustics, noise pollution, noise, rotor-airframe.

LAVAGNINO. G. R. **Aeroacoustic effect generated by the interaction rotor-airframe in an unmanned aerial vehicle's structure.** 2021. Bachelor's Thesis, Federal University of Uberlândia, Uberlândia Brazil.

RESUMO

Com o passar dos anos, os VANTs se tornam mais acessíveis, suas propriedades de operação melhoram e empresas como a Embraer se aproximam cada vez mais para incorporar este tipo de veículo em suas operações e se tornar seu futuro produto. Esses veículos estão evoluindo rapidamente e a possibilidade de os céus serem preenchidos por multicópteros zumbindo tem levantado grandes preocupações sobre segurança, saúde e controle. Por essa razão, um grande número de pesquisas, na área de Aeroacústica, precisa ser feito para resolver os principais problemas mencionados antes, incluindo também problemas como a poluição sonora em nossa sociedade moderna. Sabendo disso, o presente trabalho se dedica a estudar uma possível fonte de ruído em VANTs, conhecida como interação rotor-suporte, que provoca um ruído tonal dado pelas flutuações de pressão entre esses componentes. Como possível solução e com base em alguns estudos, foram projetados e fabricados três suportes diferentes; cada um com um conceito distinto de redução de ruído. Para testar esses conceitos, foi realizado um processo experimental utilizando um microfone de alta definição, como sistema de aquisição de dados, para medir os diferentes níveis de pressão através de um determinado período de tempo e através de um código em Matlab® interpretar e plotar os sinais como em forma de A-weighting para identificar uma possível redução de ruído em cada caso e no domínio acústico humano.

Palavras chaves: VANTs, Aeroacústica, poluição sonora, ruído, rotor-suporte.

LIST OF FIGURES

Figure 1 – Parrot Ar. Drone.....	14
Figure 2 – Height operation Dilema.....	16
Figure 3 – Comparative noise levels.....	19
Figure 4 – Human hearing domain.....	20
Figure 5 – Equal Loudness Curve for Sinusoidal Tones	20
Figure 6 – Polar plot of thickness (a) and loading noise (b) distributions.....	21
Figure 7: The progression of the ICAO Noise Standards for aircrafts.....	24
Figure 8 – Dominant engine noise sources.....	26
Figure 9 – Boeing 777 engine Chevron nozzle.....	26
Figure 10 – Flame Wheel.....	30
Figure 11 – Flame Wheel 450 Exploited.....	31
Figure 12 – Diatone GTX 549.....	32
Figure 13 – Obsidian Wasp Drone.....	32
Figure 14 – Arm 1.....	32
Figure 15 – Arm 2 (w/o FOAM).....	33
Figure 16 – Arm 2 (with FOAM).....	34
Figure 17 – Metallic Support and clamp holder.....	37
Figure 17 – Angle mapping referenced in the motor center.....	38
Figure 18 – Angle mapping.....	39
Figure 19 – Areas of the set up.....	39
Figure 20 – Areas B and C.....	40
Figure 21 – Areas B, C and D.....	40
Figure 22 – Background noise curve.....	41
Figure 23 – Microphone data of motor without rotor at angles (0°, 30°, 60° & 90°).....	42
Figure 24 – A-Weighting curves of Arm 0 at angles (0°, 30°, 60° & 90°).....	43
Figure 25 – A-Weighting curves of Arm 1 at angles (0°, 30°, 60° & 90°).....	44
Figure 26 – A-Weighting curves of Arm 2 (w/Foam) at angles (0°, 30°, 60° & 90°).....	45
Figure 27 – A-Weighting curves of Arm 2 (w/o Foam) at angles (0°, 30°, 60° & 90°).....	46
Figure 28 – BPS at 4500 RPM/angles (30°).....	47
Figure 29 – Comparison of A-Weighting curves of every arm at 4500 RPM/angles (0°, 30°, 60° & 90°).....	48

LIST OF TABLES

Table 1 – FlameWheel 450 experimental set	35
Table 2 – Data Acquisition Equipment	36

LIST OF ABBREVIATIONS AND ACRONYMS

UAV - Unmanned Aerial Vehicle

FAA - Federal Aviation Administration

EASA - European Aviation Safety Agency

NASA - National Aeronautics and Space Administration

ANC - Active Noise Control

dB - Decibel

dBA - A-weighting Decibel

RPM - Revolutions per minute

ESC - Electronic speed controller

OASPL - Overall Sound Pressure Level

SUMMARY

ACKNOWLEDGEMENTS	4
ABSTRACT	5
RESUMO	6
1. Introduction	12
1.1. Emergence of UAVs.....	12
1.2. Basics of UAVs	13
1.2.1. Pros and Cons of UAVs	14
1.3. Why exploring UAVs Aeroacoustics and Aerodynamics?	16
2. Theoretical foundation	18
2.1. Fundamentals of Sound and Noise	18
2.2. Source of Noise in UAVs and the effects in human health	21
2.3. Helmholtz Resonator concept.....	22
3. Literature review	23
3.1. Noise reduction Regulations.....	23
3.2. Noise reduction in commercial aircrafts.....	25
3.2.1. Jet engine noise reduction.....	26
3.2.2. Fan/propeller noise reduction.....	27
3.3. Noise reduction in UAVs	28
4. Methodology.....	30
4.1. Default arm (arm 0).....	30
4.1.1. Arm 1.....	31
4.1.2. Arm 2 with and without foam.....	33
4.2. Operational equipment	34
4.3. Data Acquisition Equipment.....	36
4.4. Experimental Set up.....	37
5. Results and discussion.....	41
5.1. Establishing Background noise of the environment and the motor.....	41
5.2. Analysis of every arm configuration.....	43
5.2.1. Arm 0 – A-Weighting curves.....	43
5.2.2. Arm 1 – A-Weighting curves.....	44
5.2.3. Arm 2 (with and without foam) – A- Weighting curves.....	45
5.3. Comparison between arms results at a 4500 RPM operation.....	47
6. Conclusion.....	49

BIBLIOGRAPHICAL REFERENCES	50
APPENDIX A.....	53
APPENDIX B.....	54
APPENDIX C.....	55
APPENDIX D.....	56
ANNEX A.....	57
ANNEX B.....	58
ANNEX C.....	59
ANNEX D.....	62
ANNEX E.....	63
ANNEX F.....	64
ANNEX G.....	65
ANNEX H.....	66
ANNEX I.....	67
ANNEX J.....	68
ANNEX K.....	70
ANNEX L.....	102

CHAPTER I

1. INTRODUCTION

In this chapter we are going to discuss the origins of the Unmanned Aerial Systems (UAS) or Unmanned Aerial Vehicles (UAVs), detailing major events or starting points throughout history that lead to the Modern Era of Drones. It will also be explained what is considered, nowadays, to be an UAV and some of the features that compose a basic quadcopter which is the configuration that is going to be worked in this paper. Last but not least, it is going to be presented a brief explanation of the motivation of this work such as the problems to be solved, new concepts and challenges in the ambit of aerodynamics and aeroacoustics to be considered to evolve this project and have success.

1.1. Emergence of UAVs

The UAS or UAVs are modern terms to refer to drones. These terms may be recent but their emergence can be tracked down to late 1700s. From a technical standpoint, the first record of an UAV was achieved in the year of 1783 by hot air balloons in Annonay, France. Joseph-Michel and Jacques-Étienne Montgolfier constructed and hosted the first public event of an UAV flight. Some decades after this achievement the Austrians used the hot-air balloons loaded with explosives for military purposes in the Austrian-Venice war (1849), although they were mostly ineffective. A few years passed, when the first aerial photograph was taken from a hot-air balloon in Paris, France in 1858, but this photograph ended up being lost throughout history. Even though this was a great and fast advance for the UAV history, it wasn't until 1896 when Alfred Nobel successfully adapted a camera in a rocket as an unmanned experiment system and in 1898 that the first Radio-Controlled prototype (a radio controlled boat) was presented to the public by Nicolas Tesla. Eventually, in 1907 Breguet Aviation constructed and tested the first experimental quadcopter rotary-wing aircraft, known as the Breguet-Richet Gyroplane. Even though this was a piloted flight, it was an enormous step for the quadcopter concept. In 1915, the British army used

aerial photography for reconnaissance of the German front during the Battle of Neuve Chappelle. This was the one of the earliest examples of *orthomosaic*¹.

Until 1915, the idea of the modern drone era was set. But, what is a modern drone? It is an UAV which can be used for military purposes (surveillance, reconnaissance and targeted attacks), science (monitoring migration of animals) photography and filming (concerts, large events, promotional purposes, etc.) and many others purposes. Consequently, in the further years the efforts where only focused to improve these last accomplishments. Through time the technology has played an essential role on the rapid development and evolution of UAVs, increasing structural material resistance/lightness, the quality of the cameras, electrical autonomy and reach and many other features. For this reason, in the year of 1985 the world witnessed a large increase of drone production until 1996 when the Predator Drone was developed and brought weaponized drones to the battlefield like never before. Throughout these years the drone production increased in such way that permitted civilians to have access to small/electric quadcopter such as the Parrot AR (2010). Additionally in this year, major delivery companies (FedEx, UPS, Amazon, Google, Uber, etc.) recognize drones as the future as a delivery platform [1]. A timeline of UAVs is shown in Appendix A.

1.2. Basics of UAVs

The Breguet-Richet Gyroplane could be considered to be the father of quadcopter and multi-rotor aerial vehicles. Since 1920s, these vehicles have quite a technological evolution in the stability, power and autonomy area. The year was 2010, when Parrot launches the first electrical quadcopter. This company, repurposed all the military UAV technology and direction it to small electrical quadcopter for consumer use. This model of UAV was considered to be the first one to be controlled by a simple command system, such as a smartphone (Fig. 1). Despite the 113 years of gap, the Parrot AR 2.0 and the Breguet-Richet Gyroplane present a lot of similarities in their configuration, meaning that the basics were maintained through time. The modern

¹ Orthomosaic: They are maps offer a photorealistic representation of an area that can produce surveyor-grade measurements of topography, infrastructure, and buildings. Each orthomosaic map is made up from dozens of orthoimages. (Source: <https://www.mapware.ai/blog/turning-drone-photogrammetry-into-orthomosaic-maps>)

quadcopter/multirotor configuration is composed by the following components: 4 brushless motors, propellers and Electronic Speed Controllers (ESC), a kit of connectors, a battery as the power source, a Power Distribution Board, a Flight Controller, a FPV Transmitter, a control receiver, an antenna and last but not least to mount all this the drones frame, respectably illustrated in (Appendix B).

Figure 1 – Parrot Ar. Drone²



1.2.1. Pros and Cons of UAVs

Because of their relatively simple construction and programmability to perform various type of tasks, UAVs have become interest of governmental, military and business organizations. From fast delivery in any time of the day, even rush hours, to perform accurate tasks in hard to risk places for militaries, firemen, etc. the UAVs have become synonym of work efficiency and productivity, reduction of workload, costs and risks in dangerous situations.

As reported by the Insider [2], given to this las attributes, some of the major utilities of UAVs can include:

- Aerial photography and filming

² Source: <https://www.youtube.com/watch?v=xWCYNiyqY8o>

- Express shipping and delivery
- Collecting information in disaster sites (unreachable by a man power) for search and rescue operations.
- Safety inspections of high structures or small and inaccessible sites.
- Crop monitoring
- Wild life observation
- Big site patrol, such as borders.
- Climate tracking for future storms, hurricanes and tornadoes.

In the past years, this list continues growing rapidly because of its promising future. Several uses are being developed and are underway to change the industry drastically.

Although all this is revolutionary, there are a lot of things to take in consideration, challenges and some disadvantages of the UAVs entering the society's routine. Undoubtedly the control of the demand and the users' intentions with an UAV is a major concern for governments. Besides privacy, UAV could represent a major risk to cause damages not only in houses or land structures but also in aircrafts if they are not manipulated correctly. In addition, security, flight control is another challenge considering a future usage of UAVs for delivery, surveillance and other uses. Last but not least, a major concern and disadvantage, if not improved forward in time, is the noise pollution modern multicopters generate. This type of pollution is not new, it has been present in our society since transport methods acquire an engine and has had an exponential growth in the urban areas in the cities. As constant factor of improvement, the FAA and EASA see multicopter as highly noise pollutants given their low altitude of operation and high revolution of their motors, which produce a high-pitched noise.

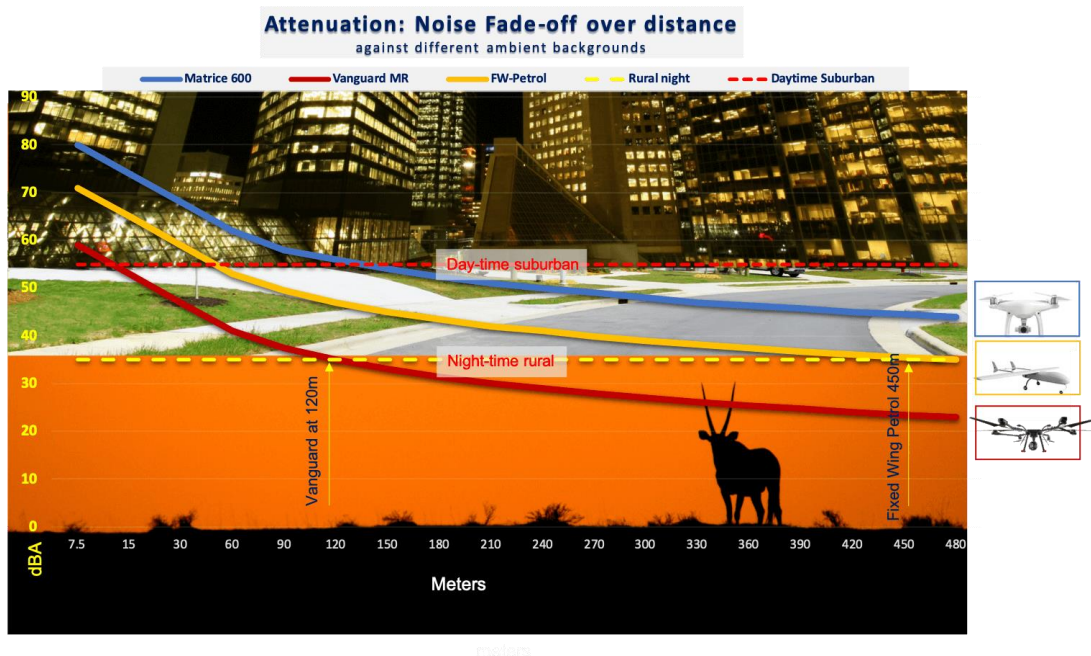
In relation to high-pitched noise, NASA performed a study [3] to understand the effect in human's behavior and resulted in an undesirable and an unwanted pitch of noise for some persons. So considering UAVs produce this type of pitch, it was concluded that for a daily basis it would be considered even more annoying than the low-pitched and brief noises.

In addition to unpleasant effect, humans can also be affected physiologically by noise pollution and some of consequences can be hypertension, insomnia,

cardiovascular problems as related by an article of National Geographic [4]. Another important study was performed by Airborne Drones [5] in which the height of operation dilemma is discussed in rural, urban and suburb areas to attenuate UAVS noise as much as possible and do not disturb humans and wild lives routine.

Evidently there are a lot of factors that need to be research and improved before UAVs adaption to our modern society. Being the noise pollution one of the major problems, it was decided to dedicate this paper to researcher to explore the quadcopter structure and see where and how can noise pollution can be reduced or at least attenuated.

Figure 2 – Height operation Dilema³



1.3. Why exploring UAVs Aeroacoustics and Aerodynamics?

As the interest in implementing UAVs in our daily routine grows, the research must grow side by side to improve and adequate these vehicles to society. Because of this, the aerodynamic and aeroacoustics characteristics of the UAVs have become areas of interest. These two areas are essential to comprehend the origins of high-

³ Source: <https://www.airbornedrones.co/drone-noise-levels/>

pitched noise produced by these vehicles and analyze in which ways this problem can be approached.

Various articles and papers have been published to explore the source of the noise emission by multicopters and fairly agree that the motors are a major source of this problem but the interaction rotor-airframe also contribute significantly. Therefore, rapid steps have been taken in the research area to examine new concepts of rotors and airframes by changing their format, material, proximity between them and so many other variables that could attenuate the noise generated. However, these changes, need a backup study to reassure they are not affecting the efficiency, stability, structure and flight control of the UAV. Having this in consideration, this work was focused in studying the interaction rotor-airframe and how changing the format using aerodynamic and aeroacoustics concepts can possibly attenuate the noise generation.

The first airframe model (Fig. 5) was design to have an airfoil type cross-section to reduce the contact area experience by the downwash flow produced by the rotor. Another concept that was used in this model, was the increase of spacing between the rotor and the airframe, to reduce the prominent tonal noise associated with proximity and their interaction [6].

The second and third models were projected as noise silencers by using a perforated surface and acoustic foam within the airframe and the other model by using the Helmholtz resonator concept [7], shown in Fig. 6 and Fig. 7, respectively. Considering the quadcopter has relatively small diameter propellers, it is needed to operate them at high RPMs and the majority of the lift is generated at the tip of the rotor. Consequently, a high source of the noise is produced when the rotor passes over the airframe, generating resonance which possibly it can be reduced by using these two methods listed above.

CHAPTER II

2. THEORETICAL FOUNDATION

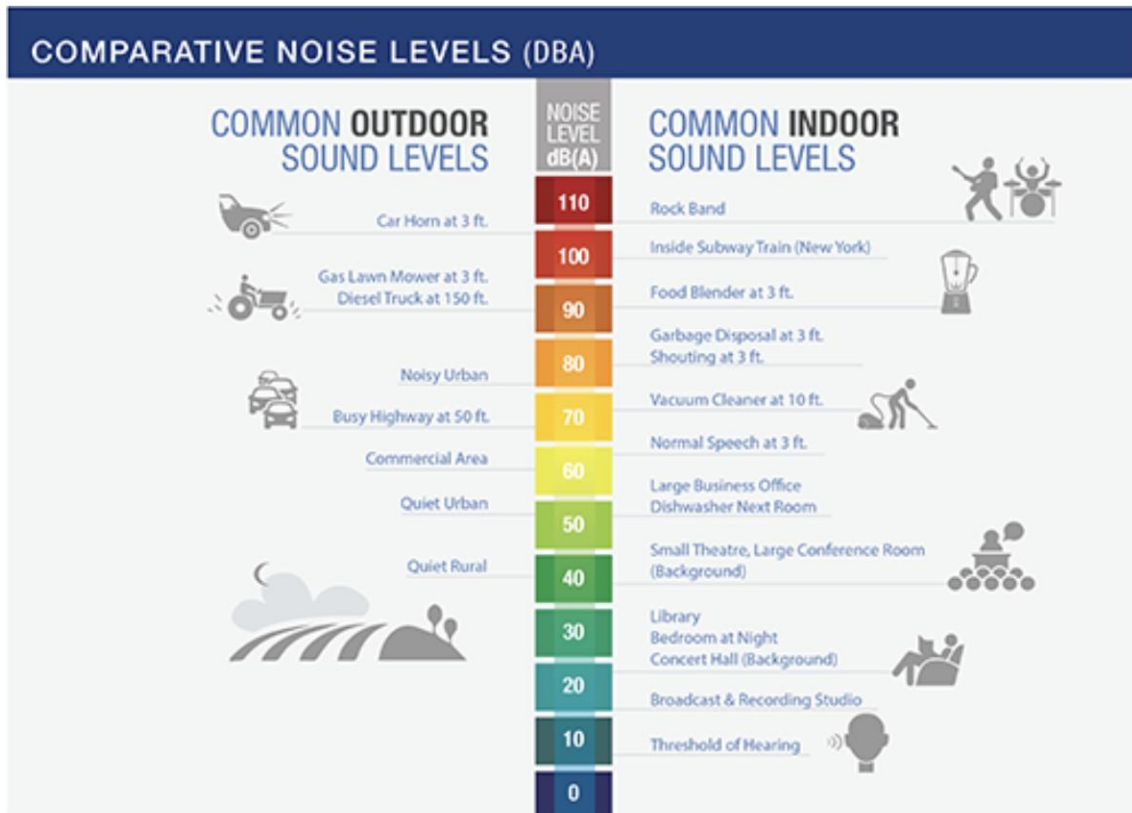
What is noise and why is it an important matter to be discussed for aircrafts and specially UAVs? Before digging into this question, it is important to set some other foundations about the origin of noise, that is sound. In this chapter it is going to be explained the fundamentals of sound and travel all the way to noise and its presence in UAVs. Additionally, it is going to be discussed some of the sources of this problem, ways to measure it and some possible solutions that have been proposed though time.

2.1. Fundamentals of Sound and Noise

Sound is nothing more than a variation of air pressure that travels in a wave form through air. This change of pressure depends on the amount of energy available to emitting the sound. So, for example the amount of energy in a whisper is totally different than a yell. It is perceptible that by yelling a larger amount of energy is disposed and it is going to be audible in a longer distance [8]. It is known that all living things have a different perception of sound intensity, animals that live in environments with less presence of light, such as moths and bats (audible spectrum up to 300,000 Hz and 9000 Hz up to 200,000 Hz, respectively), evolve a more sophisticated audition system to survive and be able to compensate their lack of vision. Humans on the other hand don't have such a sophisticated hearing system, our audible spectrum is about 20 Hz to 20 Hz and can decay through aging to 15-17kHz.

On the other hand, we have noise. This is an unwanted or annoying sound perceived by the audition system. Noise can be considered something subjective, because the level of annoyance depends on the receiving subject's sensitivity, perception or ratio to sound. The unit to measure sound's intensity is called decibel (dB). To represent the common indoor and outdoor sound levels in a human daily basis, the FAA presented a comparative graphic for Noise levels (dBA), as shown in Figure 3.

Figure 3 – Comparative noise levels⁴



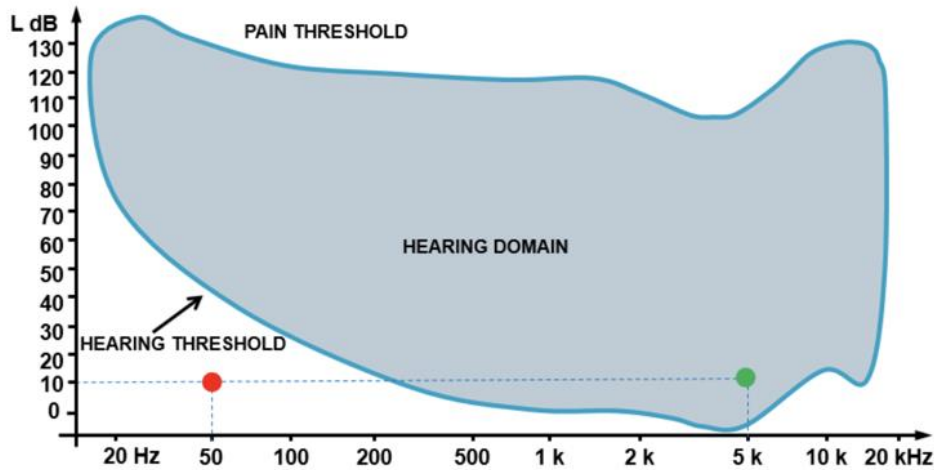
As can be seen on the scale, 0 dB represents the quietest sound a human ear can hear, or simply silence, and increases to 110 dB, which defines the threshold at which any sound beyond that level can cause hearing loss. A Jet-Engine Aircraft taking off, for example, produces sound intensity of 140 dB, which means that without sound protection, a person may suffer hearing damage.

Furthermore, diverse pitches or frequencies of sound stimulate varied reactions in the human ear, which is an essential aspect of human hearing. Low frequencies, such as thunder trembles, are harder to hear, whereas high frequencies, such as a baby’s cry, are more clearly heard. To alter the sound intensity (dB) to represent the actual sound as perceived by the ear, weights for each frequency must be considered, and these weights are shown on the A-Weighting curve (Appendix C). To further understand the attenuation and amplification of the preceding graph, it is presented (Figure 4), which shows the relationship between frequency and sound level,

⁴ Source: https://www.faa.gov/regulations_policies/policy_guidance/noise/basics/

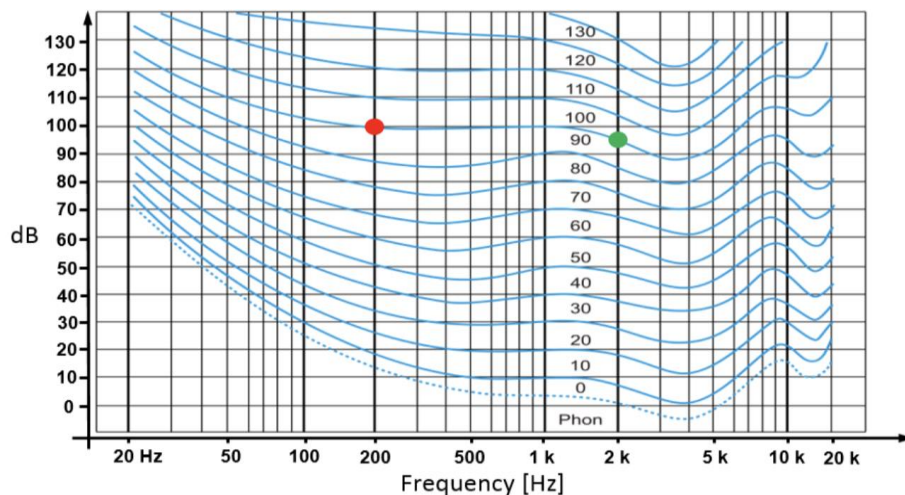
demonstrating how the threshold of hearing varies for different frequencies. Thus, a 10dB sound at 5 kHz (green dot), for example, is audible to humans, whereas a 10dB sound at 50Hz (red dot) is not.

Figure 4 – Human hearing domain⁵



Another characteristic of sound is that human hearing perception doesn't obey a linear behavior, which leads to the Equal Loudness curves. These curves demonstrate that sound perception is based on multiple acoustic characteristics.

Figure 5 – Equal Loudness Curve for Sinusoidal Tones⁶



⁵ Source: <https://community.sw.siemens.com/s/article/sound-quality-metrics-loudness-and-sones>

⁶ Source: <https://community.sw.siemens.com/s/article/sound-quality-metrics-loudness-and-sones>

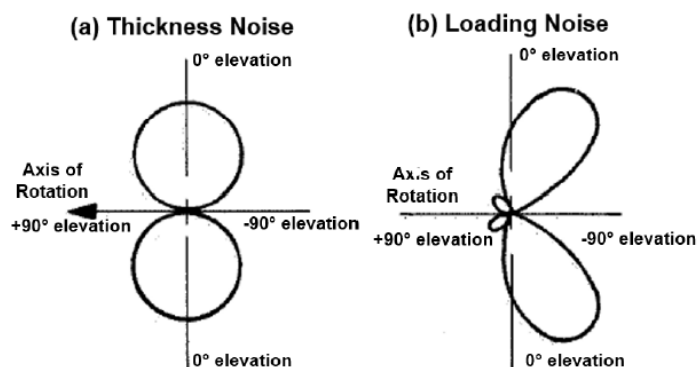
As shown in (Figure 5), in the 90 phon curve a sound with a frequency of 200 Hz and an intensity of 100 dB, is going to be as loud as a sound emitted with 2000 kHz and 95 dB. By this, it can be concluded that for a noise reduction project it's crucial to evaluate loudness and intensity additionally to the pressure level, to prevent any type of misconception of the experiments results.

2.2. Source of Noise in UAVs

The noise produced by UAVs is comparable to that produced by helicopters. Given that both types of aircraft are equipped with rotatory wings, this may be inferred. This form of noise is considered complicated and comes from a variety of sources. According to Bernandine [9] some of the major noise sources are: Thickness, Loading and Broadband noise, but Noise Quest also considers Blade Vortex Impulsive (BVI Noise) and in a secondary source engine and gearbox noise.

Thickness noise is the consequence of a sound wave pulse produced by the air being displaced by the blade in a repetitive rotation [10]. Jack E Martin, Donal W Kurtz, *“indicate that this displacement is the same as periodic mass addition and removal at each air element near the disc”*. Because of this, it can be concluded that this type of noise is relevant at higher speeds. Bernandine suggests that by changing the sweep to a narrower one or using a planform sweep, this sort of noise can be optimized. A polar plot distribution is shown in Figure x.

Figure 6 – Polar plot of thickness (a) and loading noise (b) distributions [9]



Loading Noise given by the aerodynamic loads thrust and torque that act on the blade from pressure fluctuations across the surface. Bernandine suggests that this type of noise can be decreased by optimizing the aerodynamic loads present on the blades surface [11]. This type o load is mostly present in low to moderate speeds and out of the plane.

Another sources of noise can be the broadband noise, this is a type of noise produced by a set of broad range frequencies and it is originated by turbulence flows and boundary layer noise. A possible solution is by using empirical methods, but until today is not considered to be reliable and researches are still on going for solutions and the effects in humans' health.

2.3. Helmholtz Resonator concept

Named after the German physicist Herman von Helmholtz, this concept provides a different type of resonator with an acoustic characteristic. Basically, by setting a frequency of operation, which is determined by the resonators volume (V), area (A) and length (L) of its neck, it can be produced a noise attenuation system [23]. For a better understanding of this concept follows the equation (1) that describes it and a calculus memorandum is presented in the (ANNEX F).

$$f = \left(\frac{S}{2\pi}\right) \cdot \sqrt{\frac{A}{L \cdot V}} \quad (1)$$

This concept was considered and implemented in the arm 2. The idea is to try and reduce the tonal noise that occur in the interaction rotor-airframe by implementing a resonator right below the rotor in the airframe. As (Bessa, 2018) [18] and (Zawodny, 2017) [6] propose it, the frequency set to define the Helmholtz characteristic is 4000 Hz. This frequency is considered according to the drone specifications and operation characteristics. As mentioned before the small diameter of the rotor are the cause of tonal noises, for which these types of solutions are needed.

CHAPTER III

3. LITERATURE REVIEW

Throughout this chapter, it is going to be discussed about noise reduction regulations that exist and are being proposed by the ICAO (International Civil Aviation Organization) regarding the noise pollution that exists and it is expected related to UAVs [12]. Also, it is going to be explore some old and recent researches and projects regarding techniques or methods proposed for noise reduction in aircrafts and relate these advances with challenges being faced by UAVs.

3.1. Noise reduction regulations

Since the 1970s, a worldwide concern on Noise control, related to aircrafts, emerged as this type of pollution kept growing fast and uncontrollably. This leads the ICAO (International Civil Aviation Organization) to set some control standards and recommended practices to limit noise pollution. The ICAO, hosted a convention in Chicago where more than 50 countries participated and the Annex 16 was delivered. This Annex had as a primarily objective the noise certification, to guarantee that any future aircraft design needed to include noise reduction technology. Moreover, it was required for any future project a vast number of tests were necessary to proves their effectiveness on noise attenuation. All this initial standard where set on the Annex 16 to the Convention on International Civil Aviation.

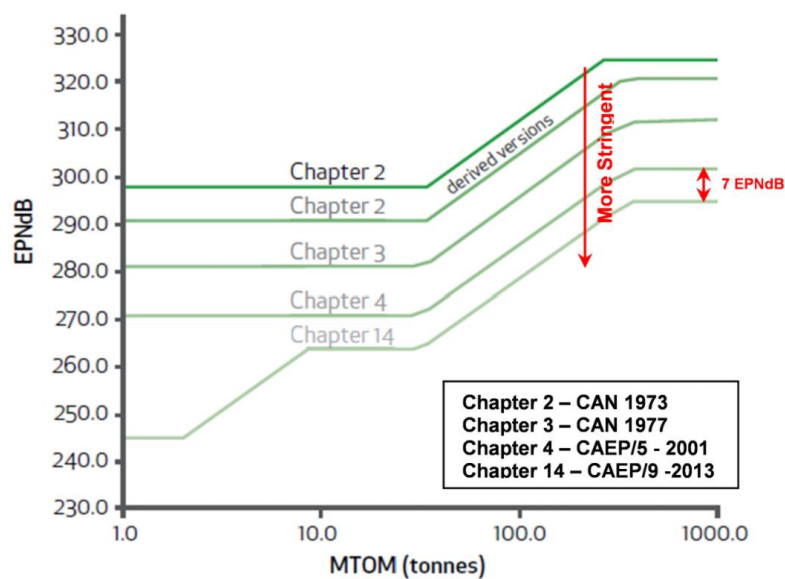
After this first convention major regulations were updated and stringent the noise standards to ensure quality of life in areas more affected bay air traffic was maintained. Here are some examples of regulations passed throughout the years after 1970:

- 1972 – Draft of International Standards and Recommended Practices for Aircraft Noise was written and applied, based on the Special Meeting on Aircrafts Noise in the Vicinity of Aerodromes (1969). This regulation defined the operation limits of aircraft operation in proximities of airdromes, such as:

Maximum Take-off Mass, angle of approach and take off, Maximum take-off thrust, etc. [12]

- 1977 – Higher bypass ratio jet engines emerged, bringing a significant improvement in noise reduction and in fuel efficiency. Important technology advances were made in the engine and airframe design in the following years allowing a significant noise decrease. Consequently, ICAO straighten even more noise standards which are contained in chapters 2, 3 and 4 of Annex 16, Volume 1.
- 2013-2014 – Chapter 14 was adapted requesting a 7EPNdB decrease for all jet and propeller-driven airplanes. Based on the previous chapters (Figure 7). This chapter aim to reduce the number of people that are affected by an aircraft noise around 55 dB daily or constantly.

Figure 7: The progression of the ICAO Noise Standards for aircrafts⁷



As our society evolves and technology develops, in this case UAVs, ICAO has an important challenge to keep up and ensure that worldwide authorities follow and implement the noise standards accordingly and respect them.

⁷ Source: <https://www.icao.int/environmental-protection/pages/reduction-of-noise-at-source.aspx>

UAVs are no exception to ICAO's regulations, this type of vehicles are only getting started and because of this they need to have strict standards since the beginning. This is a difficult challenge, but currently Brazil's involvement in the noise management aspects has been exemplary according to ICAO. Since 2017, the National Civil Aviation of Brazil (ANAC) presented an extensive and complete set of airworthiness rules [13] referring to UAVs, RBAC-E No. 94. This Amendment limits the operation of UAVs, especially near urban areas, that have a MTOM higher than 150 kg. For any unmanned vehicle with an MTOM below 150 kg there are no noise certification standards, but if it surpasses this limit the aircraft will be catalogue and applicable in the aircraft procedural and noise regulations RBAC 21 (Certification Procedures for Products and Articles) and RBAC 36 (Noise Standards: Aircraft Type and Airworthiness Certification). As various countries, Brazil is looking to increase their development of operation requirements for UAVs as they are already investing in EVTOL and foreseeing the usage of this vehicles in 2025 [12].

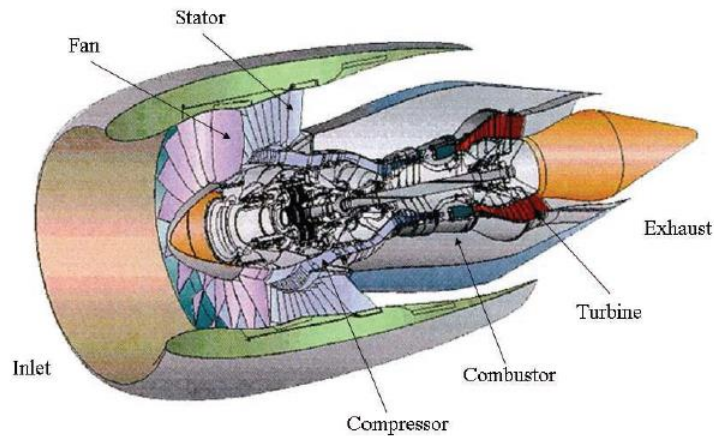
3.2. Noise reduction in commercial aircrafts

Significant progress has been made to reduce noise in the modern aircrafts, but this noise attenuation doesn't come for free. As the materials evolve through time, it has been possible to project more complex configuration, formats and parts to try and solve this problem.

NASA has conducted and sponsored a significant number of researches that aim to reduce the noise levels that our modern society is experimenting with the growing air traffic. In the aeronautical world, actions need to be taken aggressively given the long-time advances take to be researched and developed depending on the technology that is available. It is a known fact that engines are the major source of noise, especially in large aircrafts that overfly the cities constantly. But what parts of the engine could be the major contributor to the overall sound levels produced? In NASA research [14] in 2007 is postulated that the major sources of noise in a turbofan engine, commonly used in commercial aircrafts for its high performance and low noise emission, are the fan, exhaust (commonly called jet), the compressor, the combustion and the turbine (Figure 8).

A major challenge in any type of noise reduction solution, is to avoid changing the engine/motor cycle or to affect its efficiency and performance.

Figure 8 – Dominant engine noise sources [14]



3.2.1. Jet engine noise reduction

The newest and most recent example of success in noise reduction is the GE-90. This engine managed this important advance, by extracting energy from the engines core, consequently reducing de mixed velocity of the its interior and fan ducts concluding in a significant decrease of the jet exhaust velocity. Such a significant achievement, needs to be verified with a large number of tests considering this could affect the engine performance, if not evaluate correctly.

Another important solution, but this time without risking the engine’s performance integrity, was tested in 1996. The concept was called the “Chevron Nozzles” (Figure 9)⁸. This sawtooth format nozzles located on the trailing edges of some engines, are in charge of mixing the hot flow form the core of the engine and the cold flow form the bypass in a smoother way, reducing significantly the generation of turbulence

Figure 9 – Boeing 777 engine Chevron nozzles⁸



⁸ Source: https://www.nasa.gov/topics/aeronautics/features/bridges_chevron_events.html

which is a major noise generator. As mentioned in a NASA article in 2007 [14], this was one of the first and most important breakthroughs in noise reduction concepts that didn't impact in the engines thrust. Several engine and aircraft manufacturers are relying on this concept decrease the noise emission and be able to operate according to FAA and EASA regulations.

3.2.2. Fan/propeller noise reduction

Fan and propellers, present the same source of noise emission, their high-speed rotation needed to generate enough thrust to take-off or cruise through air. In 1995, NASA conducted research [15] to analyze which would be the easiest, cheapest and fastest concept to develop and try attenuate the noise produced by propellers. On the whole they concluded that the main objective should be to reduce the tip speed and the pressure ratio, but in contrast to achieve this, an increase in the diameter of the fan/propeller should be considered to compensate and achieve the thrust needed.

As mentioned in the previous section, another major noise generator is turbulence and this is a present problem when blades and propellers interact with other structures generating pressure fluctuations and unsteady flow. Consequently, researches were focused in this factor and some solution emerged as referenced in NASA's study in 2007 [14].

The "scarf inlet" emerged as a solution that redirected sound coming forward from the inlet fan and eliminate the reverse flow that is caused by distortion of the flow. After several computational and experimental tests were performed, a notorious noise reduction.

The Active noise control, was another interesting concept that was proposed in 1933 [16] as a fan tone cancellation method and has been developed until now. The idea of implementing this concept in modern engine aircrafts, emerged as the FAA and EASA regulations require more silent aircrafts and engines. The principle of functionality comes from the idea of cancelling a certain noise signal by emitting an inverse phase of it. This involves acquisition systems (microprocessors, microphones, etc.) and emission system such as speakers. This system would be installed inside the fan duct walls and the stator vanes. The purpose of this location is to identify the modes produced by the fan and try to cancel or at least reduce the noise. Although this

concept. Some other concept in development are Fan trailing edge blowing concept., Forward swept Fans and swept leaned stators.

3.3. Noise reduction in UAVs

Our actual society is experimenting a new era of aircraft, the UAVs. As mentioned before, with significant technology advances need to come strict regulations that standardize manufacturing, operation and other regulations that ensure security, health and impede any type of preventable disaster. For this to happen, extensive researches need to be performed to ensure the results fidelity and significance. With this in this section it is going to be presented a group of studies about aeroacoustics and aerodynamic optimization that can be or may be possible to apply in drones to improve the actual noise problem present in them.

In 2010, research was published in the 16th AIAA/CEAS Aeroacoustics Conference, named Aeroacoustics and Aerodynamic Optimization of Propeller Blades [17]. By using an Artificial Neural Network metamodel was possible the generation of a large number as well as individuals and applied the RANS model to secure a significant precision. The parameters optimized in the 4 different blades (FIGURE 9 AND 12) where sweep, twist, chord and thickness, which compromise the control points of b-spline parametrization of radial distributions. This article concluded, in the aerodynamic area, blades were divided in two groups swept and unswept. Swept blades presented a better performance during cruise conditions and unswept blades demonstrated a lower power requirement during take-off/landing conditions. Undoubtedly this is an important study for EVTOL area, which depend of distributed propulsion and different propellers are destined for take-off/landing and cruise operation.

In 2017, Nikolas Zowdny and Douglas Boyd published a paper [6] that discussed similar research to the present work. It was investigated the relation between noise and the interaction Rotor-Airframe. An interesting study they performed was when it was used a conical airframe, to explore the interaction rotor-airframe with different airframe diameters. In addition to experimental measurements, CFD based acoustic predictions where performed. One of the conclusions of this study, was that constant cross-section airframes had little or no effect on noise emission. Another

argument, proven with conical airframes, was that tonal noise is associated with the proximity between the rotor and the airframe, by decreasing the proximity the tonal noise will decrease too. Which is one of the major motivations for this work.

Renato Falconi, executed research [18] about noise reduction devices for UAVs in 2018. For study this, three different proplets with different winglets for each were projected and designed additionally with two ducts. Moreover, each configuration was tested and analyzed through signal acquisition of noise frequency spectrum. At the end it was shown, that ducts amplified the noise signature to high frequencies and propellers decrease noise over to 0,5 dBA in the majority of the spectrum and up to 4 DB in specific frequencies. Other studies of noise reduction were executed by modifying proplets' trailing edge's geometry as a serration, adding porous materials and boundary layer tripping in the surface [19].

CHAPTER IV

4. METHODOLOGY

This chapter covers the methodology, procedures, equipment, and materials utilized in the manufacturing process, as well as the setup and data collection for the whole experiment.

Because the quantitative component of the task focuses on attempting to reduce or eliminate any source of error, this section had to be done extremely carefully and following repetitive testing processes in order for the results to be satisfactory. Since the acquisition equipment is sensitive, climatic issues had to be taken into account to ensure the accuracy and efficacy of each measurement.

4.1. Geometry definition

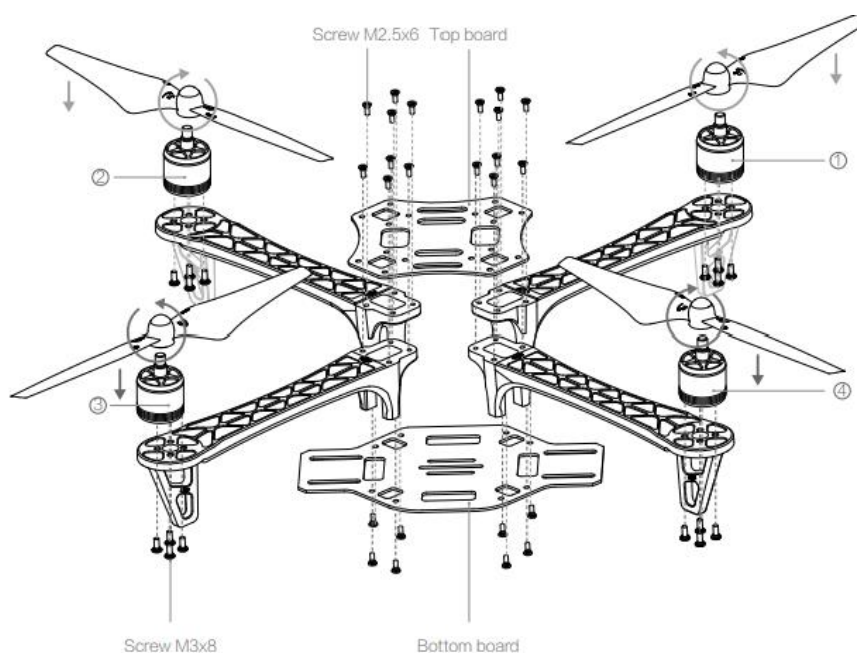
As the objective of the present work is to study the aeroacoustics effect only of the interaction rotor-airframe, it was decided to only use one airframe and rotor of the drone Flame Wheel 450. For a better representation, the physical model is shown in the Figure 10 and set as the default testing configuration (arm 0).

Figure 10 – Flame Wheel 450⁹



⁹ Source: <https://www.paybanks.ga/ProductDetail.aspx?iid=48460044&pr=>

Figure 11 – Flame Wheel 450 Exploited¹⁰



Considering the F450's significant width and contact area for the flow discharged by the rotor, a thinner or acoustically absorbent airframe must be projected. The airframe presents a perforated surface, which can maybe benefit the structural and weight properties or become a turbulence generator given the uneven surfaces. To resolve this possible problems, two airframes where designed that resulted in three different configurations, as follows.

4.1.1. Configuration - Arm 1

According to Nikolas' study, by increasing the separation rotor-airframe and lowering the airframe's width to minimize the contact area of the flow against the airframe is critical to reduce the tonal noise. Therefore, research was conducted, in pursue of an existing airframe project that had one or both of the characteristics mentioned before.

Luckily there were two that matched the lean airframe characteristic. The first one, is the Obsidian Wasp FPV racing frame (Figure 12). The second is an airframe manufactured by Diatone called GT X 549 Exorcist Moulded Carbon Quadcopter

¹⁰ http://dl.djicdn.com/downloads/flamewheel/en/F450_User_Manual_v2.2_en.pdf

Frame (Figure 13). At the end, the second airframe was chosen as the inspiration for Airframe B because it had a more aerodynamic shape.

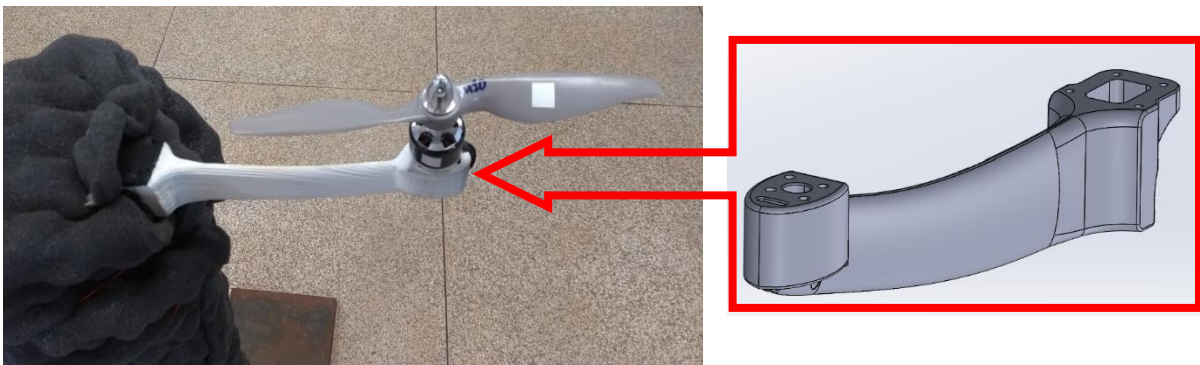
Figure 12 – Diatone GTX 549¹¹



Figure 13 – Obsidian Wasp Drone¹²



Figure 14 – Arm 1¹³ (Annex A)



¹¹ Source: <https://www.unmannedtechshop.co.uk/product/diatone-gt-x549-exorcist-frame/>

¹² Source: <https://rotoriousfpv.com/product/obsidian-wasp/>

¹³ Source: Author

Additionally, a bigger separation was added to the rotor-airframe interaction to try and match Nikolas' study. The result of the project is shown in (Figure 14).

4.1.2. Configuration - Arm 2 with and without foam

The idea behind the project of this airframe, was to project a sound absorbing or attenuator equipment to reduce the tonal noise produced by the rotor-airframe interaction. Komkin concluded in his work that for resonator installed at the end of a duct resulted in four sound absorption factors, the viscous losses at the wall of the resonator front wall, neck and its edges and the thermal loss at the wall of the resonator. Taking this into consideration, it was decided to design a perforated airframe, where its design was based using a coefficient of absorption to simulate a Helmholtz resonator and another one with an acoustic foam in its interior as a silencer or sound absorbent. It's a fact the airframe is not a duct, but if the coefficient of absorption is projected correctly and matched with the rotors frequency it is a possibility to attenuate any type o noise.

As a result with the considerations before, two airframes where manufactured. The first one, Arm 2 (w/o FOAM), which follows the Helmholtz Resonator's principle shown in (Figure 15). The properties considered for this project where (neck diameter, length, camera volume, etc), used to calculate the coefficient of absorption as referenced in the (Appendix F).

Figure 15 – Arm 2 (w/o FOAM)¹⁴ (Annex A)



¹⁴ Source: <https://rotoriousfpv.com/product/obsidian-wasp/>

As for the second arm, it was aim to design a sound absorbing equipment by perforating the top surface of the airframe and inserting acoustic foam in its interior as represented in Figure X. As explained in the theoretical foundations, acoustic foams serve as an ample attenuator of sound dissipating energy and reducing noise given its irregular shape.

Figure 16 – Arm 2 (with FOAM)¹⁵ (Annex A)



To acquire this work data a setup had to be arranged in order to produce a similar, quiet and safe environment for the drone's partial set operation. As mentioned before, only one airframe and rotor of an FlameWheel 450 was used for a better understating of the noise produced by only one set. Therefore, in this section first is going to be present every group of equipments used and the step by step of mounting the experiments set up and the acquisition of the data.

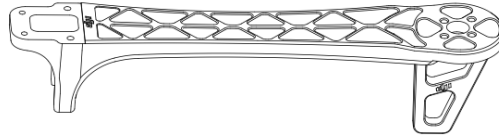
4.2. Operational equipment

The individual set of the FlameWheel 450 was constituted by the following components as shown in Table 1,

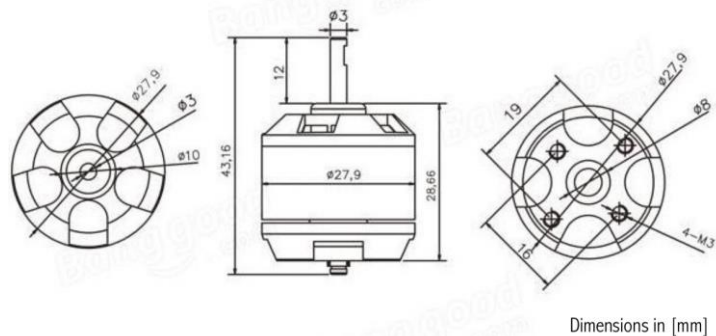
¹⁵ Source: <https://rotoriousfpv.com/product/obsidian-wasp/>

Table 1 – FlameWheel 450 experimental set

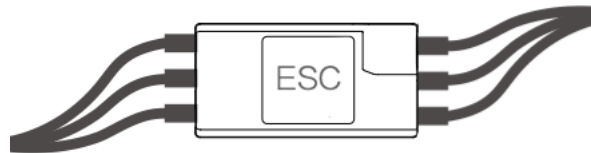
Frame Arm 450FAC



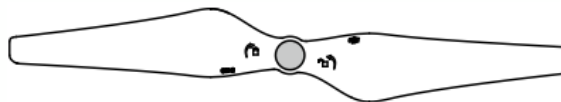
Brushless motor EMAX XA2212 1400 Kv



ESC Simonk EMAX 30 A



HQ Propeller 8'x 4'.5


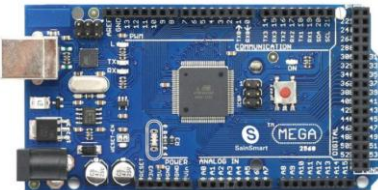


All this equipment's specifications can be found in the Appendix D. As for the power supply, instead of using the drone default battery it was decided to use a ATX Power Source 500W (PN – BLU 500R-B), shown in Annex E, to maintain a constant energy supply and don't depend on the capacity and durability of a battery.

4.3. Data Acquisition Equipment

Considering this research is about acquiring acoustic data to analyze a possible solution for noise reduction in the rotor-airframe interaction, this sub-section is essential. Equipment for this type of analyzes need to be precise and are very sensible to background effects because of which special considerations need to be acknowledge. The equipment used, are presented in the next Table 2,

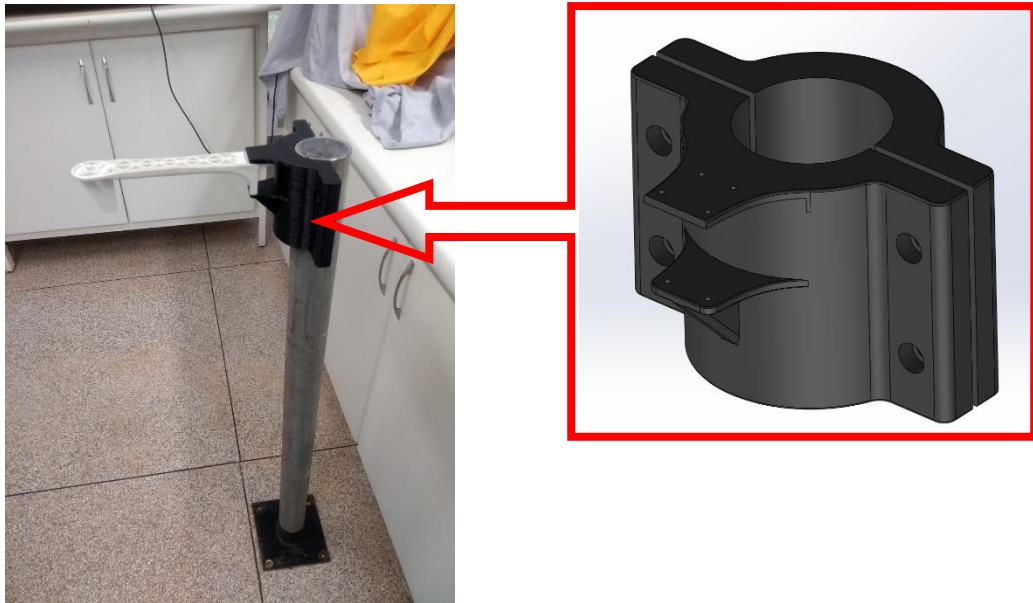
Table 2 – Data Acquisition Equipment

<p>DeltaTron Pressure-field 1/4” Microphone Type 4944B</p>	<p>National Instrument® NI 9162 USB Carrier / NI 9233</p>
	
<p>Arduino Mega 2560</p>	<p>DT-2234C+ digital tachometer</p>
	

4.4. Experimental Set Up

To adequately position all the equipment's, to prevent any type of interference or any source of error, a metallic tube-like structure was constructed using consumable material found on the laboratory (Figure 17). To secure the drones frame and rotor at a specific height (1 meter) it was projected and 3D printed a clamp holder structure considering the airframe characteristics to be able to secure it firmly (Figure 17). For more specs of the support and clamp holder see Annex B

Figure 17 – Metallic Support and clamp holder¹⁶



Continuing electrical connection needed to be performed, but not without some considerations. When connecting the ESC and the motor, before welding them, it is important to verify if the rotation of the propeller considering the thrust needs to be directed downward. Having this correctly, cables were welded and proceeded to the next step. Considering the study evaluates the interference rotor-airframe it was essential to let the area of interest (upper part of the air frame) as free as possible to prevent having any type of flow interference or turbulence generator. Because of this a cable extension was added between the ESC and the motor of about 0.60 [m] length (for each cable), which allowed cables to be installed beneath the airframe. Continuing on the other end of the ESC, the energy cable was respectively connected with the source of power and the signal acquisition ESC cable was connected in the MEGA 2560, red in channel 2 and black in GND (always respecting the polarity). Last but not least, the MEGA 2560 was connected to the computer where the commands were received from Arduino IDE-Library ESP 8266, code shown in Annex C. To ensure this code precision, a test was performed before the set-up, using the Arduino Uno to determine the motor's RPM in relation to the PWM (or signal from the computer). This

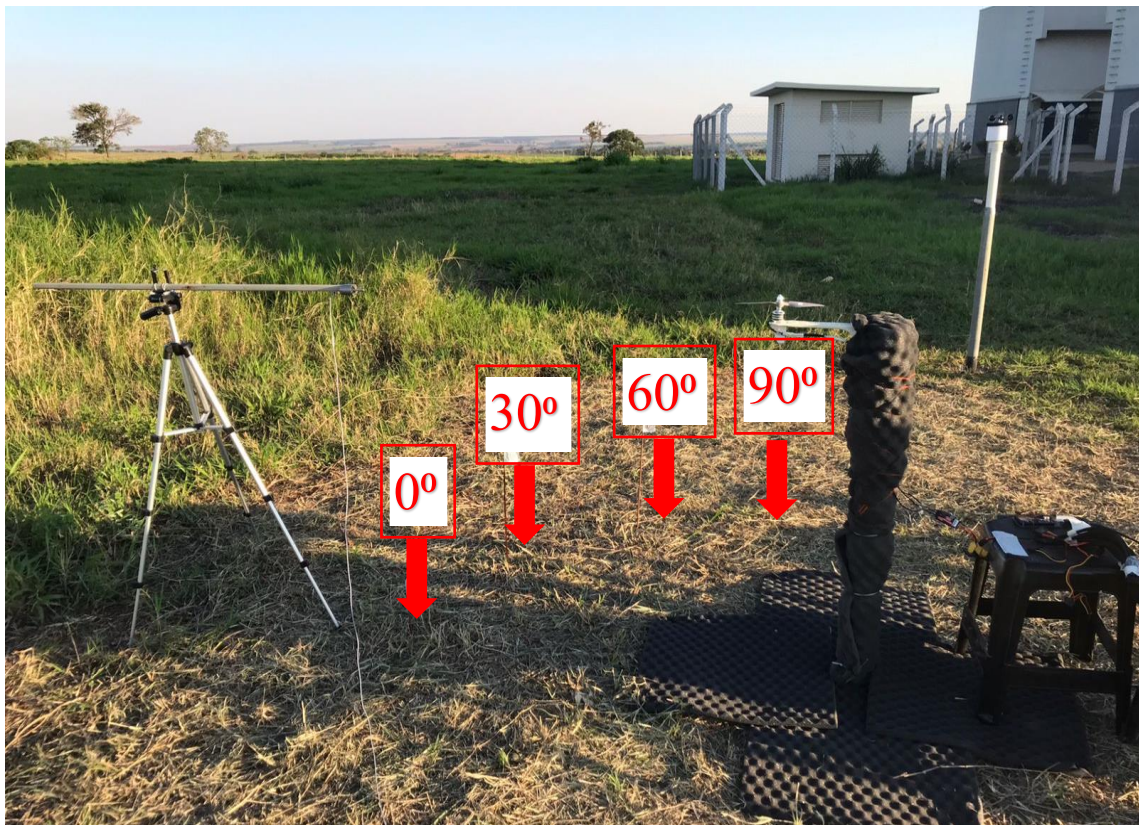
¹⁶ Source: <https://rotoriousfpv.com/product/obsidian-wasp/>

was only to set a parameter/range and obtain a more accurate reading of RPMs during the actual and final test (Annex G).

As a next step, the microphone 4944B was calibrated using the Larson Davis Calibrator Cal 200 by an emitting sound pressure level of 94 DB at 10000 Hz which is received by the microphone and if receive accurately, reliability is ensured. To acquire the data, is necessary to install the NI9162 by connecting it to the microphone and computer by running a code 20 seconds of signal (sound pressure level) are received and processed to graphs expressed in sound intensity, frequency and noise levels.

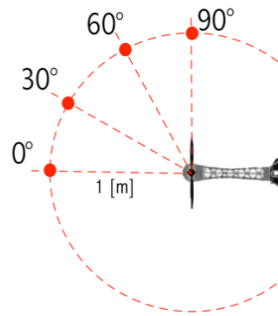
Having finish with the last steps, a mapping of the different angles that sound was measured was conducted, to establish where is the microphone is going to be positioned (Figure 17 and 18). This mapping was executed to try and identify if there is any difference of noise level according to angle. Several studies discuss the concept that noise level is the highest when measured a 45-degree angle [20].

Figure 17 – Angle mapping referenced in the motor center¹⁷



¹⁷ Source: <https://rotoriousfpv.com/product/obsidian-wasp/>

Figure 18 – Angle mapping¹⁸



Last but not least, a weather station was set up to collect some weather conditions during the experiment. Wind speed is considered to be an important factor for the microphone to be reliable, this is the reason measurements were taken after dawn so wind speed would be less than 1 [m/s]. As shown in (Figure 18), after finishing the set up the areas were divided as follows: (A) Data processing center, (B) Power supply, (C) Testing set up, (D) Microphone (acquisition system) and (E) Weather station. Another measurement, important to mention, are the coordinates (18°56'43'43"S 48°12'36" W – Uberlandia, MG 940m Elevation) of the local where the test were performed shown in (Annex D) as well as the weather conditions during experiment.

Figure 19 – Areas of the set up¹⁹



¹⁸ Source: Author

¹⁹ Source: Author

Figure 20 – Areas B and C²⁰



Figure 21 – Areas B, C and D²¹



²⁰ Source: Author

²¹ Source: Author

CHAPTER V

5. RESULTS AND DISCUSSION

After processing the data that was gather through the experimental testing for every arm, results were obtain of the measurements of levels of pressure in different angles during the drone's operation. These results are presented through A-weighting plots, as mentioned before, this is a method to filter signals to adapt to the human hearing domain. As expected in an experimental work, possible sources of error were taken in consideration.

For a deeper and better understanding of the results, this chapter was divided in the following section: Establishing background noise and broadband noises produced by the motor, results from every arm configuration and results comparison of every configuration at 4500 rpm.

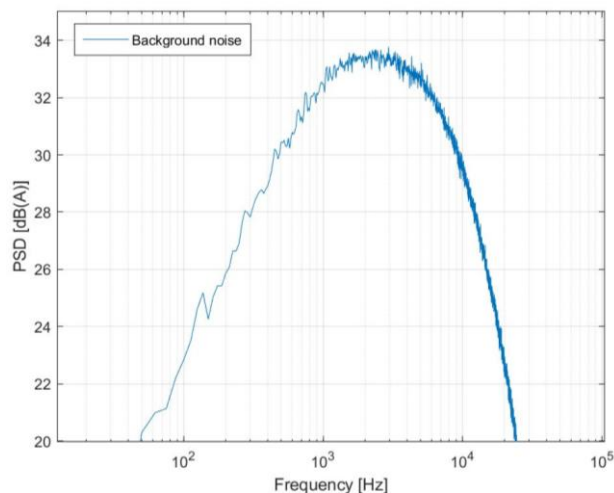
For the figures presented in this chapter, it was assumed the following nomenclature for the identification of each curve:

Microphone data + RPM + angle + type of configuration

5.1. Establishing Background noise of the environment and the motor

Before initiating any test of the configurations, it was measured the background noise experienced in the environment the measurements were performed (Figure 22). This is an important way of establishing a noise reference, considering the test were not performed in an anechoic chamber, meaning an acoustical controlled environment.

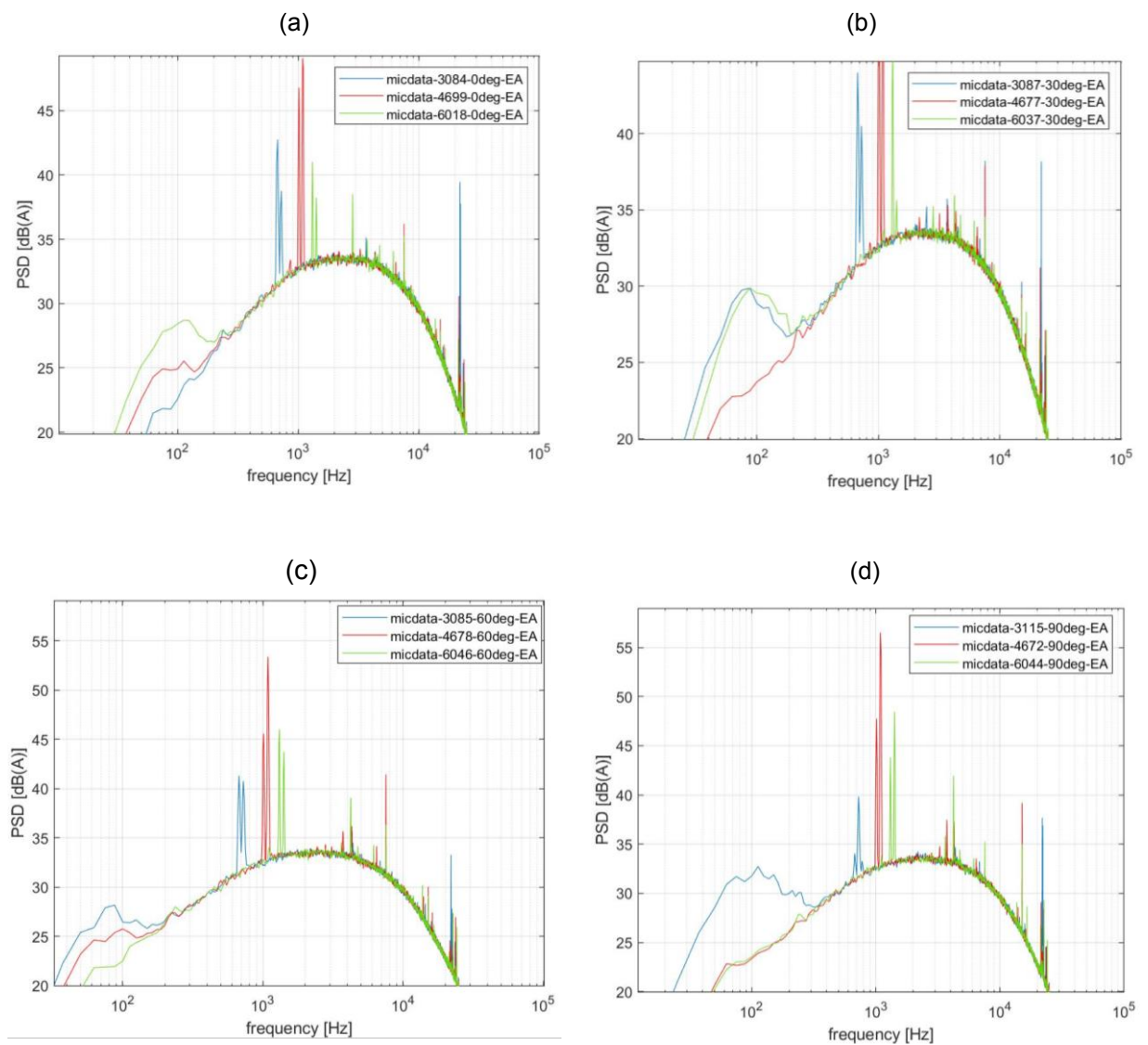
Figure 22 – Background noise curve



As mentioned in [1], ambient or background noise levels at night time are usually below the 35dBA. This confirms that (Figure 22 is coherent giving that test were performed after dawn, where noise and wind conditions are ideal for acoustic measurements.

Following this step, it was measured the level of noise generated by the motor itself (without the rotor). By identifying this noise, it can be identified and isolate it from the next measurements of noise related to the roto-airframe interaction. This data was acquired for four different angles, each angle with three different RPM velocities (Figure 22). It can be observed that the noise was practically equal for each angle.

Figure 23 – Microphone data of motor without rotor at angles (0°, 30°, 60° & 90°)



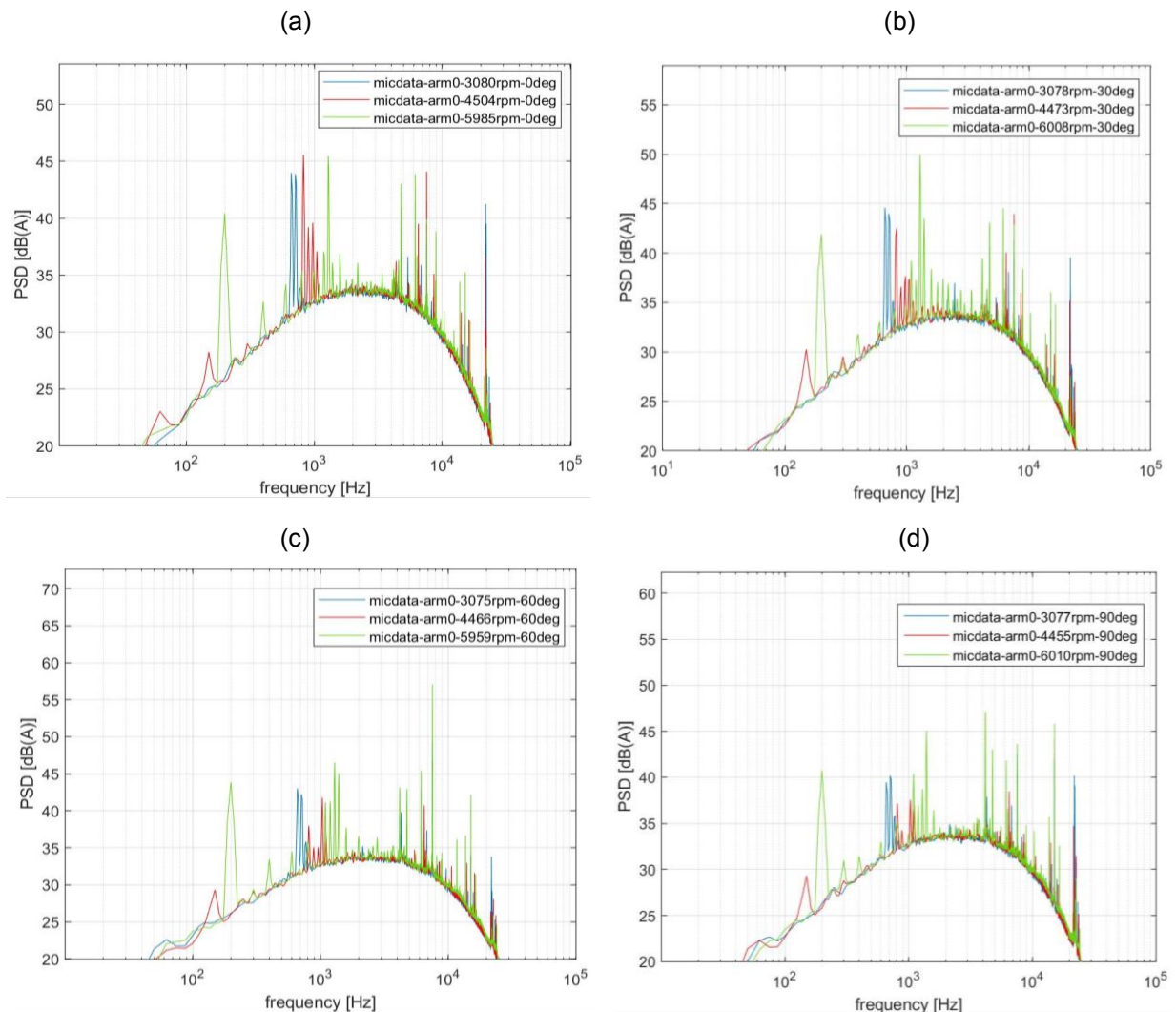
5.2. Analysis of every arm configuration

Having set the ambient and background noise levels, the next step was measuring each arm configuration with four different measuring angles for each. The result obtained did not give a clear perspective of a significant improvement in the noise aspect (Figure 24-26). Along the broadband, the arms appear to have an improvement in both low and high frequencies but this varies depending on the angle of measurement. Considering the interaction rotor-airframe is a very complicated problem to analyze given their high dependence on other aerodynamic factors such as vortex or turbulence.

By analyzing the figures of each arm separately, the A-weighting curve seems coherent and as expected they present a lot of tonal noise peaks in the regions of high frequencies.

5.2.1. ARM 0 – A-Weighting curves

Figure 24 – A-Weighting curves of Arm 0 at angles (0°, 30°, 60° & 90°)

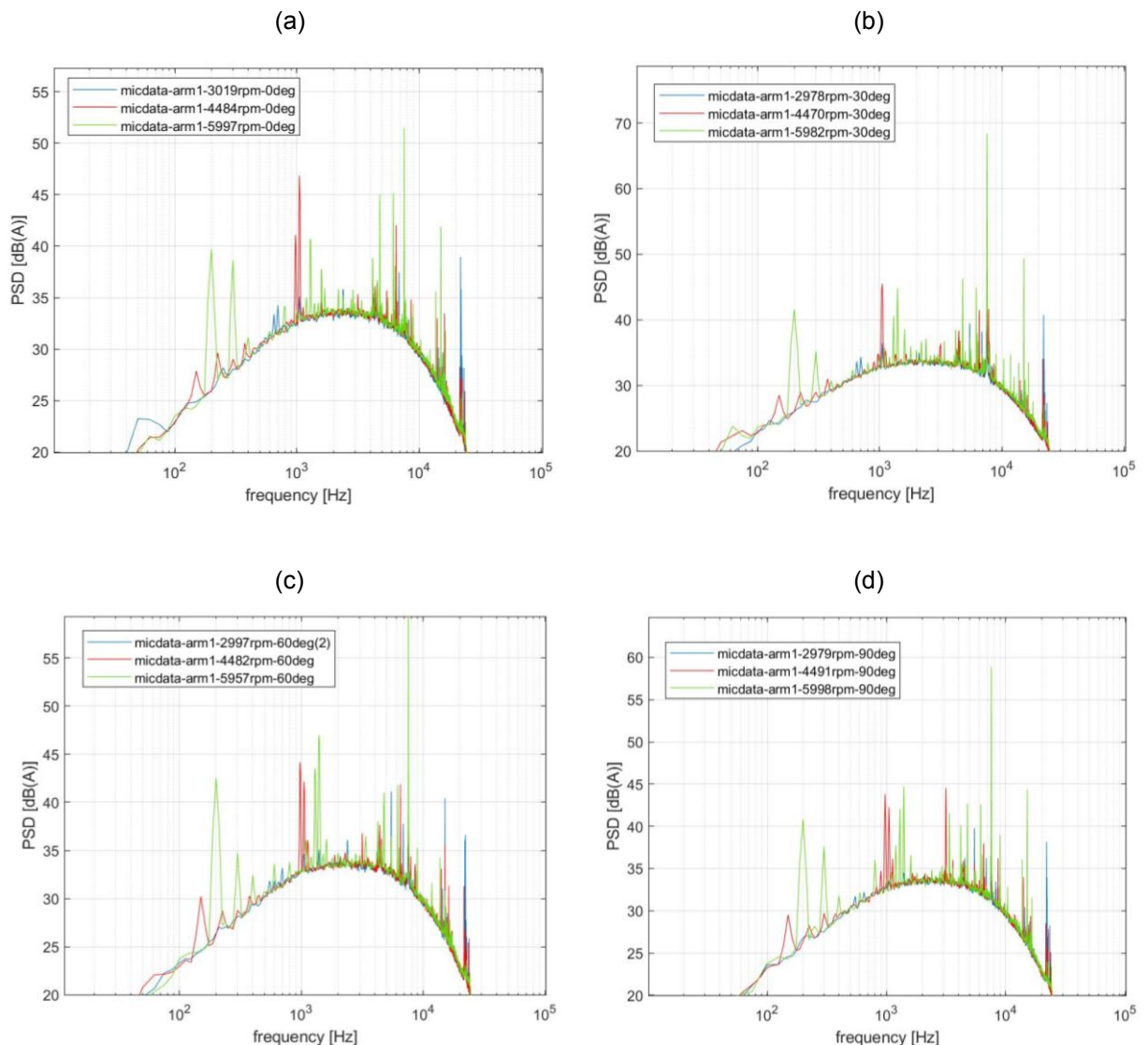


5.2.2. ARM 1 – A-Weighting curves

As for the arm 1, it is perceptively that in some regions there are high energy peaks that are not present on the other arms results. A possible reason for this is because of the shape cross-section of the arm that seem like a drop or an airfoil and may be generate sort of vortex or turbulent residuals that cause this high energy pulses. Even though the distance between the rotor and the arm was increase in this case, improvements may be opaque by some aerodynamic reasons. Another fact was time, the arm didn't go through the smoothening process as planned and may or may not affected in the flow adhering on the surface.

But still the result was not so unsatisfactory, because in some angles the broadband noise was improved and some tonal peaks in low and high frequencies were the same.

Figure 25 – A-Weighting curves of Arm 1 at angles (0°, 30°, 60° & 90°)



5.2.3. Arm 2 (with and without foam) – A-weighting curves

Continuing with arm 2 (with and without Foam), the effect of attenuation or noise reduction appear have match arm 0 results, but didn't improve as much as expected. In these two cases, there were no high energy peaks as in arm 1, but still the concept of the Acoustic foam and the Helmholtz Resonator did not surpass the noise attenuation levels of arm 0. This may have been because of the short time to print and manufacture the parts the precision of the perforations and as for the Arm 2 (w/o Foam) the neck of the perforations where decreased or vary.

By analyzing these figures and comparisons may not show a significant result, but a maybe by calculating the area below each curve or calculating the Overall Sound Pressure Level (OASPL) a more accurate and substantial result of noise attenuation. Which will be considered as future works or continuations of the present work.

Figure 26 – A-Weighting curves of Arm 2 (w/Foam) at angles (0°, 30°, 60° & 90°)

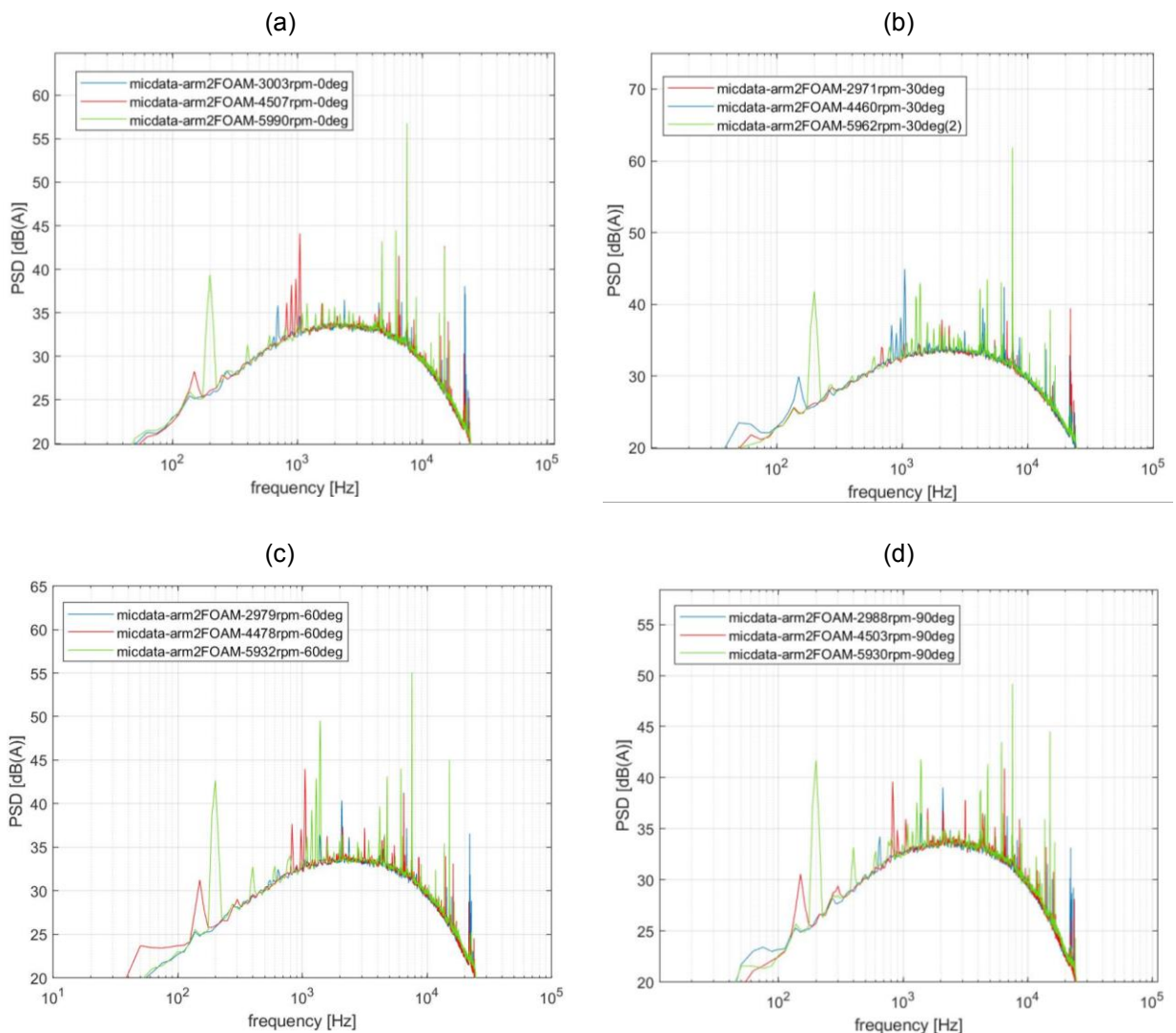
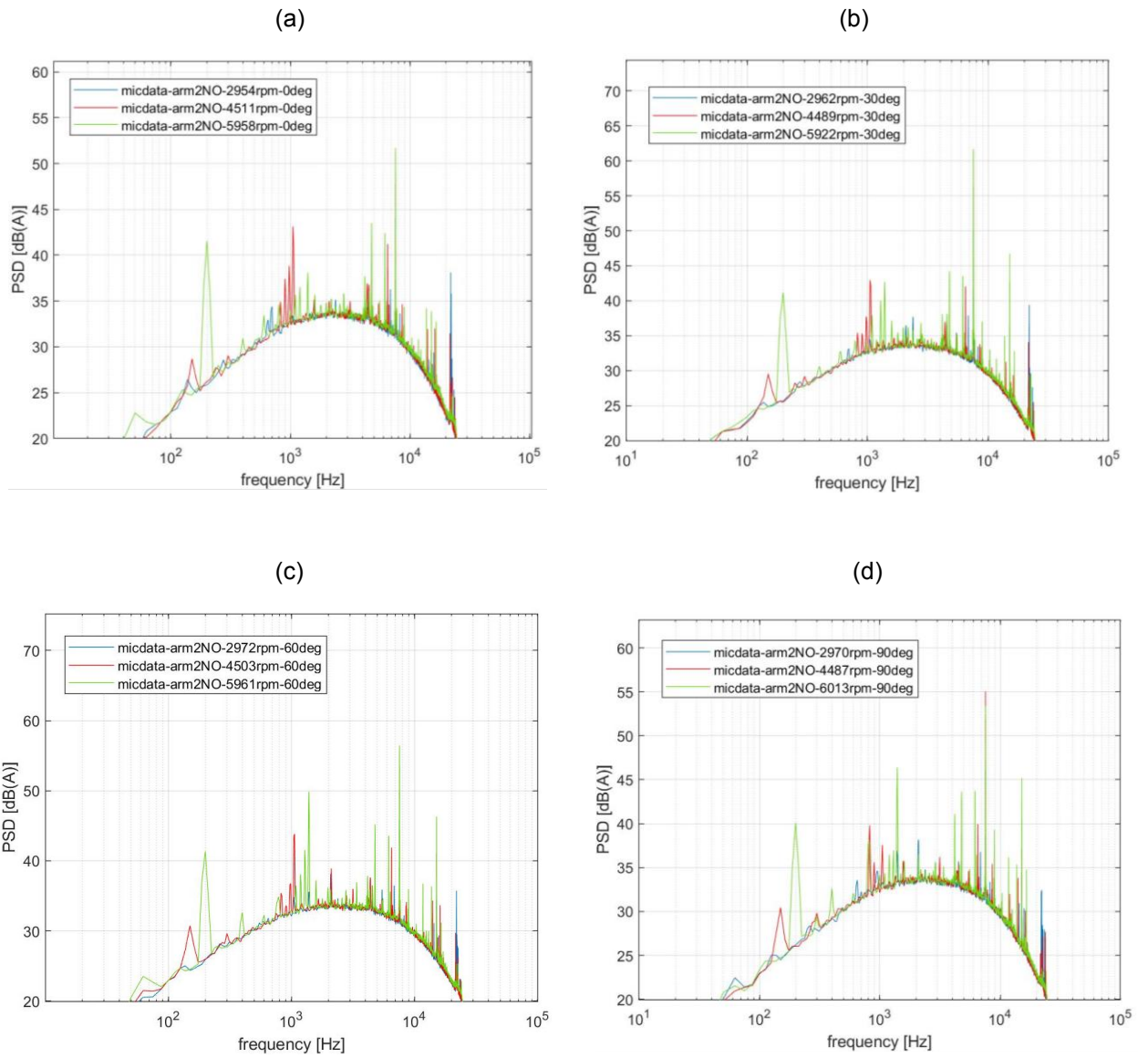


Figure 27 – A-Weighting curves of Arm 2 (w/o Foam) at angles (0°, 30°, 60° & 90°)



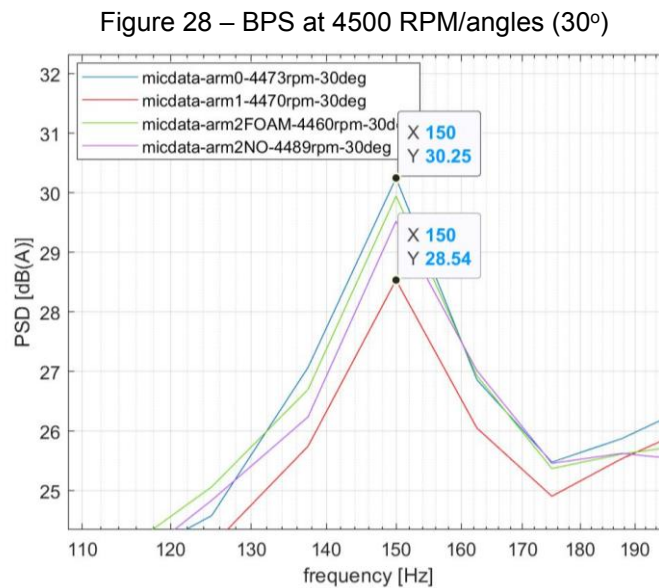
5.3. Comparison between arms results at a 4500 RPM operation

Considering the maximum operation capability of the F450 and using as reference other works [18] and [21] the default velocity to run the test would be of 4500 RPM. Therefore, the comparison of the A-Weighting curves between arms was performed in this velocity.

By observing (Figure 28), it can be notice that the four figures present a common characteristic and this is a peak at lower frequencies that is present in every arm and angle. This frequency can be explained by the concept Blade Pass Frequency (BPF) that is calculated by using the number of blades in the rotor and the RPM in analysis. some of the subjects discussed before like the high energy peaks arm 1 are more evident. This concept is nothing mora than the frequency at which the blades of the rotor pass by a static reference or a fixed position [22]. The BPF is given by the next equation,

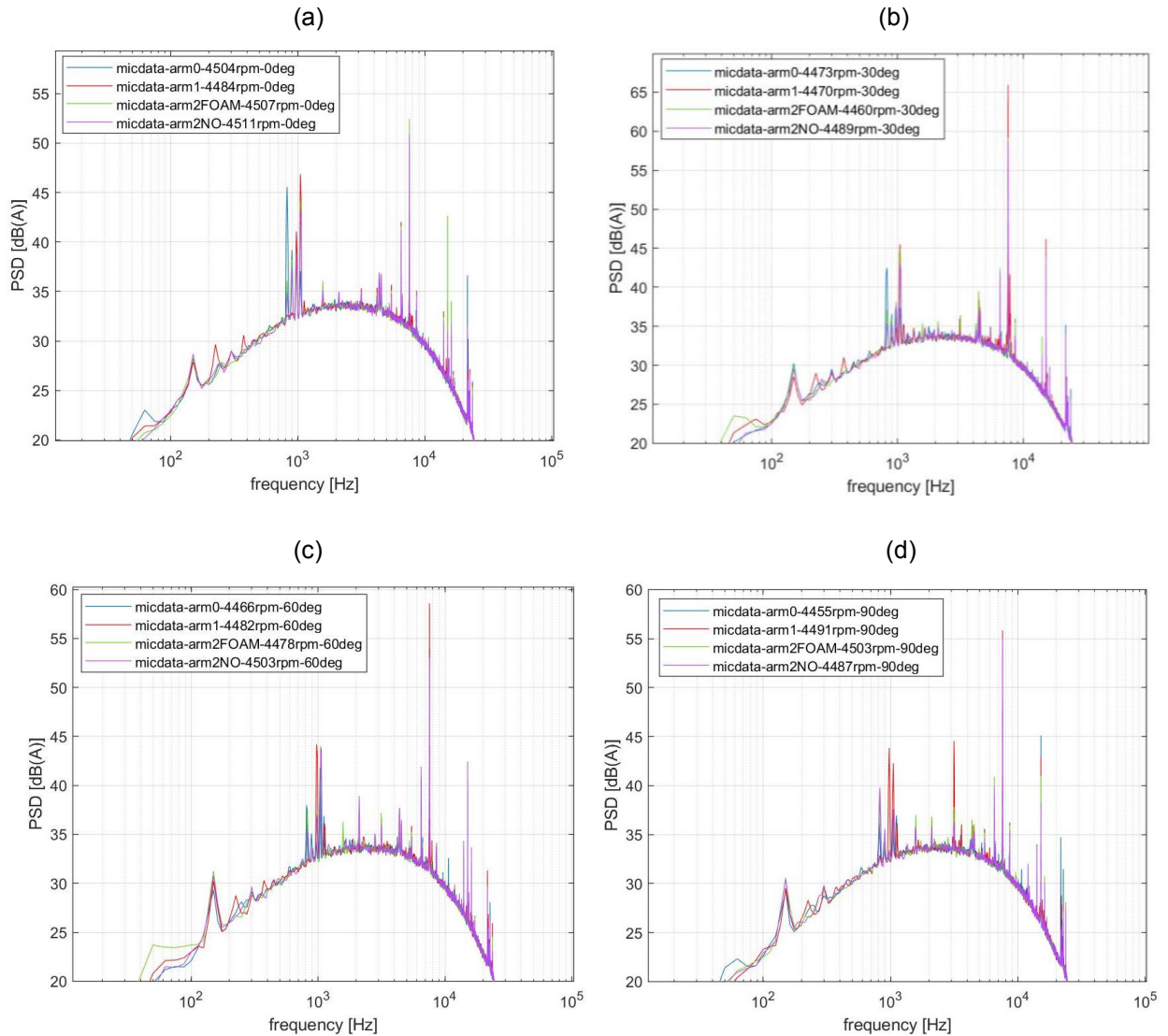
$$BPF = \frac{4500 \text{ (RPM)} \cdot 2 \text{ (blades)}}{60} = 150 \text{ [Hz]} \quad (2)$$

For better understanding, this concept is represented in (Figure 27),



As shown in the figure above, the noise attenuation effect was effective. The maximum noise reduction achieved was by arm 1 and it was a decrease of 1.71dB. For the other angles, the reduction was not significant or didn't even reduce. But again, with a naked eye analysis, it may appear as significant as expected but maybe by calculation the OASPL could be different and more substantial result.

Figure 29 – Comparison of A-Weighting curves of every arm at 4500 RPM/angles (0°, 30°, 60° & 90°)



As mentioned before, it is important to mention diverse sources of error could have affect the result. Starting with the fact that this experiment was performed in an externa area and not in an anechoic camera where conditions can be controlled better. Another source of error could be human error considering the different angles in which the microphone was positioned for each test was not extremely precise and was performed only using the angle mapping. Even though environmental factors were tried to reduce by performing the experiment at dawn and having a weather station, still may have interfered with the microphone sensibility to detect only the necessary signals. Other important factor was the limited time that was dedicated to this research because of factor as the COVID-19 pandemic which limited access to laboratories, leading to less time to manufacture the parts used in this research and other limitations.

6. CONCLUSION

The objective of this study was to conduct acoustical research to find possible way to reduce tonal noise produced by the interaction rotor-airframe. There were projected and manufactured three different airframes of an F450 drone, which was the subject of study. An acoustical acquisition test was performed to measure the different pressure levels or noise experienced in 4 different positions ((0°, 30°, 60° & 90°).

In conclusion to the data and results acquired, the arms projected produced a little noise reduction or attenuation in some low and high frequencies. Arm 1 presented some tonal high energy pulses, which might be because of some aerodynamic effect the arm is experiencing given its shape. Arm 2 (with and without the Foam) did not present this high energy pulses. As mentioned before, given the short time this research was conducted, it was not possible to analyze the aerodynamic behavior of the arms (as planned), it wasn't possible to calculate de OASPL of each curve, which could have given a more conclusive and accurate result.

Beside all this, it can be said that the study was satisfactory, the aeroacoustic area is complex by depending on flow characterization for each problem. Many tests have to be performed before finding breakthrough or just a satisfactory result. An important consideration to be taken of this work, is that an aeroacoustic study need to be done parallel to an aerodynamic study. Because turbulence also generates noise, so it's important to pair both areas to prevent this problem. Even though the arms did not surpass the default arm (arm 0) behavior, they did not present a discrepant behavior. On the contrary the noise A-Weighting curves where relatively close to what was intended in this work and even in high frequencies which is the operation set for a UAV the noise production was coherence and, in some cases, attenuated. As shown in a figure the maximum noise reduction in one of the comparisons was of 1.71 dB, which shows there must be other reduction that must have happened but were not explored or discovered.

For future research, it would be interesting to explore the aerodynamic side of this study, explore more configurations or airframes, different formats, textures, depth of perforations, etc. Also to try and understand better the results of this study, it would be interesting to perform de OASPL calculation and try to perform test in a more controlled environment to confirm the accuracy of these results.

BIBLIOGRAPHICAL REFERENCES

- [1] **“A Not-So-Short History of Unmanned Aerial Vehicles (UAV)”** (2020), By David Daly – Source: <https://consortiq.com/short-history-unmanned-aerial-vehicles-uavs/>
- [2] Insider Intelligence, **“Drone technology uses and applications for commercial, industrial and military drones in 2021 and the future”** Jul 12, 2021. Source: <https://www.businessinsider.com/drone-technology-uses-applications>
- [3] Christian, A. Cabell, Randolph. (2017). **Initial Investigation into the Psychoacoustic Properties of Small Unmanned Aerial System Noise**. NASA Langley Research Center.
- [4] National Geographic Society, Adrea Gabrielli, **“Noise Pollution”**. July 16, 2019. Source: <https://www.nationalgeographic.org/encyclopedia/noise-pollution/>
- [5] Airborne Drones, **“Drone Noise Levels”**. January 13, 2020. Source: <https://www.airbonedrones.co/drone-noise-levels/>
- [6] Zawodny N.S., Boyd D. D , **“ Investigation of Rotor-Airframe Interaction Noise Associated with Small-Scale Rotary-Wing Unmanned Aircraft Systems”** Pages 17, Presented at the AHS 73rd Annual Forum, Fort Worth, Texas, USA, May 11th, 2017.
- [7] Wolfe, J. **“Helmholtz Resonance”**. University New South Wales (UNSW) October 10th, 2003, Source: <https://newt.phys.unsw.edu.au/jw/Helmholtz.html>
- [8] **“Fundamentals of Noise and Sound”**. United States Department of Transportation. Federal Aviation Administration (FAA), July 13, 2020. Source: https://www.faa.gov/regulations_policies/policy_guidance/noise/basics/

- [9] Baeder, J. , Clark, J. , **“Computational Aeroacoustics of Various Propeller Designs for EVTOL applications”** Pages 121, Faculty of the Graduate School of the University of Maryland. Copyright by Bernandine Passe 2019.
- [10] **“Sources of Aviation Noise”**. Helicopter Noise, Noise Quest, 2018. Sources: <https://www.noisequest.psu.edu/sourcesofnoise-helicopternoise.html>
- [11] Morgans A.S., Karabasov S.A, Dowling A.P., and Hynes T.P., (2005) **“Transonic Helicopter Noise”** AIAA Journal, Vol. 43, No.7 (2005), pp. 1512-1524.
- [12] **“Enviromental Technincal Manual”** Procedures of Noise Cetification, International Civil Aviation Organization, Based on Third Edition, Vol I. 2018. Source: <https://www.icao.int/environmental-protection/pages/reduction-of-noise-at-source.aspx>
- [13] **“Noise form New Aircraft concept – Expirience from Brazil”** Enviromental Protection, ICAO Enviroment. Source: [https://www.icao.int/environmental-protection/Pages/noise new concepts brazil.aspx](https://www.icao.int/environmental-protection/Pages/noise%20new%20concepts%20brazil.aspx)
- [14] Huff. D. L. , **“Noise Reduction Technologies for Turbofan Engines”** NASA, Glenn Research Center, Cleveland Ohio. September 2007. Pp. 2-7.
- [15] Metzger, F. (1995). **An Assessment of Propeller Aircraft Noise Reduction Technology.**
- [16] Benoit, M. et al. (2012). Engineering Silence: Active Noise Cancellation. North Carolina State University
- [17] Peixun, Y., Peng, J., Bai, J., Han, X., Song, X., (2019) **“Aeroacoustic and Aerodynamic optimization of propeller blades”** Chinese Journal of Aeronautics, CSAA. Pp. 3-14.
- [18] BESSA, R. F. **Experimental Aeroacoustic Study of Noise Reduction Devices for UAVs.** 2018. 56p. Bachelor’s Thesis, Federal University of Uberlândia, Uberlândia Brazil.

[19] Candelor, P., Pagliaroli, T., Ragni, D., Di Francesco, S., (2019). “**Small-scale rotor aeroacoustics for drone propulsion a review of noise sources and control strategies**”. Universita Niccolo Cusano, Rome, Italy. Source: doi:10.20944/preprints201910.0078.v1

[20] Oleson, R., & Patrick, H. (1998). **Small aircraft propeller noise with ducted propeller**. In 4th AIAA/CEAS Aeroacoustics Conference (p. 2284).

[21] Wang, Z., Henricks, Q., Zhuang, M., (2019) “Impact of Rotor- Airframe Orientation on the Aerodynamic and Aeroacoustic Characteristics of Small Unmanned Aerial Systems”. Ohio State University, OH, USA. Pp. 1-18


[22] Blade pass frequency, (2009) AZIMA-DLI. http://www.azimadli.com/vibman/gloss_bladepassfrequency1.htm#:~:text=Blade%20Pass%20Frequency&text=In%20the%20case%20of%20a,interest%20in%20machine%20vibration%20spectra.

[23] BERG, R. “The Helmholtz resonator”. Britannica. <https://www.britannica.com/science/sound-physics/The-ear-as-spectrum-analyzer>

APPENDIX A – TIMELINE OF UAVs



A Complete History of Unmanned Aerial Vehicles

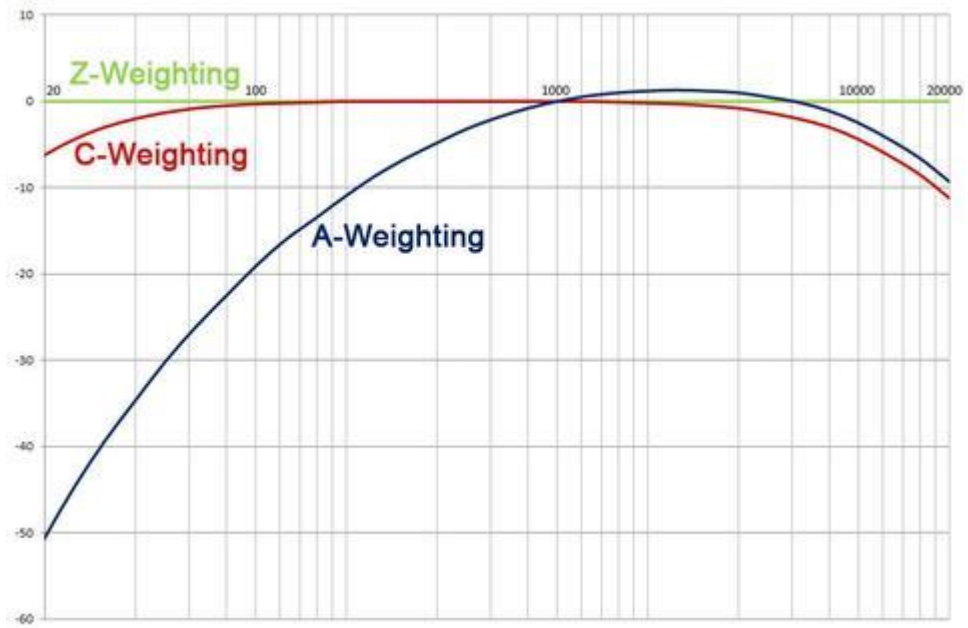
<p>1783 FRANCE</p> <p>First public demonstration of uncrewed aircraft</p> 	<p>1858 FRANCE</p> <p>First aerial photograph is taken</p> 	<p>1898 UNITED STATES</p> <p>Tesla demonstrates the first radio controlled craft</p> 
<p>1849 AUSTRIA</p> <p>Invention of the Balloon Bomb</p> 	<p>1896 SWEDEN</p> <p>First camera on an uncrewed aircraft</p> 	<p>1915 UNITED STATES</p> <p>First aerial reconnaissance photos taken</p> 
<p>1941 UNITED STATES</p> <p>First radio-controlled target plane, 'The Radioplane'</p> 	<p>1936 UNITED STATES</p> <p>U.S. Drone Program begins</p> 	<p>1917 UNITED STATES</p> <p>First UAV 'torpedo', 'The Bug' is invented</p> 
<p>1943 UNITED STATES</p> <p>First First Person View semi-uncrewed aircraft</p> 	<p>1937 UNITED STATES</p> <p>First radio-controlled UAV torpedo is unveiled</p> 	<p>1935 UNITED KINGDOM</p> <p>First low-cost radio-controlled target aircraft</p> 
<p>1973 ISRAEL</p> <p>First UAV designed for surveillance and scouting</p> 	<p>1985 UNITED STATES</p> <p>U.S. significantly scales up drone production</p> 	<p>1991 THE GULF WAR</p> <p>First conflict utilizing UAVs at all times</p> 
<p>1982 ISRAEL</p> <p>First Battlefield uncrewed aircraft</p> 	<p>1986 ISRAEL/UNITED STATES</p> <p>The US and Israel join forces to develop 'The Pioneer'</p> 	<p>1996 UNITED STATES</p> <p>The 'Predator' drone is developed</p> 
<p>2014 WORLDWIDE</p> <p>Rapid growth in the UAV industry begins</p> 	<p>2013 CHINA</p> <p>Camera equipped UAVs enter the consumer market</p> 	<p>2006 UNITED STATES</p> <p>UAVs are first permitted in U.S. civilian airspace</p> 
<p>2019 WORLDWIDE</p> <p>First episode of the Consortiq Podcast 'Unmanned Uncovered'</p> 	<p>2013 WORLDWIDE</p> <p>Major companies investigate drone delivery</p> 	<p>2010 FRANCE</p> <p>First smartphone-controlled quadcopter</p> 

APPENDIX B – Parrot AR Drone Exploited



Source: https://www.researchgate.net/figure/The-ParrotArDrone-20-components-After-Parrot-website_fig1_286926091

APPENDIX C – 'A' FREQUENCY WEIGHTING

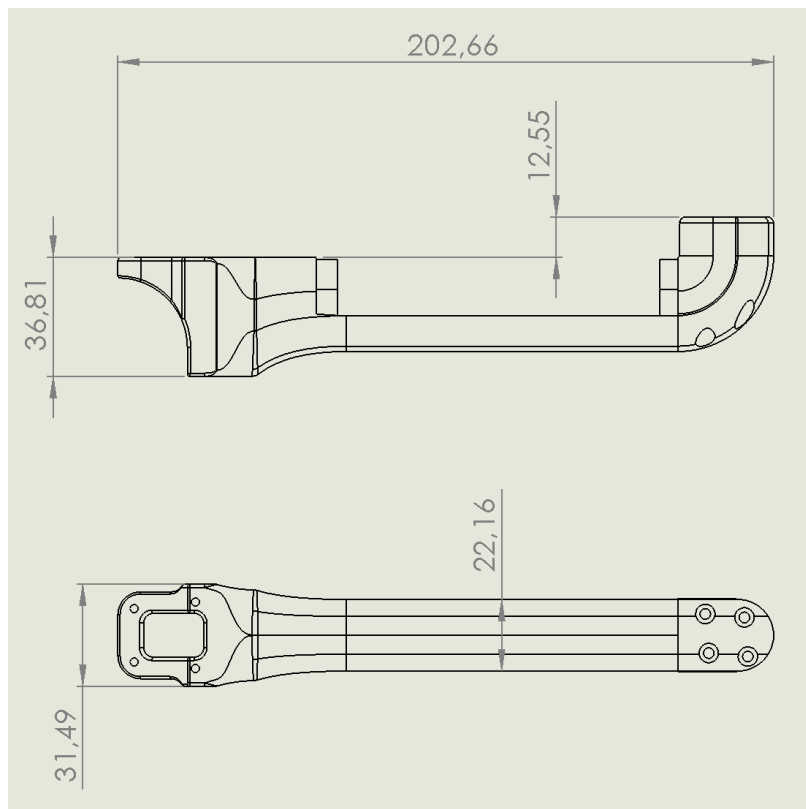
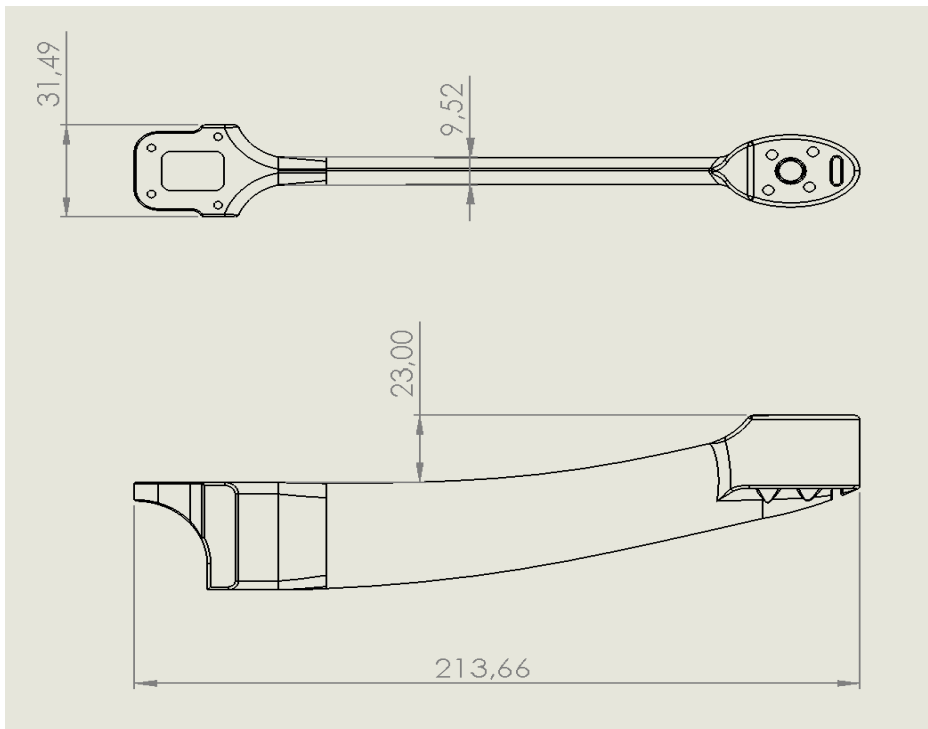


Source: <https://atp-instrumentation.co.uk/blogs/articles/a-c-z-frequency-weightings-explained>

APPENDIX D – XA 2212 MOTOR TEST RECORD

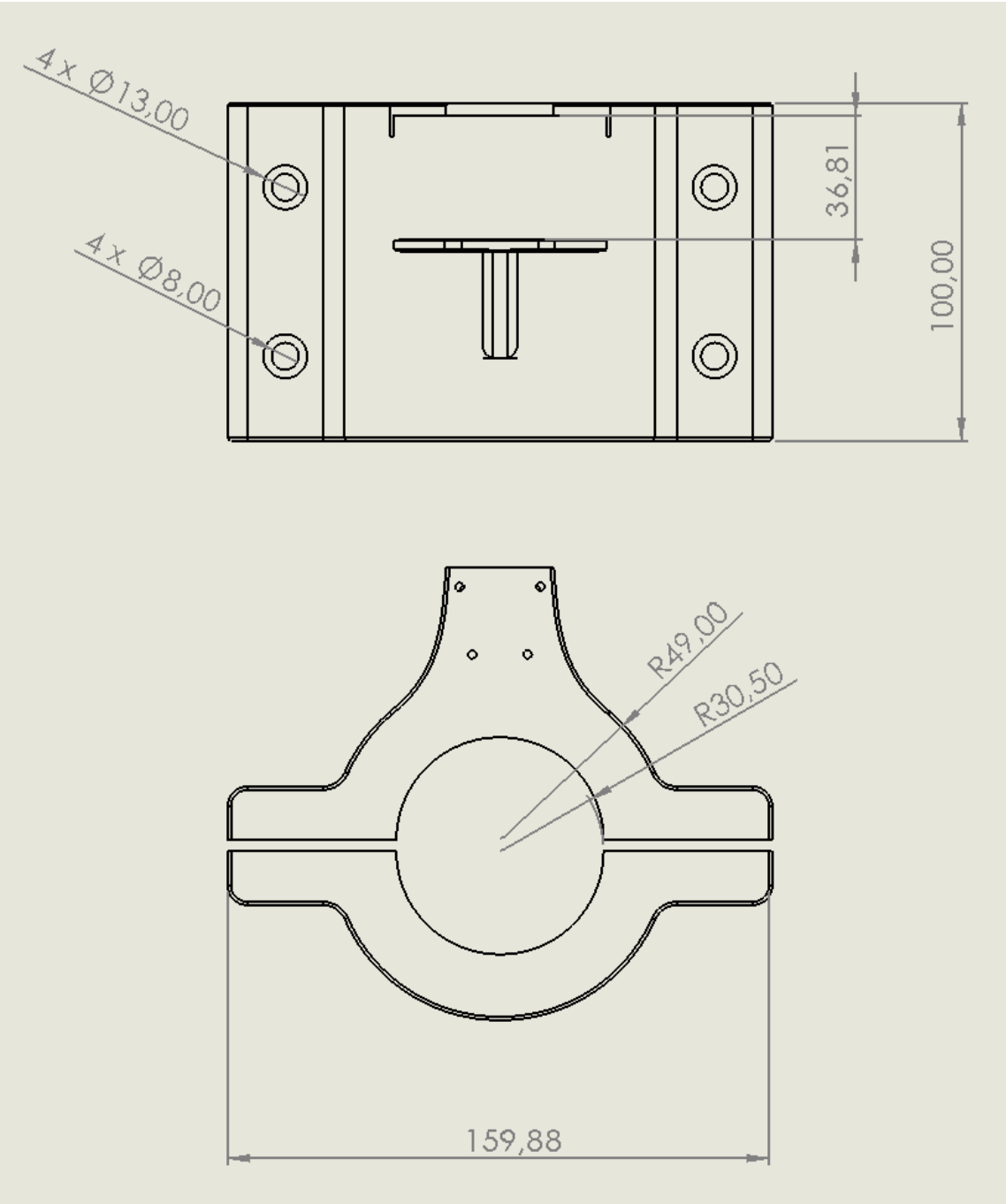
XA 2212 Brushless motor test record							
Motor type	The voltage (V)	Prop. Size	Current (A)	Thrust (G)	Power (W)	Efficiency (G/W)	RPM
XA 2212 820KV	12	APC 11*4.7	12	830	144	5.8	5720
	8	APC 11*4.7	7.3	500	58.4	8.6	4650
XA 2212 980KV	12	APC 10*4.7	15.1	880	181.2	4.9	6960
	8	APC 10*4.7	9.5	550	76	7.2	5470
	12	APC 9*6	12.3	730	147.6	4.9	8220
	8	APC 9*6	7.1	400	56.8	7.0	6090
XA 2212 1400KV	12	APC 8*4	16.4	930	196.8	4.7	12020
	8	APC 8*4	9.1	500	72.8	6.9	8900
	12	APC 8*6	20.6	940	247.2	3.8	10750
	8	APC 8*6	11.9	520	95.2	5.5	8250

ANNEX A – Arm 1 and 2 technical design



Measures in [mm]

ANNEX B – Clamp support technical design



Measures in [mm]


```

        pwm_1=1000;
        Motor2.write (0); //full reverse.
The ESC will automatically brake
the motor.
        pwm_2=1000;
        }
        }

// readSensor();
        printInfo();

while( (millis()- t_k)/1000 < Ta)
    {
        //Wait for the next
        amostragem
    }

}

//-----
// SUBROTINAS
//-----

void saturacao(){

/*Saturaçao da variavel de
comando entre 1000us e 2000us*/
//MOTOR 1 PRETO
if(pwm_1 < 1000)
    {
        pwm_1 = 1000;
    }
if(pwm_1 > 2000)
    {
        pwm_1=2000;
    }

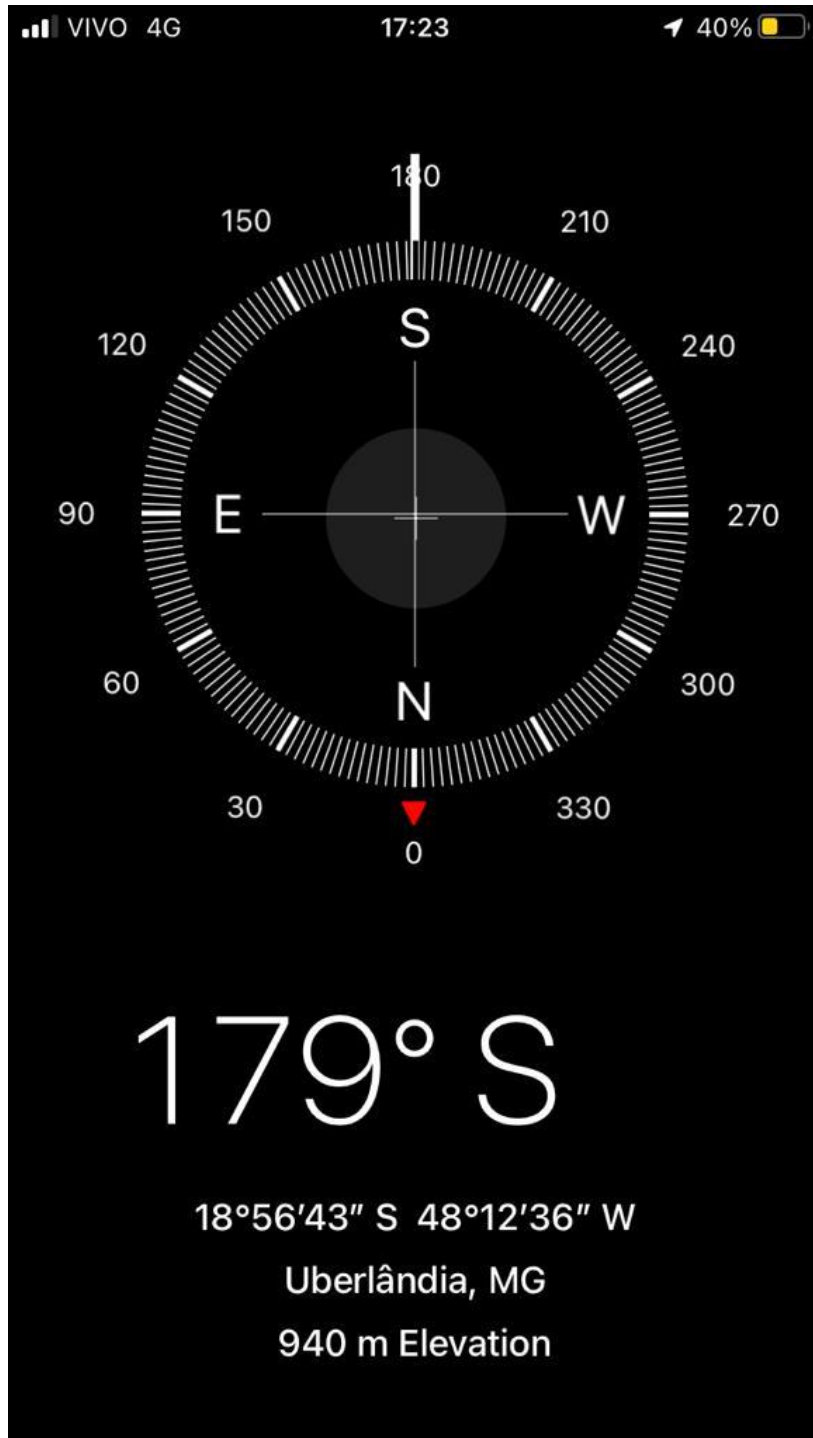
/*Saturaçao da variavel de
comando entre 1000us e 2000us*/
//MOTOR 2 PRETO
if(pwm_2 < 1000)
    {
        pwm_2 = 1000;
    }
if(pwm_2 > 2000)
    {
        pwm_2=2000;
    }
}

        void printInfo(){
//Serial.print((millis()- t_k)/1000,4);
        Serial.print((millis()/1000.00),5);
        Serial.print("\t ");
        Serial.print(pwm_1);
        Serial.print("\t ");
        Serial.print(pwm_2);
        Serial.print("\t ");
        Serial.print(force*9.81/1000);
//multiplicar por 9.81 pra ser em
        Newtons
        Serial.print("\t ");
        Serial.println(((millis()-
        t_k)/1000.00),5);
    }

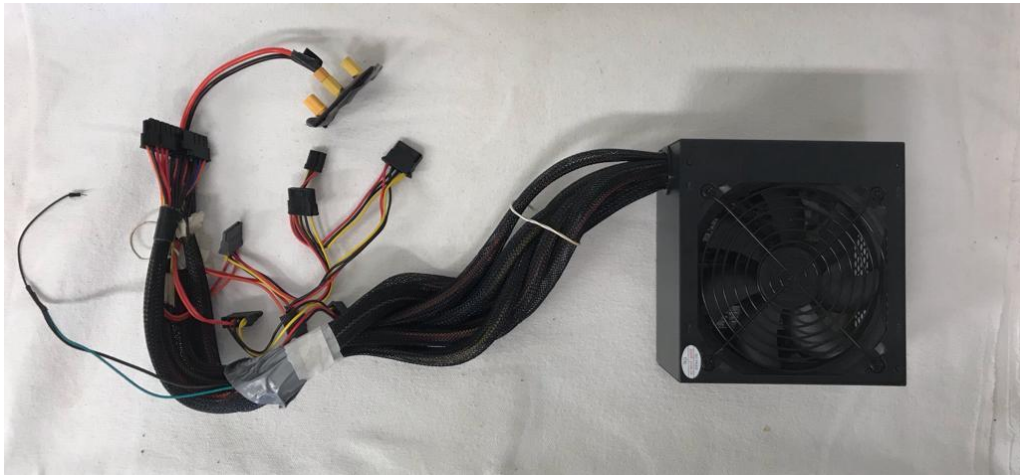
//void readSensor(){
// f_k= scale.get_units(1);
// force = ( (N1)* f_k + (N2) * f_km1
+ (N3) * f_km2 - C2 * ff_km1 - C3 *
        ff_km2 )/(C1);
// f_km2=f_km1;
// f_km1=f_k;
// ff_km2=ff_km1;
// ff_km1=force;
//}

```

ANNEX D – Experimental test's location



ANNEX E – Power source supply



Bluecase Gamer

Power Supply / Fonte ATX
500W
 BLU 500R-B

80 PLUS BRONZE

Part Number:
BLU500R-BCASE

Electrical Specification / Especificação Elétrica:

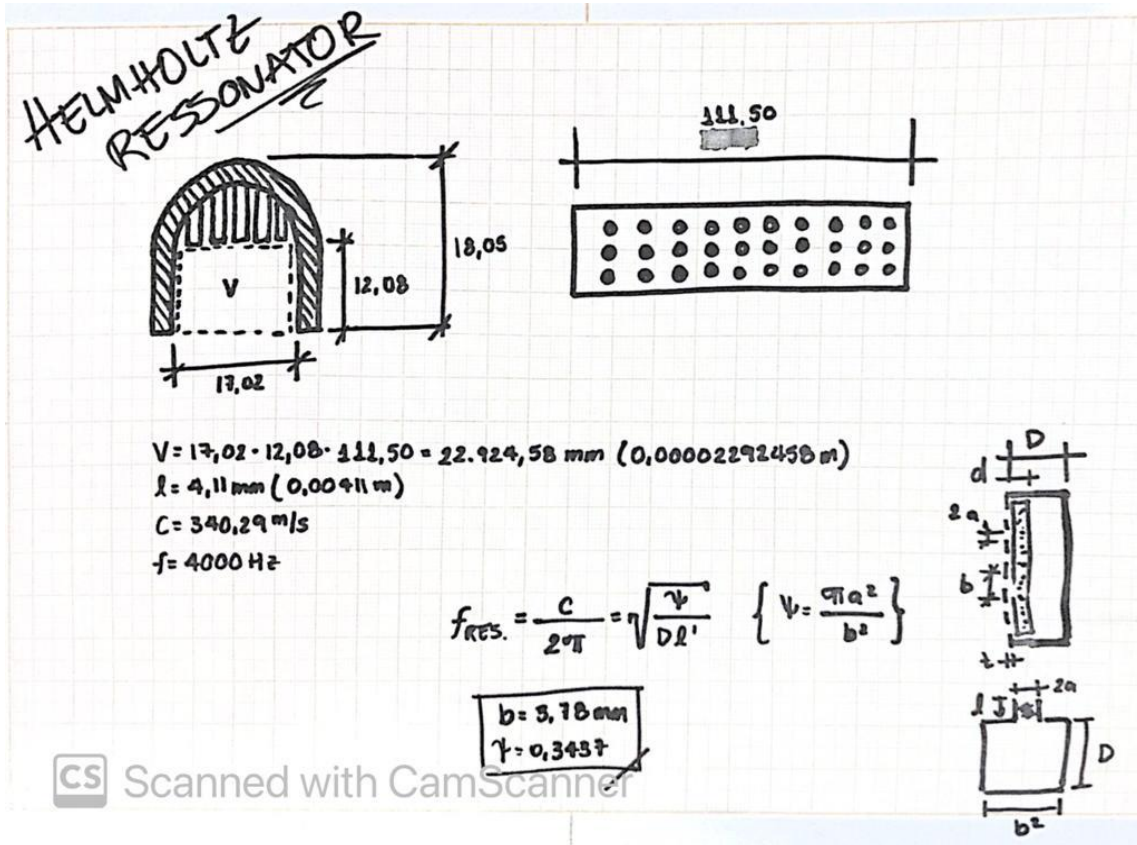
AC Input / Entrada AC:	90V - 264V 47Hz - 63 Hz				
DC Output / Saída DC:	+5V	+3.3V	+12V	-12V	+5VSB
Maximum output current / Corrente máxima de saída:	16A	16A	35A	0.3A	2.5A
Combined load / Corrente combinada:	110W		420W	3.6W	12.5W
Total power / Potência total:	500W				

EAN code / Código EAN:

Serial number / Número de Série:

Made in China / Fabricado na China
 Importado por:
 BLUEVIX COMERCIO E SERVIÇO EIRELI
 CNPJ: 39.272.778/0001-95

ANNEX F – Helmholtz Ressonator calculation memorandum



Measures in [mm]

Memorandum Nomenclature

- f = ressonance frequency
- V = Volume
- l = neck length
- C = speed of sound
- φ = perforation rate
- $2a$ = hole diameter
- b = perforation spacement

ANNEX G – Curves of Calibration during testing

INITIAL	
PWM	RPM
1187	3008
1234	4439
1300	6020

WITHOUT ROTOR	
PWM	RPM
1160	3084
1172	4672
1184	6018

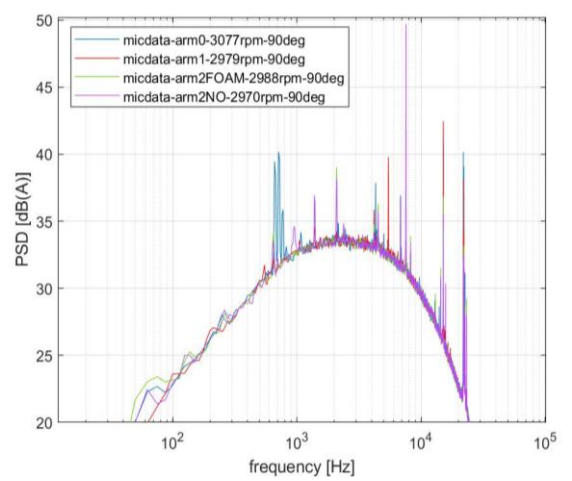
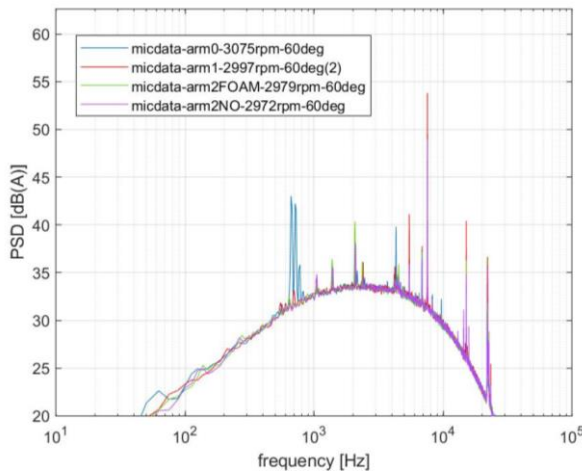
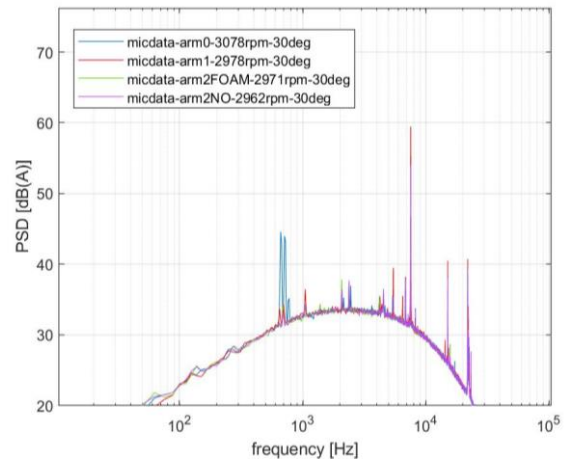
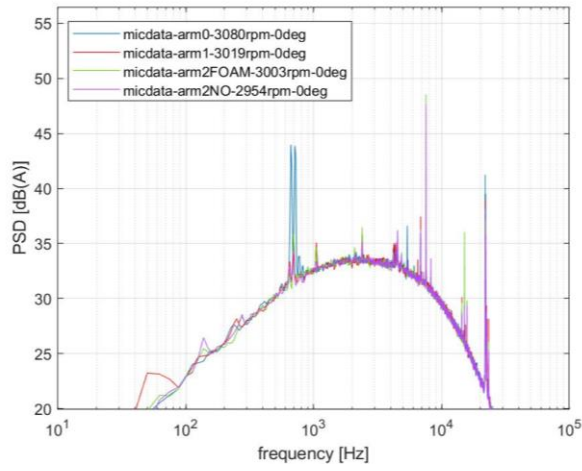
ARM 0	
PWM	RPM
1188	3077
1236	4504
1301	6010

ARM 1	
PWM	RPM
1187	3019
1237	4491
1302	5997

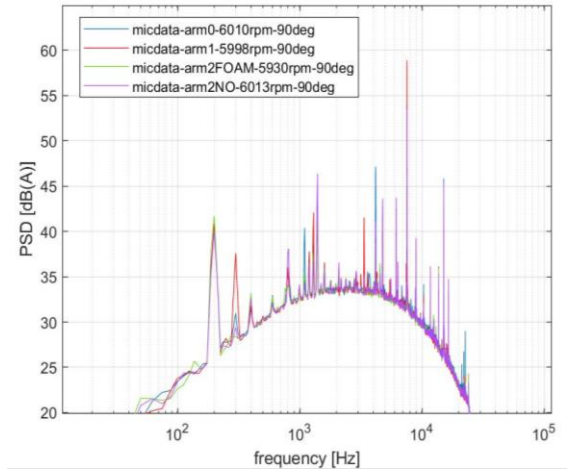
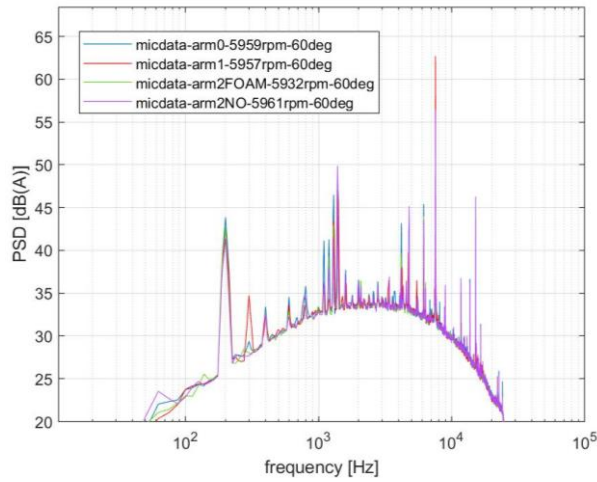
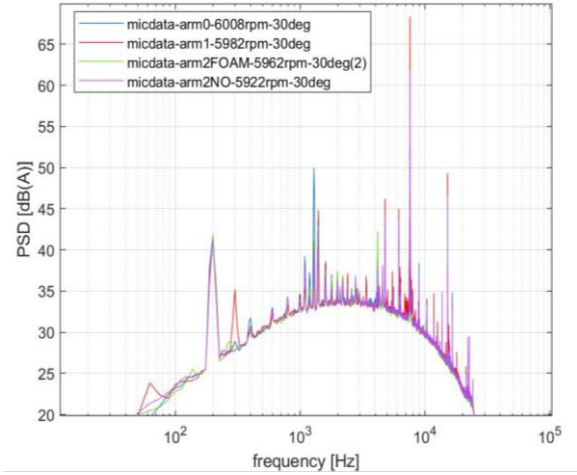
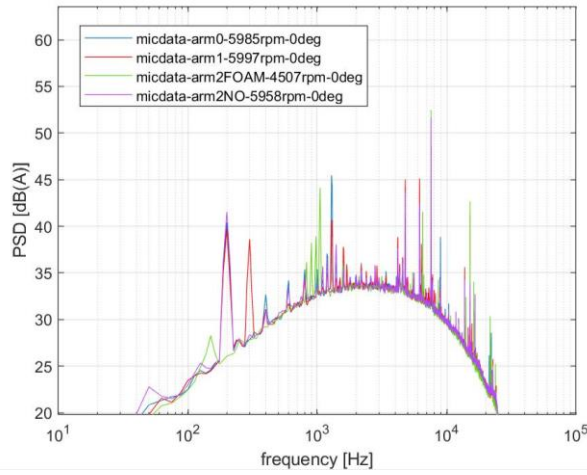
ARM 2 (w/ Foam)	
PWM	RPM
1187	3003
1238	4503
1300	5990

ARM 2 (w/o Foam)	
PWM	RPM
1187	2970
1239	4511
1300	6013

ANNEX H – Comparison of A-Weighting curves of every arm at 3000 RPM/angles (0°, 30°, 60° & 90°)



ANNEX I – Comparison of A-Weighting curves of every arm at 6000 RPM/angles (0°, 30°, 60° & 90°)



PRODUCT DATA

1/4" DeltaTron[®] Pressure-field Microphones — Types 4944-A and 4944-B

Types 4944-A and 4944-B are 1/4" Prepolarized Pressure-field Microphones laser welded to 1/4" DeltaTron preamplifiers.

The preamplifier connects to CCLD input conditioning and supports IEEE P1451.4 V 0.9 TEDS (Transducer Electronic Data Sheet).

USES

- High-level measurements
- High-frequency measurements
- Flush mounting

FEATURES

- Sensitivity: 0.9 mV/Pa
- Frequency: 16 – 70000 Hz
- Dynamic Range: 48 dB(A) – 169 dB
- Temperature: –20 to +100°C (–4 to +212°F)



- TEDS: IEEE P1451.4
- SMB or 10–32 UNF socket
- Connects to CCLD input

Description

Uses of Types 4944-A and 4944-B

A pressure-field microphone is designed to be used in small closed couplers, close to hard reflective surfaces or flush-mounted. The sensitivity has been optimised to allow measurements of high sound pressure levels without clipping in the built-in DeltaTron preamplifier.

Design and Robustness

The shape of the microphone front ensures excellent microphone performance when flush-mounted. The laser-welded diaphragm on the microphone housing ensures that the sensitivity is resistant to rough handling during flush mounting.

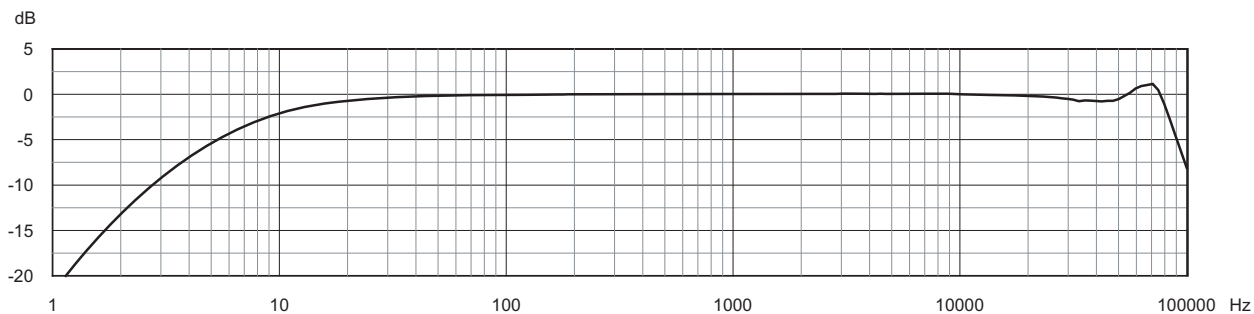
Microphone Data CD

The microphone is supplied with a mini-CD. This mini-CD carries all individual calibration data as well as random-incidence and free-field corrections. The influence of 1/4" Nose Cone UA-0385 is also available.

Calibration

The sensitivity can be calibrated at 250 Hz using Pistonphone Type 4228 with 1/4" Adaptor DP-0775. The pressure-field response can be measured using Actuator UA-0033 with Adaptor DB-0264. The pressure-field response is equal to the actuator response.

Fig. 1 Type 4944-A pressure-field response without grid



090119

Specifications – 1/4" DeltaTron Pressure-field Microphones Type 4944-A and 4944-B

CE Compliance with EMC Directive^a and Low Voltage Directive of the EU
CE Compliance with the EMC requirements of Australia and New Zealand

Typical Uses:

For measurements in confined spaces and small cavities. High-level, high-frequency measurements. Optimised for flush mounting

Nominal Diameter: 1/4"

Sensitivity (250 Hz):

-61 ± 3 dB re 1 V/Pa, 0.9 mV/Pa

Frequency Response^b:

Pressure-field Response 16 Hz to 70 kHz: ± 2 dB

Lower Limiting Frequency (-3 dB):

7 Hz to 9 Hz

Pressure Equalization Vent: Side vented

Diaphragm Resonance Frequency:

60 kHz (90° phase-shift)

Equivalent Air Volume: 0.25 mm³ (250 Hz)

Thermal Noise:

48 dB(A), 58 dB (Lin, 20 - 100 kHz)^a

a. Without conducted RF noise

b. Individually calibrated

Upper Limit of Dynamic Range (3% Distortion): > 169 dB SPL

Maximum Sound Pressure Level:

182 dB (peak)

Power Requirements:

DeltaTron Supply 2 to 20 mA, nom. 4 mA

DC Output Level: 12 V ± 2 V

Max. Output Voltage:

7 V peak for $f \leq 70$ kHz (4 mA supply)

Output Impedance: < 90 Ω, typ. 60 Ω

ENVIRONMENTAL

Operating Temperature Range:

-20 to +100°C (-4 to +212°F)

Storage Temperature:

In case: -25 to +70°C (-13 to +158°F)

With data CD: 5 to 50°C (41 to 122°F)

Temperature Coefficient (250 Hz):

+0.008 dB/°C (-10 to +50°C, 14 to 122°F)

Pressure Coefficient:

-0.003 dB/kPa, typical

Operating Humidity Range:

0 to 90% RH (without condensation)

Influence Of Humidity:

< 0.1 dB in the absence of condensation

Vibration Sensitivity (< 1000 Hz):

69 dB equivalent SPL for 1 m/s²

Magnetic Field Sensitivity:

< 48 dB(A), 58 dB (Lin, 20 - 100 kHz for

80 A/m, 50 Hz field)

Estimated Long-term Stability:

> 1000 years/dB at 20°C (68°F) and dry air

> 40 years/dB at 20°C (68°F) and 90% RH

> 1 year/dB at 50°C (122°F) and 90% RH

DIMENSIONS

Diameter with Grid: 7 mm (0.28")

Diameter without Grid: 6.35 mm (0.25")

Length with Grid: 65 mm (2.56")

Length without Grid: 63.5 mm (2.50")

Output Socket:

4944-A: SMB coaxial socket, male

4944-B: 10-32 UNF socket

Note: All values are typical at 23°C (73.4°F), 101.3 kPa, 50% RH and ≥ 4 mA power supply, unless measurement uncertainty or tolerance field is specified. All uncertainty values are specified at 2σ (i.e., expanded uncertainty using a coverage factor of 2)

Ordering Information

Type 4944-A 1/4" DeltaTron Pressure-field Microphone with SMB socket

Type 4944-B 1/4" DeltaTron Pressure-field Microphone with 10-32 UNF socket

Include the following accessories:

BC-5002 Microphone Data CD^c

c. Quote microphone serial number if re-ordering

Optional Accessories

- Type 4231: Sound Calibrator
- DP-0775: Calibration Adaptor for 1/4" Microphones
- DB-0264: 1/2" to 1/4" Adaptor for UA-0033
- UA-0033: Electrostatic Actuator
- UA-0385: Nose Cone for 1/4" Microphones
- UA-1588: 1/4" Microphone Holder

- AO-0587-D-030: SMB-BNC Cable 3 m (10 ft.)

- ZG-0328: DeltaTron Power Supply (for Brüel & Kjær 7-pin sockets)

Service Products

- 4944-CAF: Accredited Calibration
- 4944-CFF: Factory Standard Calibration (included with delivery)

Brüel & Kjær reserves the right to change specifications and accessories without notice

HEADQUARTERS: DK-2850 Nærum · Denmark · Telephone: +45 4580 0500
 Fax: +45 4580 1405 · www.bksv.com · info@bksv.com

Local representatives and service organisations worldwide





Manual de Instruções

ESTAÇÃO METEOROLÓGICA COM DISPLAY TOUCH SCREEN

(VENTO E PRESSÃO DO AR) ITWH-1080

www.instrutemp.com.br

Sobre este manual

Parabéns por adquirir esta estação meteorológica profissional! Temos certeza que você irá desfrutar de seus benefícios e precisão nas medições climáticas.

Este manual irá guiá-lo passo a passo sobre o ajuste de sua estação ITWH-1080. Leia este manual para se familiarizar com todas as funções deste aparelho, e o mantenha guardado para consultas futuras sempre que necessário.

Glossário de termos comuns

DCF/WWVB/MSF

O sinal DCF WWVB ou MSF é um sinal de tempo ajustado em AM transmitido pelo governo federal da Alemanha, NIST é originário dos Estados Unidos ou Laboratório Nacional de Física. A hora base é gerada por um gerador de tempo atômico cuja precisão é de 10 bilhões por segundo.

LCD

“LCD” significa Display de Cristal Líquido. É um tipo comum de tela utilizado em televisões, computadores, relógios etc.

Barômetro e Pressão Barométrica

Um barômetro é um dispositivo que mede a pressão do ar - esta pressão é chamada de pressão barométrica. Nós geralmente não sentimos a pressão barométrica pois a pressão do ar é igual em todas as direções.

Pressão relativa do ar

Pressão relativa do ar é o mesmo que pressão barométrica. O cálculo da pressão relativa do ar é a combinação da pressão absoluto do ar e a altitude.

Polegadas de Mercúrio (inHg)

Polegadas de mercúrio são unidades de medição da pressão do ar comuns nos Estados Unidos.

Hectopascals (hPa)

Hectopascals são unidades de medição da pressão do ar comuns no Sistema Internacional (SI) de medição.

Nota Importante:

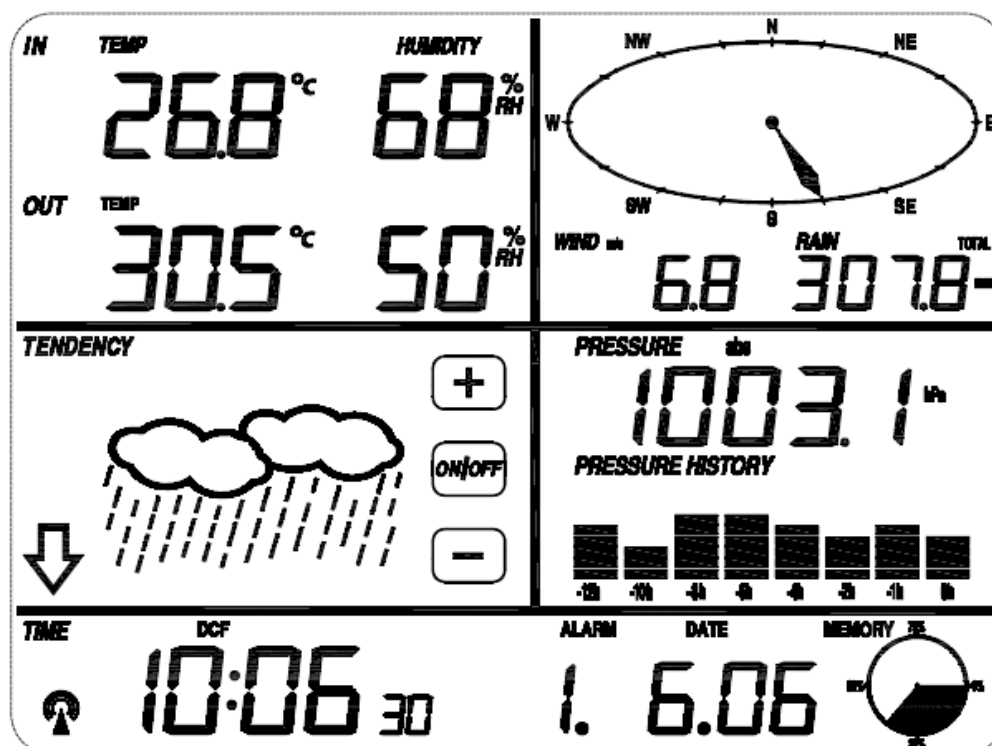
Antes de inserir as baterias, leia cuidadosamente este manual.

Esta estação meteorológica digital Touch Screen ITWH-1080 inclui uma estação base (receptor), uma unidade transmissora, um sensor de direção do vento, um indicador de chuva, cabo USB e software para PC.

A estação base é equipada com um display LCD Touch Screen que permite uma grande variedade de ajustes de tempo e data.

Superior Esquerdo LCD	temperatura de entrada e saída / umidade
Superior Direito LCD	medição de vento e chuva
Meio Esquerdo LCD	previsão do tempo
Meio Direito LCD	Pressão do ar e histórico da pressão
Linha de Fundo	tempo e data, dados armazenados

Nota: o sinal de “alarme ativado” no aparelho indica que o alarme foi ativado.



Esta Estação possui uma função adicional de leitura de todas as medições e dados em um PC.

Notas importantes de funcionamento

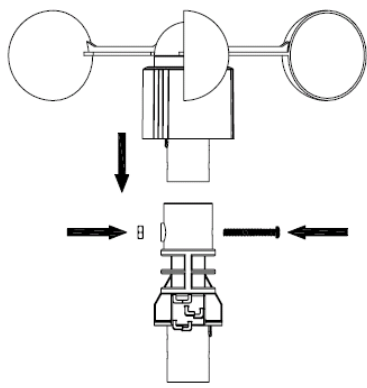
Todas as ações e funções da estação meteorológica são iniciadas através de sensíveis toques no display Touch Screen (não pressione o display!), toque a área selecionada e (+), ON/OFF ou (-) para fazer a seleção desejada ou acrescentar valor.

Toda vez que uma programação for iniciada ao tocar o display, o aparelho emitirá um som e a luz de fundo será ligada por alguns segundos.

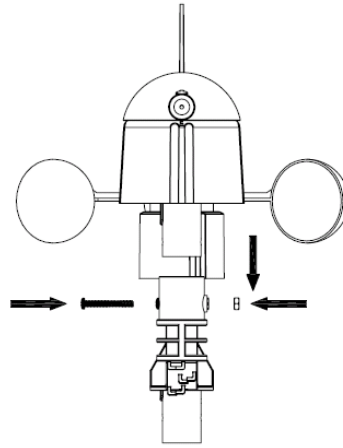
Caso nenhuma área seja pressionada por 30 segundos, o display retornará automaticamente para o modo normal.

Iniciando

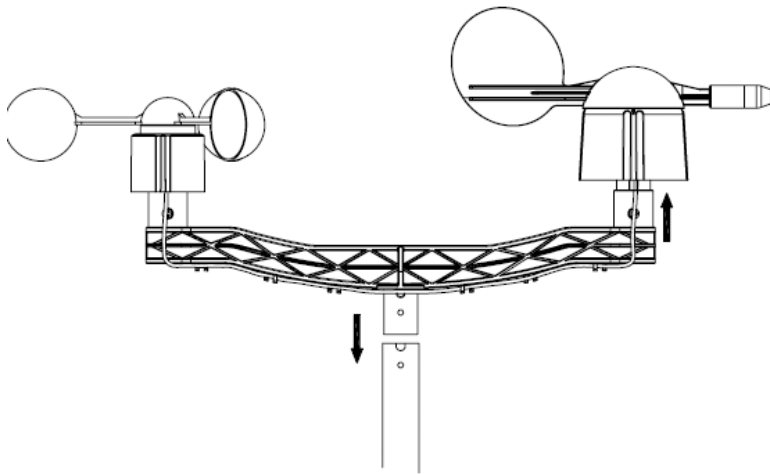
Sensores de ajuste



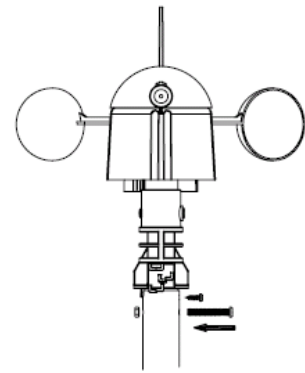
1

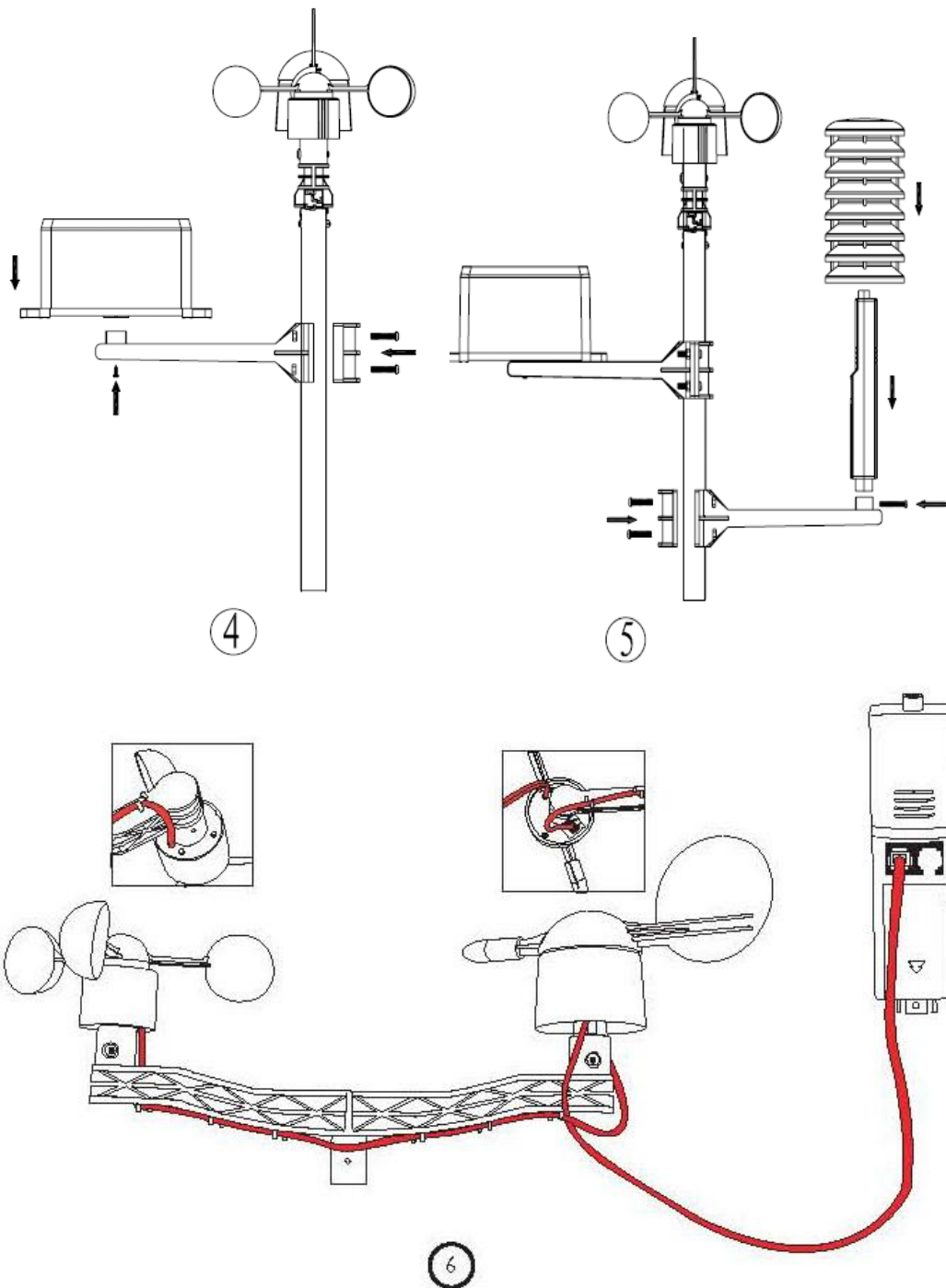


2

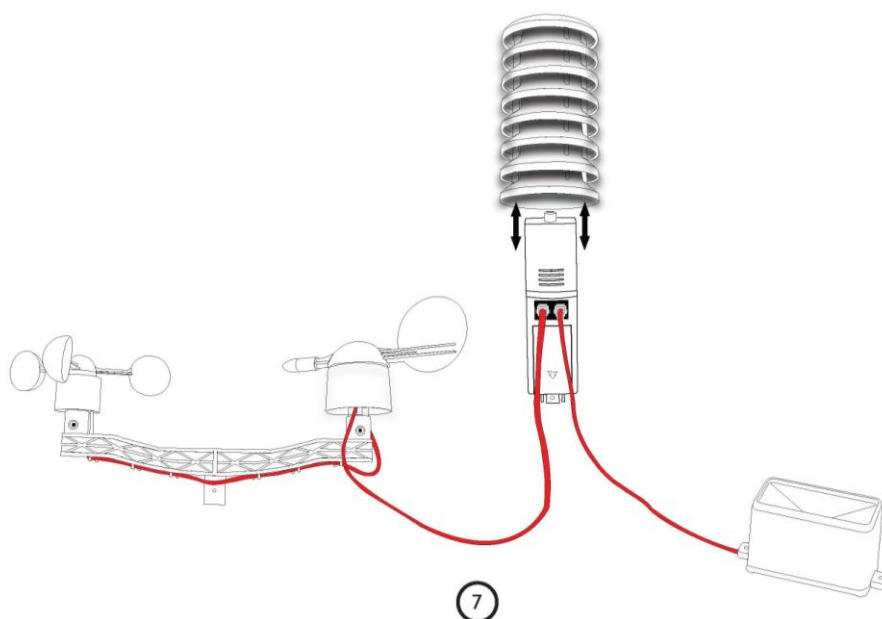


3

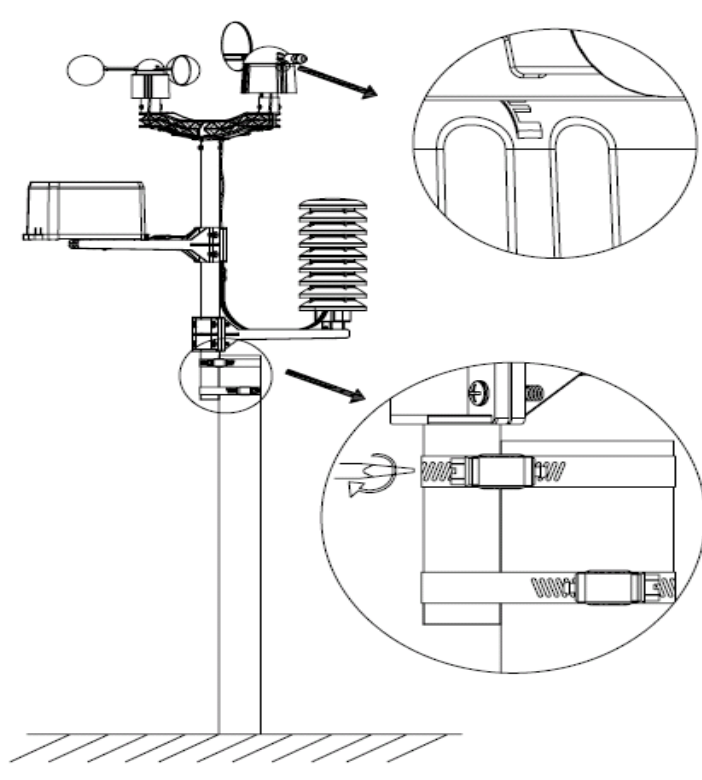




O cabo do indicador de vento é conectado à entrada do sensor de direção do vento.
 O cabo do sensor de direção do vento é conectado na entrada marcada como **Wind** no sensor do termo-higro.



O cabo do sensor de chuva é conectado à entrada marcada como **RAIN** no sensor do termo-higro.



Notas importantes:

Na borda do sensor de direção do vento, há quatro letras do alfabeto: “N”, “E”, “S” e “W”, que representam as direções: North (norte), East (leste), South (sul) e West (oeste). O sensor de direção do vento deve estar ajustador corretamente para que a

direção apontada seja a correta. Caso o sensor não esteja ajustado corretamente haverá erro permanente na medição de sua direção.

O fio do sensor de velocidade do vento deve ser inserido no sensor de direção do vento.

O fio do sensor de direção do vento deve ser inserido na entrada de telefone localizada no sensor do termo-higro com a identificação marcada “Wind”.

O fio do sensor de chuva deve ser inserido na entrada de telefone localizada no sensor do termo-higro com a identificação marcada “Rain”.

Iniciando o sistema

Insira duas baterias LR6 (pilhas AA) no transmissor, um LED localizado na parte frontal do estojo do transmissor acenderá por 4 segundos, e então desligará. O aparelho está pronto para uso. O transmissor fará uma transmissão de dados e então o rádio receptor iniciará a rotina de recepção. Caso o sinal não seja detectado corretamente, um LED piscará 5 vezes indicando que o sinal não foi encontrado. Quando o sinal for fraco e sua recepção não for possível, o transmissor terminará a transmissão para o rádio em um minuto, e então retornará para o modo normal do aparelho. Quando acontecer uma transmissão de dados, o LED acenderá por 20 ms. Durante o período de recepção do rádio controlado, não haverá transmissão e uma nova transmissão normal somente ocorrerá depois de completada a rotina de recepção. O tempo máximo de recepção do rádio controlado é de 5 minutos.

Após inserir as baterias na estação meteorológica, todos os segmentos do display LCD acenderão por alguns segundos.

Após isto, a estação meteorológica fará a medição inicial e iniciará a registrar a transmissão. (o ícone de recepção do rádio aparecerá no display). Antes de haver recepção de dados externos, não toque o display LCD, caso contrário o sensor externo será desativado logo após o toque no display. Quando registrado uma transmissão externa, a estação meteorológica Touch Screen irá automaticamente para o modo normal e todos os ajustes seguintes poderão ser feitos pelo usuário.

Caso nenhum sinal RCC seja detectado na configuração inicial, o transmissor tentará uma vez a cada hora localizar um sinal RCC até que faça esta localização. Assim que o transmissor localizar o sinal RCC, será transmitido no monitor, e o ícone RCC será

mostrado no display. Caso o monitor não receba o sinal RCC, ou perca o sinal, o ícone RCC não será mostrado.

Nota: A melhor condição para recepção do sinal é durante a noite, entre meia noite e 6:00 horas da manhã, quando há menor interferência atmosférica.

Posicionamento do aparelho

Uma vez que verificado todos os componentes e a estação meteorológica está funcionando, podem-se posicionar os itens em seus lugares permanentes. Antes da montagem permanente, certifique-se que todos os componentes estejam funcionando corretamente e em conjunto. Exemplo: caso haja problemas com o rádio transmissor 868MHz, isto pode ser facilmente corrigido apenas mudando sua localização.

Nota: De modo geral, a localização entre o receptor e o transmissor, considerando um campo aberto, pode ser de até 330 pés, considerando que não existam obstáculos como construções, árvores, veículos, linhas de alta voltagem etc.

Pode ainda haver interferências de sinal de rádio, TV, nestes casos desligue a comunicação de rádio do transmissor. Leve isto em consideração quando escolher os locais fixos para instalação do aparelho.

Ajustes iniciais

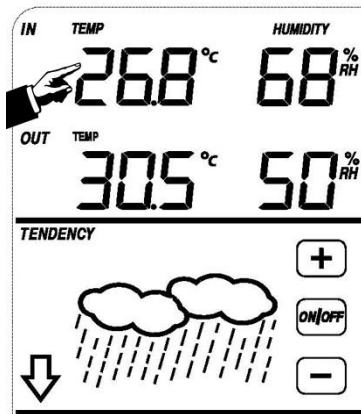
Nota: Os ajustes iniciais são pré-determinados pelo fabricante, e na grande maioria dos casos não é necessário refazer estes ajustes – exceto para obter Pressão Relativa do Ar (veja na seção específica neste manual). Entretanto, alterações nestes ajustes podem ser facilmente realizadas.

Para ajustes básicos, o menu seguinte é iniciado tocando o display Touch Screen na área desejada.

Os ajustes básicos podem ser feitos na ordem a seguir:

Nota: ajustes podem ser interrompidos a qualquer momento apenas pressionando alguma outra área no display (exceto +, - ou ON/OFF).

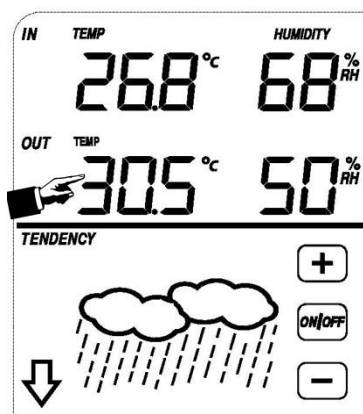
Temperatura Interna



Para ativar o ajuste de temperatura interna:

- 1) Toque a seção INDOOR TEMPERATURE (temperatura interna), os botões + e - piscarão no display. Toque os botões + ou - para selecionar a unidade de temperatura entre °C e °F.
- 2) Toque a seção IN TEMP novamente para ajustar o alarme de alta temperatura, os botões +, - e ON/OFF piscarão no display. o ícone HI AL aparecerá. Toque os botões + ou - para alterar o valor, pressione os botões + ou - por 3 segundos para alterar valores em grande escala. Pressione o botão ON/OFF para ativar ou desativar o alarme (caso o alarme esteja ligado, será mostrado um ícone no display para indicar seu funcionamento).
- 3) Toque a seção IN TEMP pela terceira vez para ajustar o alarme de baixa temperatura, os botões +, - e ON/OFF piscarão no display. o ícone LO AL aparecerá. Toque os botões + ou - para alterar o valor, pressione os botões + ou - por 3 segundos para alterar valores em grande escala. Pressione o botão ON/OFF para ativar ou desativar o alarme (caso o alarme esteja ligado, será mostrado um ícone no display para indicar seu funcionamento).
- 4) Toque a seção IN TEMP pela quarta vez para mostrar o valor máximo de temperatura interna registrado, o valor máximo piscará no display. o ícone MAX será mostrado. Pressione por 3 segundos o valor máximo e o valor no display voltará para o modo de medição normal.
- 5) Toque a seção IN TEMP pela quinta vez para mostrar o valor mínimo de temperatura interna registrado, o valor mínimo piscará no display. o ícone MIN será mostrado. Pressione por 3 segundos o valor mínimo e o valor no display voltará para o modo de medição normal.

Temperatura Externa



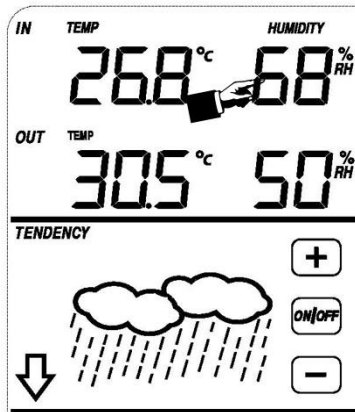
Para ativar o ajuste de temperatura externa:

- 1) Toque a seção OUTDOOR TEMPERATURE (temperatura externa), os botões + e - piscarão no display. Pressione estes botões para alterar entre os modos Temperatura Externa, Vento Frio e Ponto de Orvalho.
- 2) Toque a seção OUT TEMP novamente, os botões + e - piscarão no display. Toque os botões + ou - para selecionar a unidade de temperatura entre °C e °F.
- 3) Toque a seção OUT TEMP pela terceira vez para ajustar o alarme de alta temperatura, os botões +, - e ON/OFF piscarão no display. o ícone HI AL aparecerá. Toque os botões + ou - para alterar o valor, pressione os botões + ou - por 3 segundos para alterar valores em grande escala. Pressione o botão ON/OFF para ativar ou desativar o alarme (caso o alarme esteja ligado, será mostrado um ícone no display para indicar seu funcionamento).
- 4) Toque a seção OUT TEMP pela quarta vez para ajustar o alarme de baixa temperatura, os botões +, - e ON/OFF piscarão no display. o ícone LO AL aparecerá. Toque os botões + ou - para alterar o valor, pressione os botões + ou - por 3 segundos para alterar valores em grande escala. Pressione o botão ON/OFF para ativar ou desativar o alarme (caso o alarme esteja ligado, será mostrado um ícone no display para indicar seu funcionamento).
- 5) Toque a seção OUT TEMP pela quinta vez para mostrar o valor máximo de temperatura externa registrado, o valor máximo piscará no display. o ícone MAX será mostrado. Pressione por 3 segundos o valor máximo e o valor no display voltará para o modo de medição normal.
- 6) Toque a seção OUT TEMP pela sexta vez para mostrar o valor mínimo de temperatura externa registrado, o valor mínimo piscará no display. o ícone MIN

será mostrado. Pressione por 3 segundos o valor mínimo e o valor no display voltará para o modo de medição normal.

Umidade Interna

Para ativar o ajuste de umidade interna:

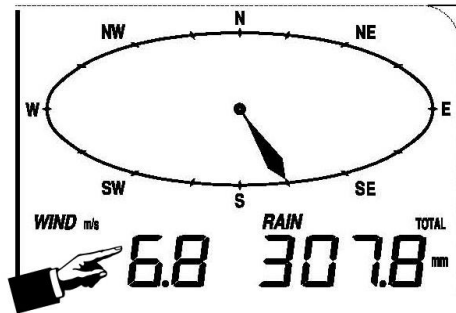


- 1) Toque a seção INDOOR HUMIDITY (umidade interna) para ajustar o alarme de alta umidade interna, os botões +, - e ON/OFF piscarão no display. o ícone HI AL aparecerá. Toque os botões + ou - para alterar o valor, pressione os botões + ou - por 3 segundos para alterar valores em grande escala. Pressione o botão ON/OFF para ativar ou desativar o alarme (caso o alarme esteja ligado, será mostrado um ícone no display para indicar seu funcionamento).
- 2) Toque a seção IN HUMIDITY novamente para ajustar o alarme de baixa umidade interna, os botões +, - e ON/OFF piscarão no display. o ícone LO AL aparecerá. Toque os botões + ou - para alterar o valor, pressione os botões + ou - por 3 segundos para alterar valores em grande escala. Pressione o botão ON/OFF para ativar ou desativar o alarme (caso o alarme esteja ligado, será mostrado um ícone no display para indicar seu funcionamento).
- 3) Toque a seção IN HUMIDITY pela terceira vez para mostrar o valor máximo de umidade interna registrado, o valor máximo piscará no display. o ícone MAX será mostrado. Pressione por 3 segundos o valor máximo e o valor no display voltará para o modo de medição normal.
- 4) Toque a seção IN HUMIDITY pela quarta vez para mostrar o valor mínimo de umidade interna registrado, o valor mínimo piscará no display. o ícone MIN será mostrado. Pressione por 3 segundos o valor mínimo e o valor no display voltará para o modo de medição normal.

Umidade Externa

Procedimentos e ajustes são similares aos ajustes da umidade interna.

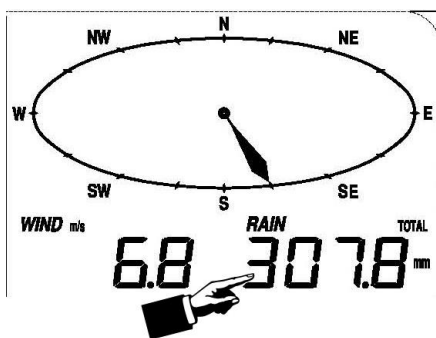
Velocidade do vento



Para ativar o ajuste de velocidade do vento:

- 1) Toque a seção WIND SPEED (velocidade do vento), os botões + e – piscarão no display. Pressione os botões + e – para alterar entre Média de Velocidade do Vento e Velocidade de Rajada do Vento.
- 2) Toque a seção WIND SPEED novamente, os botões + e – piscarão no display. Pressione os botões + e – para selecionar a unidade de velocidade do vento entre km/h, mph, m/s, knots, bft.
- 3) Toque a seção WIND SPEED pela terceira vez para ajustar o alarme de alta velocidade, os botões +, - e ON/OFF piscarão no display. o ícone HI AL aparecerá. Toque os botões + ou – para alterar o valor, pressione os botões + ou – por 3 segundos para alterar valores em grande escala. Pressione o botão ON/OFF para ativar ou desativar o alarme (caso o alarme esteja ligado, será mostrado um ícone no display para indicar seu funcionamento).
- 4) Toque a seção WIND SPEED pela quarta vez para ajustar o alarme a função do alarme de direção do vento. A seta de direção do vento piscará no display. Pressione os botões + e – para selecionar a direção desejada para ativar o alarme, e pressione ON/OFF para ligar ou desligar o alarme.
- 5) Toque a seção WIND SPEED pela quinta vez para visualizar o valor de velocidade máxima mostrado no display, o valor máximo piscará no display. O ícone MAX será mostrado. Pressione por 3 segundos o valor máximo e o valor no display voltará para o modo de medição normal.

Chuva

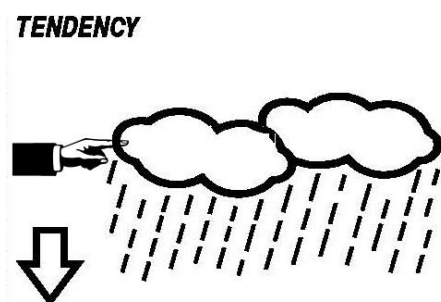


Para ativar o ajuste de chuva:

- 1) Toque a seção RAIN (chuva), os botões + e – piscarão no display. Toque os botões + e – para alterar entre 1h, 24h, semana, mês e chuva total.
- 2) Toque a seção RAIN novamente, os botões + e – piscarão no display. Toque os botões + e – para selecionar a unidade de queda de chuva entre mm e inch.
- 3) Toque a seção RAIN pela terceira vez para ajustar o alarme, os botões +, - e ON/OFF piscarão no display. o ícone HI AL aparecerá. Toque os botões + ou – para alterar o valor, pressione os botões + ou – por 3 segundos para alterar valores em grande escala. Pressione o botão ON/OFF para ativar ou desativar o alarme (caso o alarme esteja ligado, será mostrado um ícone no display para indicar seu funcionamento).
- 4) Toque a seção RAIN pela quarta vez para mostrar o valor máximo de queda de chuva registrado. Pressione a seção RAIN por 3 segundos para apagar o valor máximo e voltar ao valor corrente.
- 5) Toque a seção RAIN pela quinta vez para apagar o valor de chuva para 0, pressionando por 3 segundos, então o valor de 1h, 24h, semana, mês e total de chuva retornará para 0.

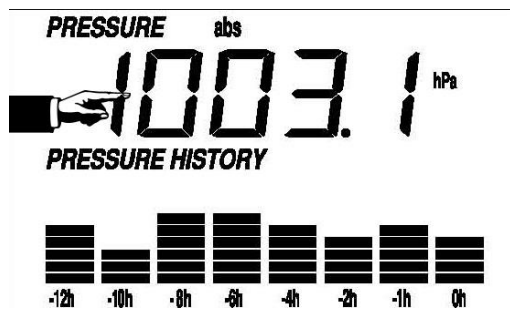
Previsão do tempo

TENDÊNCIA



- 1) Toque a seção WEATHER FORECAST (previsão do tempo), os botões + e – piscarão no display. Toque os botões + e – para alterar entre os ícones SUNNY (ensolarado), PARTLY CLOUDY (parcialmente nublado), CLOUDY (nublado) e RAINY (chuvoso).
- 2) Toque a seção WEATHER FORECAST novamente, os botões + e – piscarão no display. Toque os botões + e – para ajustar a pressão entre 2-4hPa (pré ajuste 2hPa).
- 3) Toque a seção WEATHER FORECAST pela terceira vez, os botões + e – piscarão no display. Toque os botões + e – para ajustar a tempestade entre 3-9hPa (pré ajuste 4hPa).

Pressão



- 1) Toque a seção PRESSURE (pressão), os botões + e – piscarão no display. Toque os botões + e – para alterar entre Pressão Absoluta e Pressão Relativa.
- 2) Toque a seção PRESSURE novamente, os botões + e – piscarão no display. Toque os botões + e – para alterar a unidade entre hPa, inHg e mmHg.
- 3) Toque a seção PRESSURE pela terceira vez para ajustar o valor de Pressão Relativa. Os botões + e – piscarão no display, e o ícone rel aparecerá. Toque os botões + ou – para alterar o valor, pressione os botões + ou – por 3 segundos para alterar valores em grande escala.
- 4) Toque a seção PRESSURE pela quarta vez para ajustar o alarme de alta pressão, os botões +, - e ON/OFF piscarão no display. o ícone HI AL aparecerá. Toque os botões + ou – para alterar o valor, pressione os botões + ou – por 3 segundos para alterar valores em grande escala. Pressione o botão ON/OFF para ativar ou desativar o alarme (caso o alarme esteja ligado, será mostrado um ícone no display para indicar seu funcionamento).
- 5) Toque a seção PRESSURE pela quinta vez para ajustar o alarme de baixa pressão, os botões +, - e ON/OFF piscarão no display. o ícone LO AL aparecerá.

Toque os botões + ou – para alterar o valor, pressione os botões + ou – por 3 segundos para alterar valores em grande escala. Pressione o botão ON/OFF para ativar ou desativar o alarme (caso o alarme esteja ligado, será mostrado um ícone no display para indicar seu funcionamento).

- 6) Toque a seção PRESSURE pela sexta vez para visualizar o valor de pressão máxima mostrado no display, o valor máximo piscará no display. O ícone MAX será mostrado. Pressione por 3 segundos o valor máximo e o valor no display voltará para o modo de medição normal.
- 7) Toque a seção PRESSURE pela sétima vez para mostrar o valor mínimo de pressão registrado, o valor mínimo piscará no display. o ícone MIN será mostrado. Pressione por 3 segundos o valor mínimo e o valor no display voltará para o modo de medição normal.

Nota: quando o modo pressão absoluta for selecionado, a etapa 3 deverá ser pulada.

Barra gráfica de pressão

Toque a seção de Barra gráfica de pressão e então pressione os botões + ou – para alternar a escala da barra gráfica entre 12hrs ou 24hrs, para exibir o histórico da pressão.

Hora



- 1) Toque a seção TIME (hora), os botões + e – piscarão no display. Toque os botões + ou – para ajustar o nível de contraste de 0 a 9 (pré ajustado em 5).
- 2) Toque a seção TIME novamente, os botões + e – piscarão no display. Toque os botões + ou – para ajustar o fuso horário.

Nota: Na Europa, 0 para fuso horário GMT+1, 1 para fuso horário GMT+2, -1 para fuso horário GMT.

Na América, -4 para fuso horário do Atlântico, -5 para fuso horário Oriental, -6 para fuso horário Central, -7 para fuso horário das Montanhas, -8 para fuso horário do Pacífico, -9 para fuso horário do Alaska, -10 para fuso horário do Havai.

- 3) Toque a seção TIME pela terceira vez, os botões + e – piscarão no display. Toque os botões + ou – para ajustar o formato de hora entre 12/24 horas.

- 4) Toque a seção TIME pela quarta vez, os botões + e – piscarão no display. Toque os botões + ou – para ajustar a função DST On ou Off. (esta função está disponível apenas na versão WWWB, enquanto que na versão DCF, esta função não está ativada).

Nota: “DST OFF” indica que esta função está desligada e a hora interna não mudará automaticamente. “DST ON” indica que esta função está ativa e a hora interna mudará automaticamente de acordo com a hora DST ajustada.

- 5) Toque a seção TIME pela quinta vez para ajustar a hora. Os botões + e – piscarão no display. Toque os botões + e – para ajustar os valores.
- 6) Toque a seção TIME pela sexta vez para ajustar os minutos. Os botões + e – piscarão no display. Toque os botões + e – para ajustar os valores.

Data



- 1) Toque a seção DATE (data), os botões + e – piscarão no display. Toque os botões + ou – para alterar entre hora, data e semana.
- 2) Toque a seção DATE novamente, os botões + e – piscarão no display. Toque os botões + ou – para alterar entre os formatos DD-MM e MM-DD.
- 3) Toque a seção DATE pela terceira vez, os botões + e – piscarão no display. Toque os botões + ou – para ajustar o ano. Mantenha pressionado o botão + ou – por 3 segundos para ajustar em grande escala.
- 4) Toque a seção DATE pela quarta vez, os botões + e – piscarão no display. Toque os botões + ou – para ajustar o mês. Mantenha pressionado o botão + ou – por 3 segundos para ajustar em grande escala.
- 5) Toque a seção DATE pela quinta vez, os botões + e – piscarão no display. Toque os botões + ou – para ajustar o dia. Mantenha pressionado o botão + ou – por 3 segundos para ajustar em grande escala.
- 6) Toque a seção DATE pela sexta vez, os botões + e – piscarão no display. Toque os botões + ou – para ajustar a hora do alarme. Mantenha pressionado o botão + ou – por 3 segundos para ajustar em grande escala.

- 7) Toque a seção DATE pela sétima vez, os botões + e – piscarão no display. Toque os botões + ou – para ajustar o minuto do alarme. Mantenha pressionado o botão + ou – por 3 segundos para ajustar em grande escala.

Memória

- 1) Toque a seção Memória (Memory) para mostrar o histórico de dados armazenados no display, os botões + e – piscarão no display. Pressione – para visualizar os dados mais recentes, e + para visualizar os dados mais antigos. Quando um dado é mostrado, aparecerá sua data correspondente. O intervalo do histórico de dados salvos apenas pode ser alterado no PC, através do software que acompanha este produto, o intervalo pré ajustado de histórico de dados é de 30 minutos.
- 2) Toque a seção Memória novamente para iniciar o procedimento de limpeza da memória: a palavra “CLEAR” piscará no display. o ícone de memória cheia aparecerá no display, pressione este ícone por 3 segundos para limpar a memória do aparelho.

Conexão com PC

Como uma importante função para análise e visualização de todos os dados de medição e leitura, este aparelho possui software que possibilita a leitura completa de seus dados em PC.

Armazenamento de Dados

Para efeito de histórico, esta estação meteorológica permite armazenagem interna de até 4080 medições incluindo a hora e data. Esta estação perderá todos os dados caso haja uma interrupção em seu fornecimento de energia. Caso a capacidade de memória se esgote, esta estação armazenará dados novos sobrescrevendo os mais antigos.

Recuperando Dados

Os dados das medições e ajustes dos valores podem ser processados e mostrados em um PC. Também os ajustes dos intervalos de 5 minutos a 240 minutos dos dados armazenados podem ser lidos e ajustados no PC.

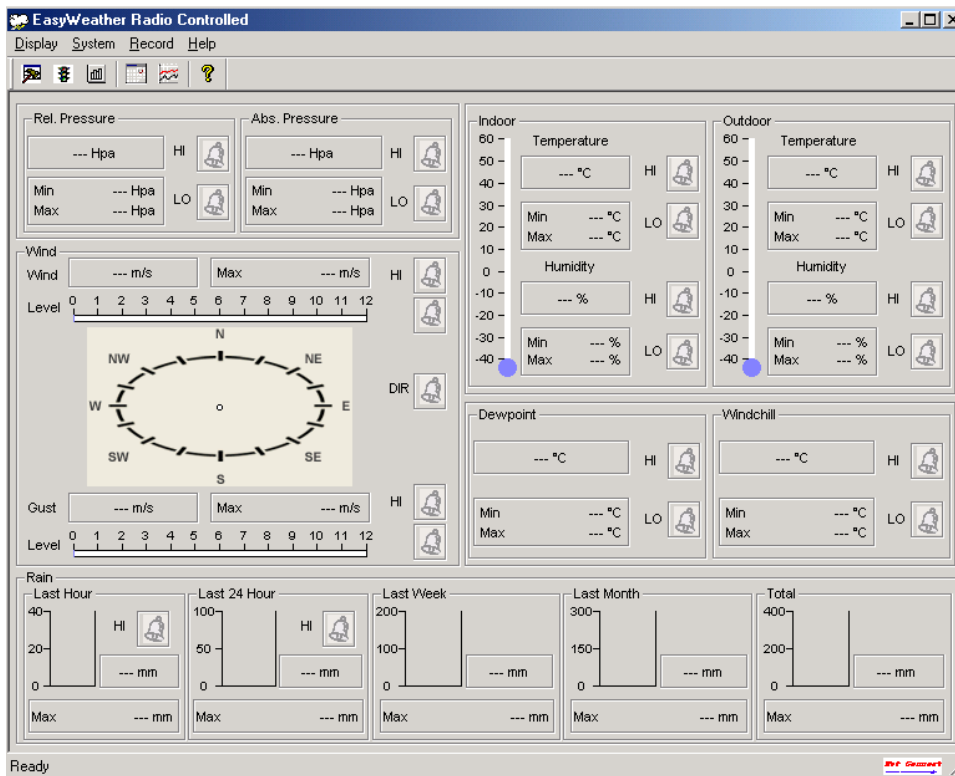
Instalação do Software

A instalação do software da estação meteorológica ITWH-1080 é muito simples: dê um duplo clique no setup.exe e siga os passos mostrados na tela.

Certifique de estar executando o programa em seu computador como administrador da máquina. Caso contrário, a função de gráficos pode não funcionar corretamente.

Ao executar o programa pela primeira vez, o valor corrente será mostrado no display e a aba do software no Windows mostrará informações relacionadas ao histórico da leitura.

Considere que, quanto maior o volume de dados a ser transferido para o PC, mais lento será o processo e o sistema não responderá a seus ajustes enquanto estiver transferindo os dados, caso contrário o display mostrará “read weather data fail”, e esta mensagem de erro indicará que a porta USB está lendo os dados da memória e o sistema não pode responder a nenhuma outra função.





Quando a memória estiver completa, a transferência de dados para o PC pode levar até 2 minutos, e o software pode levar até outros 2 minutos para processar os dados e mostrar o gráfico.

Dados adicionais sobre o software podem ser encontrados no menu HELP.

Especificações

Dados Externos

Distância do campo de transmissão	100 metros (300 pés)
Frequência (América do Norte)	868 MHz (Europa)/915 MHz
Faixa de Temperatura	-40°C a 65°C (-40°F a 149°F)
Precisão	±1°C
Resolução	0.1°C
Faixa de Medição Umidade Relativa	10% a 99%
Precisão	±5%
Volume de chuva ---)	0 a 9999mm (fora de faixa mostrará ---)

Precisão	±10%
Resolução 1000mm)	0.3mm (caso volume de chuva < 1mm (caso volume de chuva > 1000mm)
Velocidade do vento faixa mostrará ---	0-160 km/h (0-100 mph) – fora de
Precisão 10m/s)	±1 m/s (velocidade do vento < ±10% (velocidade do vento >
10m/s)	

Dados Internos

Intervalo de medição pressão/temperatura	48 segundos
Faixa temperatura interna faixa mostrará ---	0°C a 50°C (32°F a 122°F) – fora de
Resolução	0.1°C
Faixa de medição de umidade relativa	10% a 99%
Resolução	1%
Faixa de medição de pressão do ar	300-1100hPa (8.85-32.5 inHg)
Precisão	±3hPa entre 700-1100 hPa
Resolução	0.1 hPa (0.01 inHg)
Duração do alarme	120 segundos

Alimentação

Estação base	3 pilhas alcalinas AA 1.5V
Sensor remoto	2 pilhas alcalinas AA 1.5V
Vida útil base e de 24 meses para o sensor.	Mínimo de 12 meses para a estação

Nota: caso a temperatura externa seja inferior a -20°C , certifique-se que o tipo de bateria suporte esta temperatura, a maioria das pilhas alcalinas não podem ser utilizadas em temperaturas inferiores a -20°C , pois elas podem descarregar e danificar o aparelho.

(figura 17)

Preserve o meio ambiente. Descarte as baterias utilizadas somente em postos de coleta autorizados.

Manual de Instalação do Software da Estação Meteorológica

1.0 Informações Gerais

Esta é uma estação meteorológica de alta qualidade, fácil de utilizar e monitorar seu sistema e leituras em seu sistema de armazenamento interno. Embora possua este dispositivo de armazenamento interno, os valores de temperatura, umidade, pressão do ar, vento e chuva podem ser vistos e armazenados em um PC.

Após instalar o programa da Estação Meteorológica neste CD-ROM em seu PC, você poderá visualizar todos os dados recebidos da Estação Base dos sensores externos. Utilize o cabo USB fornecido e conecte a Estação Base em seu PC. A partir daí, você poderá visualizar os dados atuais e os já armazenados.

2.0 Requerimentos de Sistema

Antes de instalar o software em seu PC, veja a configuração mínima exigida:

Sistema: Windows NT4, Windows 2000, Windows XP, Windows Vista, Windows 7.

Internet Explorer 6.0 ou superior

Processador: Pentium III 500 MHz ou superior

Memória: mínimo 128MB, ideal 256MB.

Drive de CD-ROM

A conexão entre a Estação Base e o PC é feita através de cabo USB.

3.0 Instalação do software “EASYWEATHER”

Primeiramente, certifique-se que a Estação Base e os Sensores Externos estejam conectados corretamente (veja o manual de instruções para a Estação Meteorológica Touch Screen para estes ajustes). Após esta verificação, instale o software em seu PC seguindo os passos abaixo:

1. Ligue o seu PC e insira o CD-ROM no drive CD-ROM
2. Dê um duplo clique em “Setup.exe”
3. Selecione o idioma para o processo de instalação e clique em “next”
4. Clique em “next” e selecione a pasta de destino
5. Clique em “next” e o software instalará automaticamente
6. Pressione “ok” para finalizar o processo de instalação
7. Vá ao menu Iniciar / Todos os Programas / EasyWeather e clique no ícone EasyWeather para iniciar o programa.

Nota: Para que a função gráfica funcione, é necessário que o programa seja instalado pelo administrador do PC. Caso seja instalado em outro perfil, algumas funções do programa podem não funcionar corretamente.

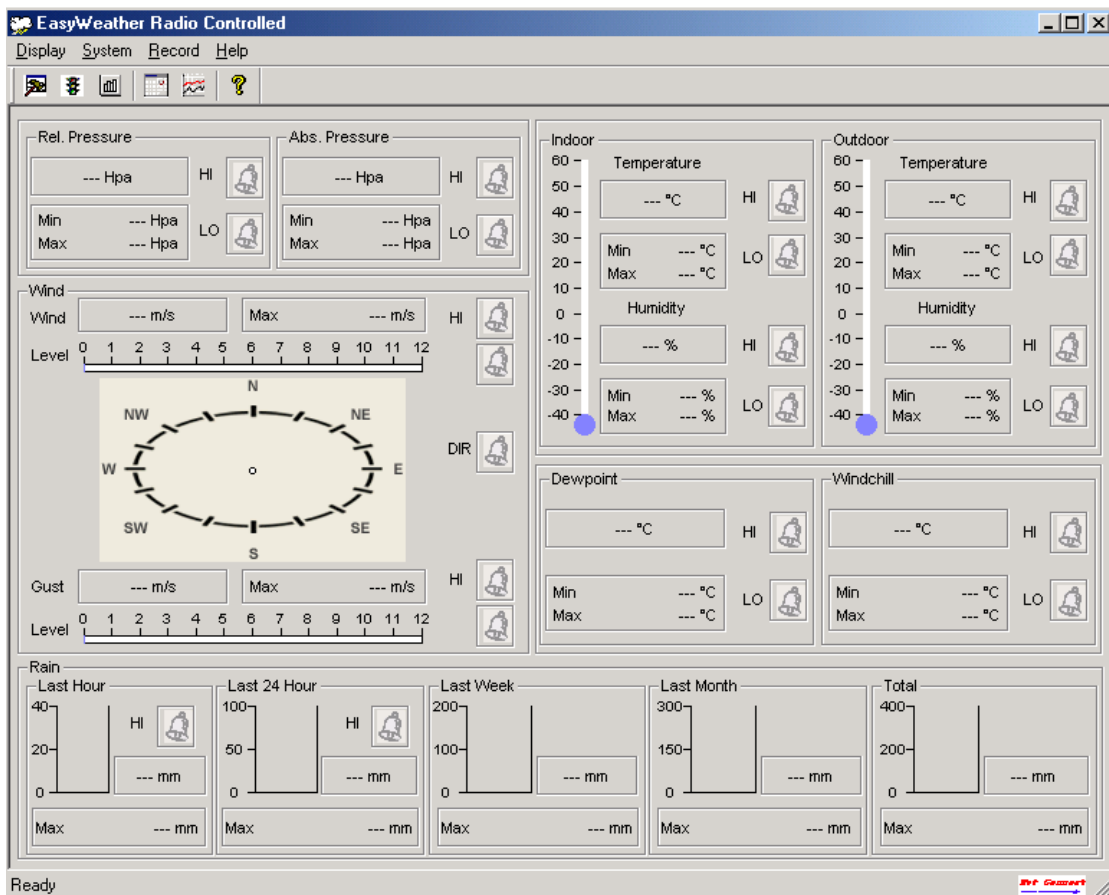
Iniciando o EasyWeather no Windows 7

Certifique-se de estar registrado como administrador em seu PC.



1. Clique em iniciar
2. Localize o ícone EasyWeather e clique com o botão direito do mouse
3. Clique em “run as administrator”

4.0 Ajustes Básicos

Após iniciar o programa EasyWeather.exe, a seguinte tela aparecerá em seu display.



Todos os ajustes feitos na estação base são espelhados no software, portanto uma vez que você tenha feito um ajuste na estação base, não precisará fazer este ajuste no software. Entretanto, você poderá facilmente fazer algum ajuste no PC e transmiti-lo para a estação base (este processo pode levar alguns minutos).

Quando a estação base estiver conectada no PC, o ícone  aparecerá. Quando a estação base não estiver conectada, o ícone  será mostrado.

Botões



Display e ajuste das configurações de sistema

Setup

Time Zone: [Dropdown]

Interval: [Text] Minute

Unit

Indoor Temperature: [Dropdown] °C

Outdoor Temperature: [Dropdown] °C

Pressure: [Dropdown] Hpa

Wind Speed: [Dropdown] m/s

Rainfall: [Dropdown] mm

Display

Format: [Dropdown] Full Date

Day: [Dropdown] mm-dd-yy

Time: [Dropdown] 24H

Axis: [Dropdown] 12 Hours

Outdoor Temperature: [Dropdown] Temperature

Pressure: [Dropdown] Absolute

Velocity: [Dropdown] Wind

Rainfall: [Dropdown] Hour

Alarm Enable

<input type="checkbox"/> Time	<input type="checkbox"/> Wind Direct		
<input type="checkbox"/> Indoor Humidity Low	<input type="checkbox"/> Indoor Humidity High	<input type="checkbox"/> Outdoor Humidity Low	<input type="checkbox"/> Outdoor Humidity High
<input type="checkbox"/> Indoor Temperature Low	<input type="checkbox"/> Indoor Temperature High	<input type="checkbox"/> Outdoor Temperature Low	<input type="checkbox"/> Outdoor Temperature High
<input type="checkbox"/> Windchill Low	<input type="checkbox"/> Windchill High	<input type="checkbox"/> Dewpoint Low	<input type="checkbox"/> Dewpoint High
<input type="checkbox"/> Absolute Pressure Low	<input type="checkbox"/> Absolute Pressure High	<input type="checkbox"/> Relative Pressure Low	<input type="checkbox"/> Relative Pressure High
<input type="checkbox"/> Wind Speed High	<input type="checkbox"/> Gust Speed High	<input type="checkbox"/> Hour Rainfall High	<input type="checkbox"/> Day Rainfall High

Pressure

Relative: [Text] Hpa

Absolute: [Text] Hpa

[Save] [Cancel]

Esta seção é utilizada para ajustar o software, as unidades da estação base, bem como habilitar ou desabilitar as funções correspondentes de alarme. Assim que escolher as unidades / funções desejadas, pressione “Save” para assegurar que o ajuste tenha sido salvo.

 Display e ajuste dos valores do alarme do sistema

Alarm [X]

Time
 Hour: Minute:

Indoor Humidity
 High: % Low: %

Outdoor Humidity
 High: % Low: %

Indoor Temperature
 High: °C Low: °C

Outdoor Temperature
 High: °C Low: °C

Windchill
 High: °C Low: °C

Dewpoint
 High: °C Low: °C

Absolute Pressure
 High: inHg Low: inHg

Relative Pressure
 High: inHg Low: inHg

Wind
 High: km/h bft

Gust
 High: km/h bft

Rain
 High Hour: mm High 24 Hour: mm

Wind Direct

Esta seção é utilizada para ajustar a hora desejada, alarme alto ou baixo para a estação base. Assim que escolher os valores desejados, pressione “Save” para assegurar que o ajuste tenha sido salvo. Caso não queira fazer nenhuma alteração, clique em “Cancel” para não fazer nenhum ajuste.

Valor mínimo e máximo

Scope			
Indoor Humidity		Outdoor Humidity	
Maximum	Time	Maximum	Time
76 %	2007-01-02 11:14	78 %	2007-01-03 23:48
Minimum	Time	Minimum	Time
63 %	2007-01-02 15:04	57 %	2007-01-02 08:20
Indoor Temperature		Outdoor Temperature	
Maximum	Time	Maximum	Time
34.0 °C	2007-01-02 16:12	45.8 °C	2007-01-01 12:02
Minimum	Time	Minimum	Time
28.9 °C	2019-05-24 13:14	27.4 °C	2007-01-02 18:40
Windchill		Dewpoint	
Maximum	Time	Maximum	Time
45.8 °C	2007-01-01 12:02	39.8 °C	2007-01-01 12:02
Minimum	Time	Minimum	Time
27.4 °C	2007-01-02 18:40	19.8 °C	2007-01-03 15:27
Absolute Pressure		Relative Pressure	
Maximum	Time	Maximum	Time
29.59 inHg	2007-01-02 04:51	29.86 inHg	2007-01-03 12:25
Minimum	Time	Minimum	Time
29.34 inHg	2019-05-28 16:09	29.47 inHg	2007-01-03 12:51
Wind		Gust	
Maximum	Time	Maximum	Time
9.7 km/h	2007-01-02 19:18	84.6 km/h	2007-01-03 12:05
Rain Maximum		24 Hours	
Hour	Time	Maximum	Time
0.0 mm	2007-01-03 11:14	0.0 mm	2007-01-03 11:14
Week	Time	Month	Time
0.0 mm	2007-01-03 11:14	0.0 mm	2007-01-03 11:14
Total	Time	OK	
0.0 mm	2007-01-03 11:14		

Esta seção é utilizada para mostrar os valores max e min de leituras armazenadas, bem como sua data e hora. Os valores Max e Min somente podem ser apagados através de operação na estação base.




Lista de histórico de dados

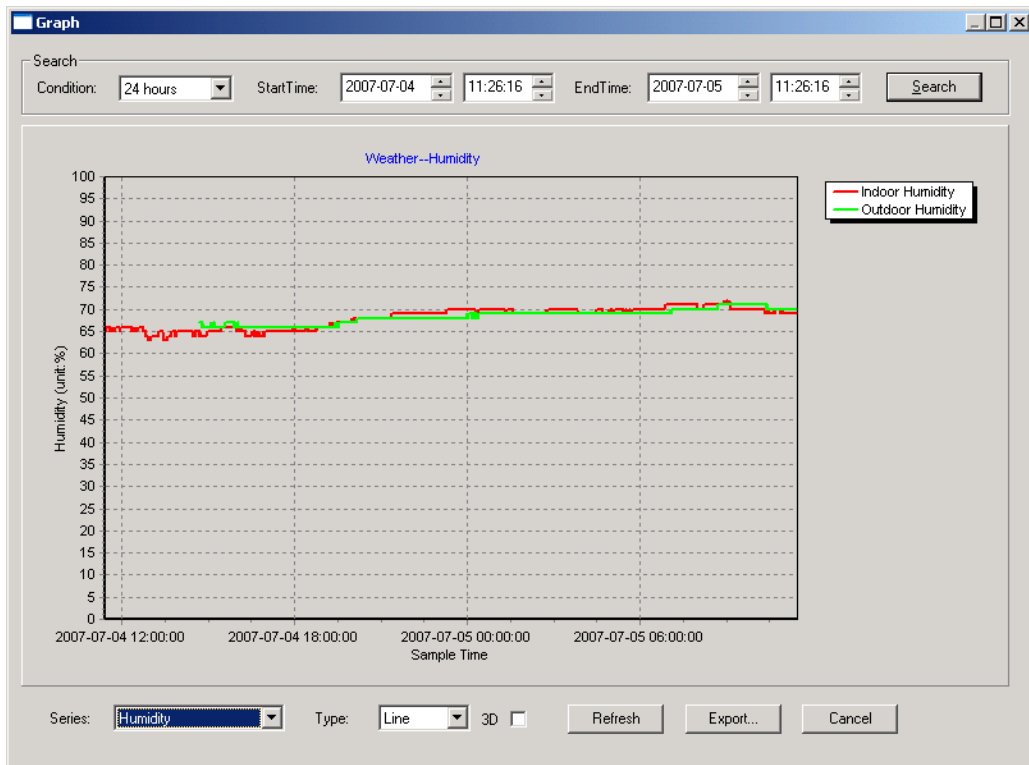
No	Time	Interval(mi)	Indoor Humidity(%)	Indoor Temperature(°C)	Outdoor Humidity(%)	Outdoor Tem
34	2007-07-10 11:59	1	65	32.8	65	32
35	2007-07-10 12:00	1	65	32.8	65	32
36	2007-07-10 12:01	1	65	32.8	65	32
37	2007-07-10 12:02	1	93	33.5	65	32
38	2007-07-10 12:03	1	93	33.5	65	32
39	2007-07-10 12:04	1	93	33.5	65	32
40	2007-07-10 12:05	1	95	34.1	65	32
41	2007-07-10 12:06	1	95	34.1	65	32
42	2007-07-10 12:07	1	95	34.1	65	32
43	2007-07-10 12:08	1	95	34.1	65	32
44	2007-07-10 12:09	1	94	34.0	65	32
45	2007-07-10 12:10	1	95	34.3	65	32
46	2007-07-10 12:11	1	90	33.9	65	32
47	2007-07-10 12:12	1	96	34.0	65	32
48	2007-07-10 12:13	1	92	33.4	65	32
49	2007-07-10 12:14	1	93	33.6	64	32
50	2007-07-10 12:14	1	84	33.0	64	32
51	2007-07-10 12:15	1	74	32.9	64	32
52	2007-07-10 12:16	1	70	33.0	64	32
53	2007-07-10 12:17	1	66	33.1	64	32
54	2007-07-10 12:18	1	66	33.1	64	32
55	2007-07-10 12:19	1	65	33.1	64	32
56	2007-07-10 12:20	1	65	33.1	64	32
57	2007-07-10 12:21	1	64	33.1	64	32
58	2007-07-10 12:22	1	64	33.1	63	32
59	2007-07-10 12:23	1	63	33.0	63	32
60	2007-07-10 12:24	1	63	33.0	63	32
61	2007-07-10 12:25	1	63	33.0	63	32

Esta seção é utilizada para mostrar o histórico de dados em formato de planilha. Caso queira ver o histórico de dados em um período específico, selecione a duração e pressione “Search” para carregar os dados. Através do botão “Export” você poderá exportar os dados em formato de arquivo texto para outras aplicações que necessitar.

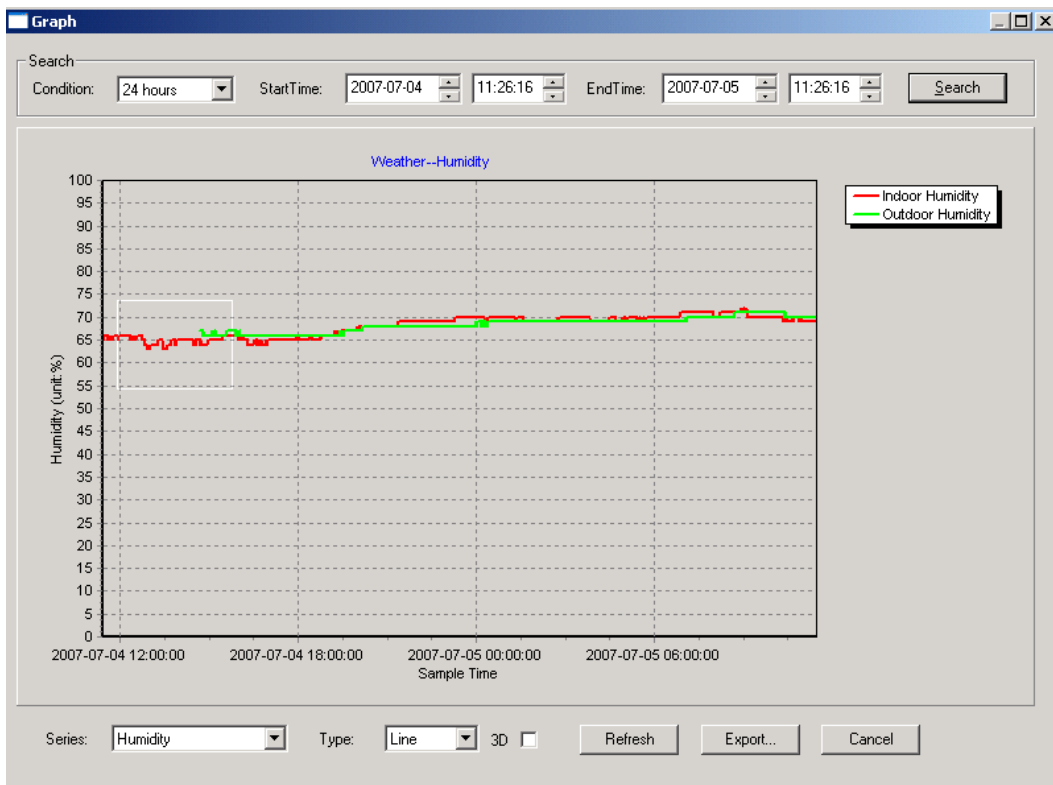
Quando a memória da estação base estiver cheia, pressione “Clear Memory” para limpar a memória da estação base (lembre-se de ter transmitido todos os dados para o PC antes de utilizar esta função).

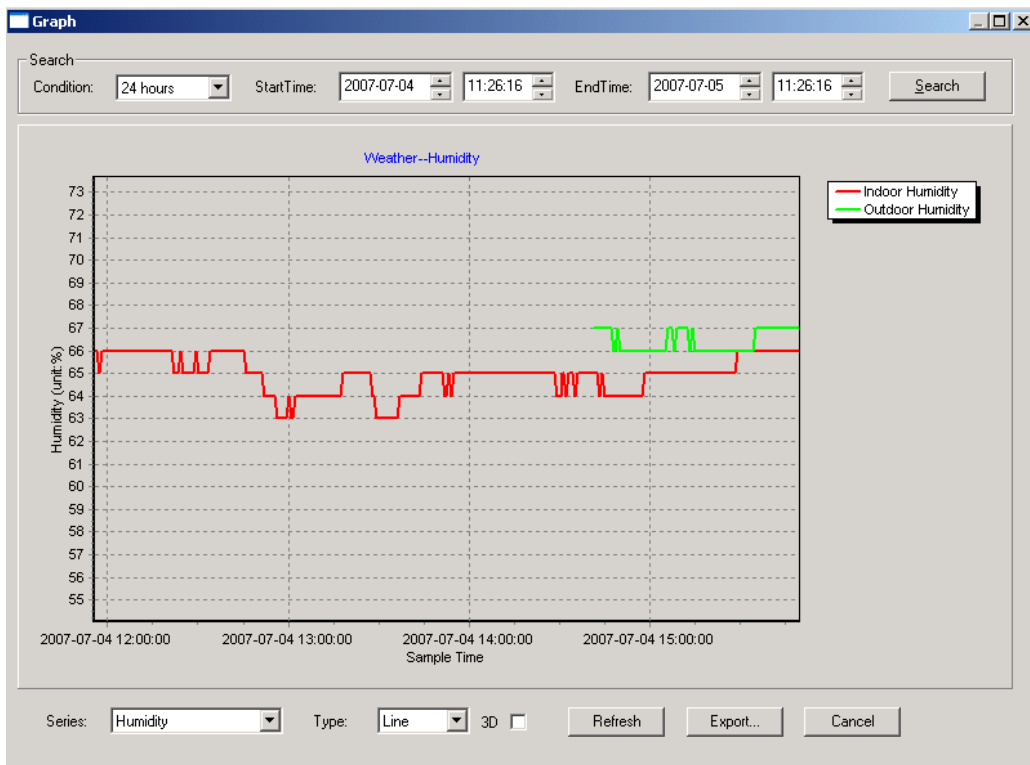
Caso queira iniciar um novo histórico de gravação de dados, pressione “Clear Data” e todos os dados armazenados serão deletados (caso queira, faça um backup dos dados antes de apagá-los, fazendo uma cópia do arquivo “easyweather.dat” em outra pasta, renomeie o arquivo como “jan-07.dat”, por exemplo, para consultas futuras).

 Gráfico do histórico de dados

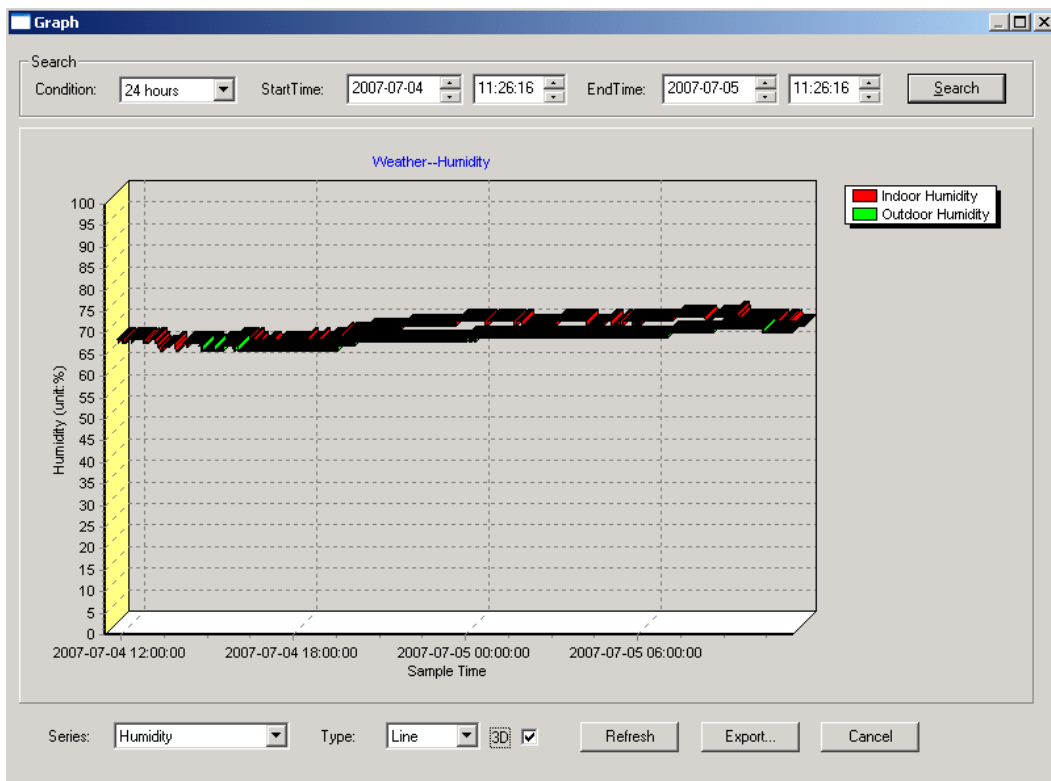


Nesta seção, você poderá visualizar os dados armazenados em formato de gráfico, para uma observação mais fácil. Caso queira ver mais detalhes, passe seu mouse sobre a área desejada e o display mostrará automaticamente a escada detalhada.





Você também pode visualizar o gráfico em 3D, marque esta opção na caixa “3D”.

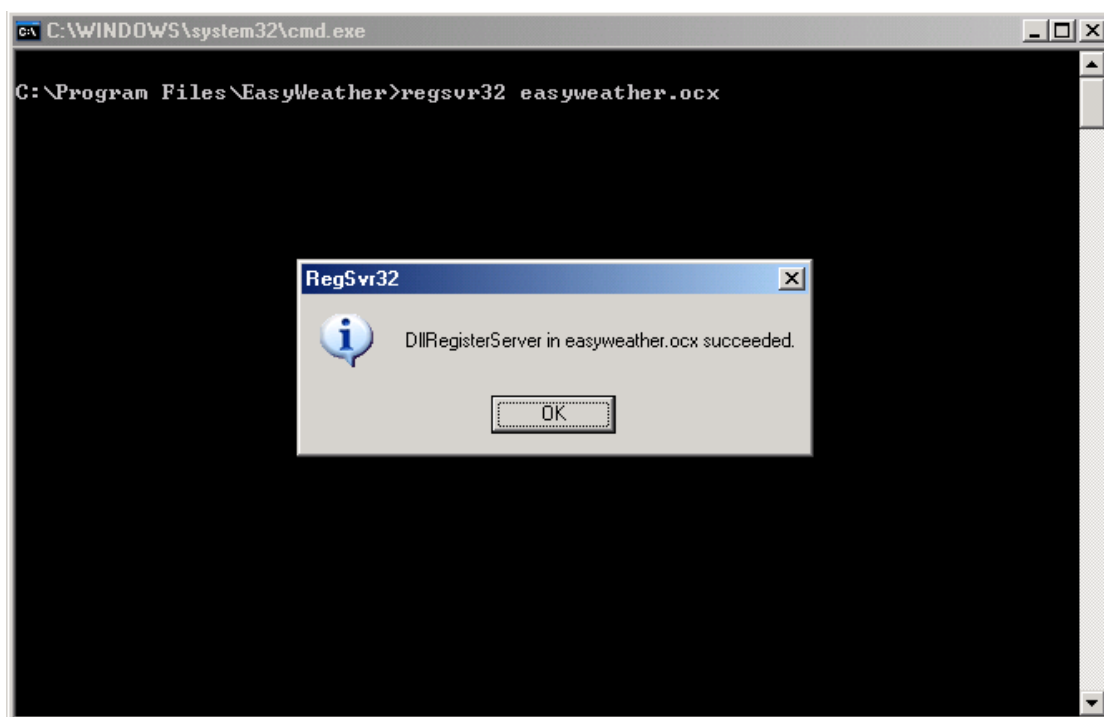


Você poderá alterar a coluna Y movendo seu mouse para cima ou para baixo.

O que fazer caso a função gráfico não funcione

Este é o problema mais comum que pode haver durante a utilização do software. Para se certificar de que a função gráfico esteja funcionando, siga os passos abaixo:

- 1) Localize onde o arquivo “easyweather.exe” está localizado.
- 2) Crie um arquivo com o nome “reg_graph.bat” no word ou bloco de notas.
- 3) Digite “regsvr32 easyweather.ocx” e salve o arquivo “reg_graph.bat”.
- 4) Dê um duplo clique no arquivo “reg_graph.bat” e registre o driver gráfico novamente. Caso a operação funcione, a janela abaixo será mostrada:



Notas Especiais sobre a sincronização entre o PC e a estação

O software do PC obteve sua própria escala de tempo por meio do marcador de intervalo de tempo a partir do histórico de dados da estação base. O software do PC sincroniza automaticamente os dados do clima com uma marca de tempo calculado. Dessa maneira a pasta com o histórico de dados pode ter diferentes horas quando a hora do PC for diferente da hora da estação base. Para ajustar a mesma escala de tempo, lembre-se de configurar tanto a hora do PC quanto a da estação base corretamente, sendo ambas iguais, nenhum dado sobre o clima corre o risco de ser perdido ou substituído. Se o histórico de dados sobre o clima na estação base for removido manualmente, então o histórico de dados do clima estará perdido permanentemente desde a última atualização.

Antes que a memória esteja cheia (um ícone de memória mostrando que está 100% cheia), lembre-se de atualizar o histórico de dados do PC periodicamente.

Se houver uma redefinição causada pela queda de chuva na estação base, então haverá uma discrepância do valor de chuva entre o PC e a estação base.

Notas Legais

- Nós reservamos o direito de apagar ou mudar qualquer imagem de clima ou atualizações não propositais no nosso servidor por um usuário do WH1080 e produtos e software EasyWeather.
- O software EasyWeather e seus componentes são protegidos por leis de direito autoral e acordos internacionais assim como outras leis de propriedade intelectual.
- Você não pode copiar os materiais impressos que acompanham os produtos.



Instrutemp Instrumentos de Medição Ltda

Rua Fernandes Vieira, 156 - Belenzinho - São Paulo/SP - Cep: 03059-023

Tel: (11) 3488-0200 - Fax: (11) 3488-0208

www.instrutemp.com.br / email: vendas@instrutemp.com.br

DIGITAL PHOTO TACHOMETER OPERATION MANUAL

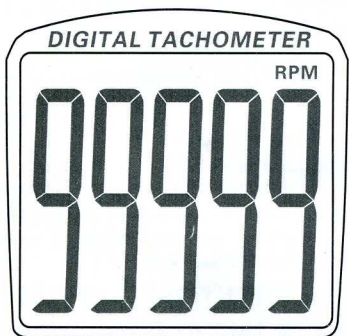


TABLE OF CONTENTS

1. FEATURES	1
2. SPECIFICATIONS	1
3. FRONT PANEL DESCRIPTIONS	2
4. MEASURING PROCEDURE	3
5. MEASURING CONSIDERATION	3
6. MEMORY	4
7. BATTERY REPLACEMENT	4

CAUTION
BEAM OF LIGHT-DO NOT
STARE INTO EYE BEAM!

1. FEATURES

- * Large LCD displaying.
- * Wide measuring range & high resolution.
- * Digital display gives exact RPM with no guessing or errors.
- * The last value/max. value/min. value will be automatically stored in memory and can be displayed by turn anytime.
- * The use of durable, long-lasting components, including a strong, light weight ABS - plastic housing assures maintenance free performance for many years. The housing has been carefully shaped to fit comfortably in either hand.

2. SPECIFICATIONS

Display:	5 digits, 31mm LCD (Liquid Crystal Display), with function annunciation.
Test Range:	2.5 to 99,999 RPM (r/min).
Resolution:	0.1 RPM (2.5 to 999.9 RPM). 1 RPM (over 1,000 RPM).
Accuracy:	$\pm(0.05\%+1 \text{ digit})$.
Sampling Time:	0.8 sec. (over 60 RPM).
Test Range Select:	Automatic.
Memory:	Max.Value, Min.Value, Last.Value.
Detecting Distance:	50 to 200mm / 2 to 8 inch (LED) 50 to 500mm / 2 to 20 inch (Laser)
Time Base:	Quartz crystal.
Circuit:	Exclusive one-chip of microcom- puter LSI circuit.
Battery:	UM-3 1.5V x 3
Operation Temp.:	0 to 50° C (32 to 122° F)

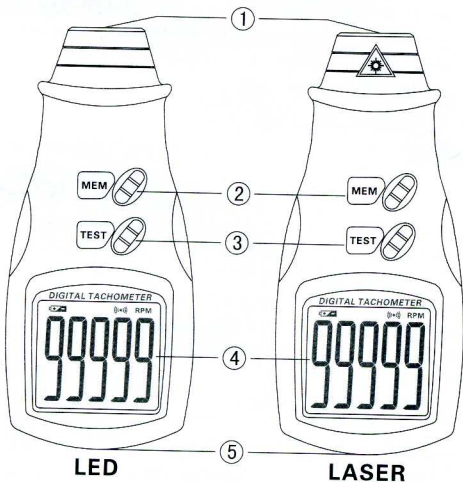
Power Consumption: Approx. 35mA (LED)
 Approx. 30mA (Laser)

Dimensions: 160×76×40mm

Weight: Approx. 280g (including battery)

Accessories: Carrying case 1 pc.
 Reflecting tape marks (600mm)
 Operation manual..... 1 pc.

3. FRONT PANEL DESCRIPTIONS



- | | |
|------------------------------|------------------|
| 1, Signal light beam | 2, Memory button |
| 3, Measure button | 4, Display |
| 5, Battery Compartment/Cover | |

4. MEASURING PROCEDURE

Apply a reflective mark to the object being measured. Depress the MEASURE BUTTON and align the visible light beam with the applied target. Verify that the MONITOR INDICATOR lights when the target aligns with the beam (about 1 to 2 seconds).

5. MEASURING CONSIDERATION

5-1 REFLECTIVE MARK

Cut and peel adhesive tape provided into approx. 12mm (0.5") squares and apply one square to each rotation shaft.

- a. The non-reflective area must always be greater than the reflective area.
- b. If the shaft is normally reflective, it must be covered with black tape or black paint before attaching reflective tape.
- c. Shaft surface must be clean and smooth before applying reflective tape.

5-2 VERY LOW RPM MEASUREMENT

As it is easy to get high resolution and fast sampling time. If measuring the very low RPM values, suggest user to attach more " REFLECTIVE MARKS " averagely. Then divide the reading shown by the number of " REFLECTIVE MARKS " averagely. Then divide the reading shown by the number of " REFLECTIVE MARKS" to get the real RPM.

5-3 BATTERY REMOVAL

If the instrument is not be used for any extended period, remove batteries.

6. MEMORY

6-1 A readout (the last value, max. value, min.Value) obtained immediately before turning off the MEASURE BUTTON is automatically memorized. For example, please ref. following fig. 1.

6-2 That Memorized value can be displayed on the indicator by turn once depressing the memory button. The Symbol "UP" represents the Max. Value and "dn", the Min Value; "LA", the last Value.

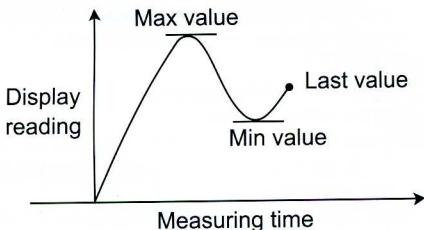


Fig.1

7. BATTERY REPLACEMENT

- (1) If is necessary to replace battery, when left corner of LCD display show " $\square + \square$ ".
- (2) Slide the battery cover (3-5) away from the instrument and remove the battery.
- (3) Install the batteries UM-3 correctly into the case.